Modèle de forêts enracinées sur des cycles et modèle de perles via les dimères

Wangru Sun

Thèse de doctorat

Discipline : Mathématiques

Université Pierre et Marie Curie

École Doctorale des Sciences Mathématiques de Paris Centre
Laboratoire de Probabilités et Modèles Aléatoires

présentée par

Wangru Sun

Modèle de forêts enracinées sur des cycles et modèle de perles via les dimères

---

co-dirigé par Cédric Boutillier et Béatrice De Tilière

Presentée et soutenue le 7 fvrier 2018 devant le jury composé de :

M. Cédric Boutillier	Université Pierre et Marie Curie	Directeur
M. David Cimasoni	Université de Genève	Rapporteur
Mme. Béatrice De Tilière	Université Paris-Est Créteil	Directrice
M. Nathanaël Enriquez	Université Paris Sud	Examinateur
M. Thomas Fernique	Université Paris 13	Rapporteur
M. Arnaud Le Ny	Université Paris-Est Créteil	Examinateur
M. Zhan Shi	Université Pierre et Marie Curie	Examinateur

Abstract

The dimer model, also known as the perfect matching model, is a probabilistic model originally introduced in statistical mechanics. A dimer configuration of a graph is a subset of the edges such that every vertex is incident to exactly one edge of the subset. A weight is assigned to every edge, and the probability of a configuration is proportional to the product of the weights of the edges present.

In this thesis we mainly study two related models and in particular their limiting behavior. The first one is the model of cycle-rooted-spanning-forests ($CRSF$) on tori, which is in bijection with toroidal dimer configurations via Temperley's bijection. This gives rise to a measure on $CRSF$. In the limit that the size of torus tends to infinity, the $CRSF$ measure tends to an ergodic Gibbs measure on the whole plane. We study the connectivity property of the limiting object, prove that it is determined by the average height change of the limiting ergodic Gibbs measure and give a phase diagram.

The second one is the bead model, a random point field on $\mathbb{Z} \times \mathbb{R}$ which can be viewed as a scaling limit of dimer model on a hexagon lattice. We formulate and prove a variational principle similar to that of the dimer model [CKP01], which states that in the scaling limit, the normalized height function of a uniformly chosen random bead configuration lies in an arbitrarily small neighborhood of a surface h_0 that maximizes some functional which we call as entropy. We also prove that the limit shape h_0 is a scaling limit of the limit shapes of a properly chosen sequence of dimer models.

There is a map form bead configurations to standard tableaux of a (skew) Young diagram, and the map is measure preserving if both sides take uniform measures. The variational principle of the bead model yields the existence of the limit shape of a random standard Young tableau, which generalizes the result of [PR07]. We derive also the existence of an arctic curve of a discrete point process that encodes the standard tableaux, raised in [Rom12].

Keywords. dimer model, tilings, cycle-rooted-spanning-forests, random walks, bead model, standard (skew) Young tableaux, limit shapes.

Résumé

Le modèle de dimères, également connu sous le nom de modèle de couplage parfait, est un modèle probabiliste introduit à l'origine dans la mécanique statistique. Une configuration de dimères d'un graphe est un sous-ensemble des arêtes tel que chaque sommet est incident à exactement une arête. Un poids est attribué à chaque arête et la probabilité d'une configuration est proportionnelle au produit des poids des arêtes présentes.

Dans cette thèse, nous étudions principalement deux modèles qui sont liés au modèle de dimères, et plus particulièrement leur comportements limites. Le premier est le modèle des forêts couvrantes enracinées sur des cycles ($CRSF$) sur le tore, qui sont en bijection avec les configurations de dimères via la bijection de Temperley. Dans la limite quand la taille du tore tend vers l'infini, la mesure sur les $CRSF$ converge vers une mesure de Gibbs ergodique sur le plan tout entier. Nous étudions la connectivité de l'objet limite, prouvons qu'elle est déterminée par le changement de hauteur moyen de la mesure de Gibbs ergodique et donnons un diagramme de phase.

Le second est le modèle de perles, un processus ponctuel sur $\mathbb{Z} \times \mathbb{R}$ qui peut être considéré comme une limite à l'échelle du modèle de dimères sur un réseau hexagonal. Nous formulons et prouvons un principe variationnel similaire à celui du modèle dimère [CKP01], qui indique qu'à la limite de l'échelle, la fonction de hauteur normalisée d'une configuration de perles converge en probabilité vers une surface h_0 qui maximise une certaine fonctionnelle qui s'appelle "entropie". Nous prouvons également que la forme limite h_0 est une limite de l'échelle des formes limites de modèles de dimères.

Il existe une correspondance entre configurations de perles et (skew) tableaux de Young standard, qui préserve la mesure uniforme sur les deux ensembles. Le principe variationnel du modèle de perles implique une forme limite d'un tableau de Young standard aléatoire. Ce résultat généralise celui de [PR07]. Nous dérivons également l'existence d'une courbe arctique d'un processus ponctuel discret qui encode les tableaux standard, defini dans [Rom12].

Mots-clés. modèle de dimères, pavages, forêts couvrantes enracinées sur cycles, marches aléatoires, modèle de perles, tableaux de Young standard, forme limite.

Contents

Chapter 1

Introduction

The *dimer model*, also called the perfect matching model, was first introduced in physics and chemistry to model the adsorption of di-atomic molecules on the surface of a crystal [FR37]. It is a statistical mechanics model in dimension 2. In the 1960's Kasteleyn [Kas61, Kas63, Kas67], Fisher and Temperley [TF61] have shown how to calculate the partition function. Many progresses have been made since the late 1990s, see [Ken97, CKP01, KO06, KOS06] for example.

The dimer model is related to many other probabilistic models on graphs embedded in 2-dimensional surfaces. For example, the free-Fermion six-vertex models, the 2-d Ising model, spanning trees, etc. In this thesis, we mainly focus on two statistical mechanical models closely related to the dimer model, use the tools or existing results of the dimer model to study the properties of these two models (mainly their asymptotic behaviors).

The first one is the model of spanning trees and spanning forests. These classical objects are first found to be related to the dimer model by Temperley [Tem74] by a bijection. In this thesis, we consider a variation of the original model: the cycle-rooted-oriented spanning forests. The second one is the bead model [Bou09], and it is shown to be closely related to the standard (skew) Young tableaux.

In this chapter we give a general introduction of the notions, the existing results and tools we use and the main results proved in this thesis. This includes informal definitions, intuitive explanations and an outline of the whole thesis. They are organized in the order of the three main models.

1.1 Dimer model

We begin with a general introduction of the dimer model, which plays a central role in this thesis. A more detailed and formal introduction can be found in Chapter 2.

The model can be briefly described as follows: consider a connected graph $G = (V, E)$. Every edge $e \in E$ is equipped with a weight $c(e)$ which is a positive real number. A dimer configuration M is a subset of edges such that every

vertex $v \in V$ is incident to exactly one edge in M. An edge of M is called a *dimer*.

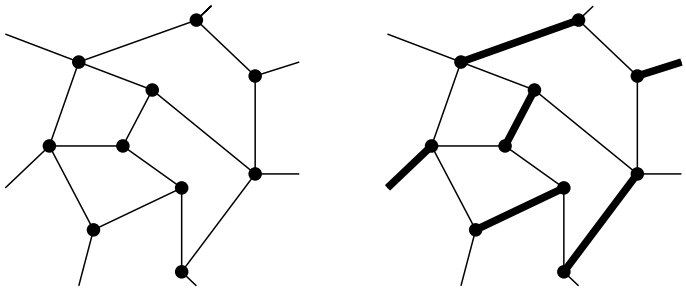

Figure 1.1: An example of a dimer configuration on a graph.

Throughout this thesis, we consider a dimer model embedded in a 2 dimensional surface. In this case, a more intuitive way to interpret the model is via tilings. The most classical examples are domino tilings or lozenge tilings, which respectively can be viewed as the dimer model on the $\mathbb{Z}^2$ lattice or honeycomb lattice (hexagon lattice), see Figures 1.2 and 1.3 below.

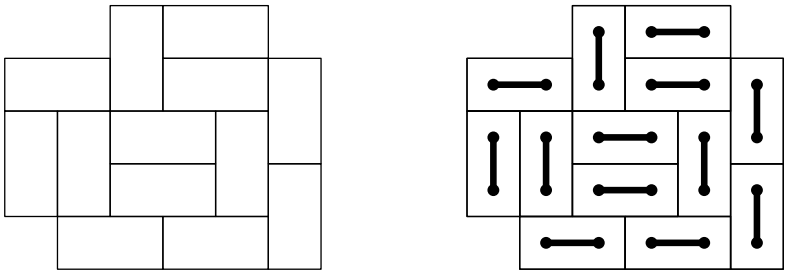

Figure 1.2: Domino tiling and dimers on a portion of $\mathbb{Z}^2$.

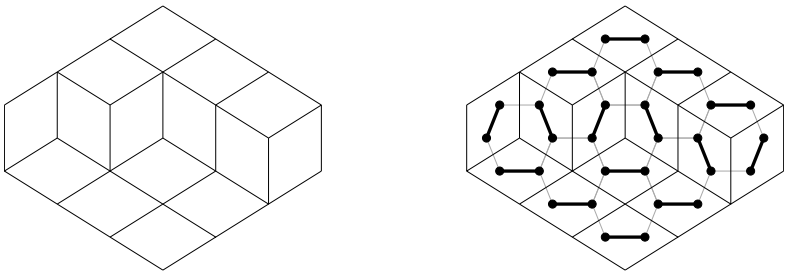

Figure 1.3: Lozenge tiling and dimers on the honeycomb lattice.

The lozenge tiling in Figure 1.3 can be naturally viewed as a pile of cubes on a domain D. The horizontal lozenges can be viewed as faces parallel to the $x-y$ plane, and if we choose the "lowest" such face to have 0 height, then every other horizontal face has a integer "height" which is the number of cubes underneath the horizontal face. The maximal height is given by the boundary condition. For example, in

Figure 1.3 the maximal height is equal to 1. Moreover, there is a constraint on these height functions: if we think of the height as a function on the integer points of the $x - y$ plane, then along each row (resp. column) of the cubes, the heights are monotone. Such an integer function is called a *plane partition*.

This simple relation between plane partitions and lozenge tilings is one of the main inspiration of our Chapter 6. We will talk more about it later in Section 1.3. Also, the definition of the height function is something more general, see Section 2.3.1.

Now we consider a measure defined on the set of configurations. When the graph is finite, the measure is taken to be proportional to the product of the weights of the present edges, which we call a *weighted measure* or a *Boltzmann measure*.

For the infinite case, a natural idea is to define the measure as the limit of a sequence of measures which are the measures defined on bigger and bigger graphs. However, choosing different sequences can lead to completely different measures as the measure strongly depends on the boundary conditions. A trivial example is given by the following graphs, where we see that a tiny change on the boundary will greatly change the measure.

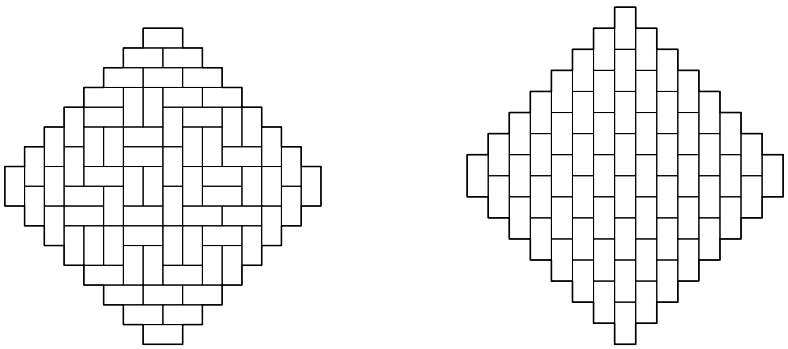

Figure 1.4: Domino tiling of two domains of similar shape.

The left domain in Figure 1.4 is called the *Aztec diamond*, because of its obvious similarity with an Aztec pyramid. The right domain in Figure 1.4 can only be tiled in this way, and we call it a frozen phase. Meanwhile, the way to tile the left domain (an Aztec diamond) is much richer. When the domain is large, in the middle of an Aztec diamond there are always interesting behaviors, what is to be called as a liquid phase, and at the corners we have a frozen phase. For more details about the phases, see Section 2.3.4. This phenomena is studied in [CEP96], where the four corners with frozen behavior are called the polar regions. The boundary between the frozen regions and other parts is thus called the arctic curve.

By this toy example, we see that the asymptotic behavior is not simply determined by the asymptotic shape of the domain. It is proved [CKP01] to be determined by the height function on the boundary of the domain, see Section 2.4.

Rather than choosing the asymptotic boundary condition among the height functions defined on the boundary of planar domains, the authors of [KOS06] consider

periodic boundary conditions. More precisely, they consider a $\mathbb{Z}^2$-periodic graph G_∞, and the measure of dimer configurations of G_∞ is taken to be the limit of a family of magnetically altered dimer measures on $\mathcal{G}_N := G_\infty/(N\mathbb{Z}^2)$. Here "magnetically altered" means that rather than considering the usual weighted measure, the authors consider a family of measures where the weights of the edges crossing the boundary between different copies of the original graph $\mathcal{G}_1$ are multiplied by the exponential of some parameters that are called *magnetic field*. They correspond to the two extra degrees of freedom of the dimer measure in the toroidal case. When $n \to \infty$ such measures converge to an ergodic Gibbs measure depending on the magnetic field, and the limiting measure is characterized by the *slope*, the expected height between neighboring copies of the fundamental domain. See Section 2.3.4.

Authors of [CKP01] reveal that the toroidal dimer measure is the good tool to describe the local measure for our earlier question about the dimer measure in the infinite limit with an asymptotic boundary condition. A variational principle is established, which proves the existence and uniqueness of the limiting behavior, see Section 2.4.

All the properties and results mentioned above are the inspirations of our study of the following two models: spanning trees, spanning forests and cycle rooted spanning forests in Section 1.2, the bead model and standard skew Young tableaux in Section 1.3.

1.2 Spanning trees/forests, cycle rooted spanning forests

Temperley [Tem74] first introduced a measure preserving bijection on the square grid between spanning trees and dimer configurations. Consider a square grid G, and consider its double graph G^d, which can be viewed as if we divide each square face of G into 4 smaller ones. Choose any vertex v_0 of G on the boundary, then the spanning trees of G are in bijection with dimer configurations of $G^d\backslash\{v_0\}$: for every dimer configuration M, and for each dimer $e \in M$, chose among its two incident vertices the one which is a vertex of G, then take this vertex as the departing point and go along the dimer e until it meet another vertex of G. What we get is a spanning tree of G. Conversely, given a spanning tree of G, the reverse procedure generates a set of dimers of $G^d\backslash\{v_0\}$, and there is a unique way to extend this to a dimer configuration of $G^d\backslash\{v_0\}$, see Figure 1.5.

This bijection was generalized by Burton and Pemantle in [BP93] and Kenyon, Propp and Wilson [KPW00] to more general cases: between spanning trees of directed weighted planar graphs and dimer configurations of its double graph, see Section 3.4.1. The generalized bijection is measure preserving if we properly choose the weights. A detailed explanation is given in Section 3.4.2.

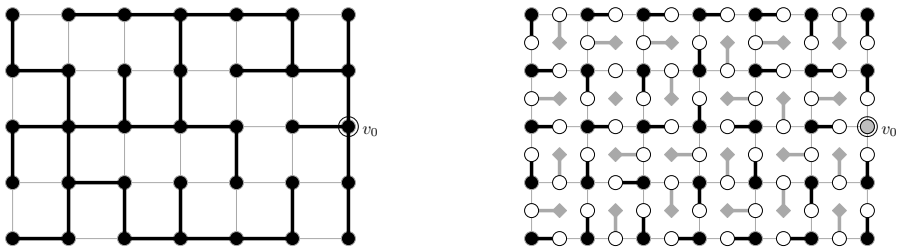

Figure 1.5: Temperley's bijection on a square grid.

In this thesis, we are mainly interested in the case of toroidal graphs. If we apply such a bijection to the toroidal case, then from every dimer configuration on the double graph $\mathcal{G}^d$ of some toroidal graph $\mathcal{G}$, we get a cycle rooted spanning forest (CRSF), see Section 3.1.

By [KOS06], if we take larger and larger toroidal graphs where every one is a quotient of the same $\mathbb{Z}^2$-periodic graph, then the dimer measures converge to an ergodic Gibbs measure of some slope, so the measure on *CRSF* via Temperley's bijection is also an ergodic Gibbs measure. Some asymptotic properties can be obtained directly as analogues of the corresponding results of the dimer model, for example, the edge-edge correlations and variations of the height function.

However, in this thesis, the property we mainly focus on is a specific property for trees and forests that doesn't have its counter part in the dimer model: the connectivity. This question in fact comes from [Pem91], where the author studies the limiting behavior (mainly connectivity) of a spanning tree on larger and larger graphs as subgraphs of $\mathbb{Z}^d$, d fixed, see Section 3.3.

As for the toroidal case, the question can be briefly stated as follows: in the limit when the size of the torus tends to infinity, the *CRSF* as a union of edges of an infinite $\mathbb{Z}^2$-periodic graph without cycles (the cycles of *CRSF* are of non-trivial homotopy so they disappear in the limit), is it a spanning tree (connected) or a spanning forest (not connected)?

We answer this question by giving and proving Theorems 4.3.2 and 4.4.3, summarized by Theorem 1.2.1 here below, which says that the connectivity of the limiting object of the *CRSF* measure depends on the slope of the corresponding limiting dimer measure.

Theorem 1.2.1. *When the slope of the limiting dimer measure is non-zero, under the corresponding CRSF measure there are a.s. infinitely many connected components, and when it is zero, if the graph verifies a technical assumption (Condition* $(\star)$*, see Definition 4.4.2), then there is a.s. one connected spanning tree.*

Here is an outline of the organization of Chapters 3 and 4, which are the chapters on spanning trees/forests and *CRSF*. Chapter 3 of this thesis is mainly devoted to an introduction of the basic structures and fundamental properties related to this

topic. A crucial fact that relates the height change (which in the limit corresponds to the slope) of a dimer configuration and the homology (which yields an estimation of the number of connected components) of its corresponding *CRSF* is proved in Proposition 3.4.1.

In Chapter 4, we define the limiting measure of *CRSF*, characterize the measure with the discrete Laplacian (Theorem 4.2.3) and study the connectivity properties of the limiting object. We prove Theorem 1.2.1, and as a corollary we give a full picture of the phase diagram of the connectivity of the limiting *OCRSF* measure on graphs verifying Condition ($\star$).

1.3 Bead model, standard (skew) Young tableaux

In Chapter 5 and 6 we consider a random point field on $\mathbb{Z}\times\mathbb{R}$ or a subset of it, which is called the *bead model* because of its similarity to a collection of beads on parallel threads. The vertical positions of the beads are asked to be interlacing: between any two successive beads on a thread, on either of its neighboring threads, there should be exactly one bead whose vertical position is between these two beads.

Figure 1.6 gives an example of a bead configuration. Consider for example the third thread counted from right. Given all the beads on the other threads (the black ones), on this thread there should be exactly one bead (the red one) on the piece that is incident to both of the grey regions generated by the beads on neighboring threads.

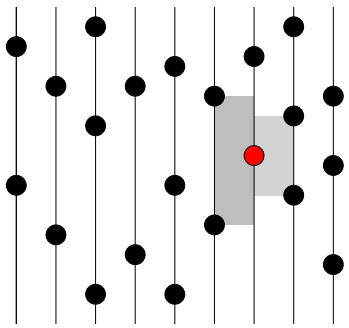

Figure 1.6: A bead configuration.

Boutillier [Bou09] constructs a family of ergodic Gibbs measures of the bead model on $\mathbb{Z}\times\mathbb{R}$ as continuous limits of a lozenge tiling when some weight tends to 0. The author's work can be viewed as a limiting case of the dimer model on a periodic graph.

In this thesis, we are interested in the counter part of the dimer model (lozenge tiling) on finite domains. In particular, we consider a very tall region tileable by lozenges and consider a unit square D whose boundary condition is given by that of the tileable region, see Chapter 5 for the detailed construction or Figure 1.7 for an illustration. The bead model normalized into the unit square is in fact a normalized

continuous limit of the tiling of the region when the height of that region tends to infinity.

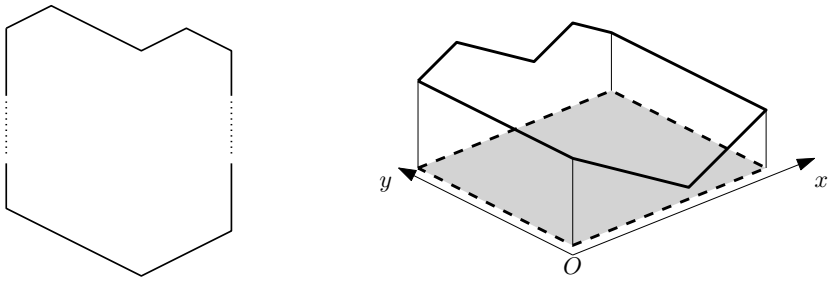

Figure 1.7: A very tall domain tileable by lozenges vs. corresponding boundary condition of the bead model.

We are interested in the limiting behavior of the bead model when the number of threads tends to infinity while the normalized boundary conditions are fixed. We know by [CKP01] (see Section 2.4 for a summary) that if the relative height of the tall region is fixed, there is a variational principle that proves that in the limit the random surface given by a random tiling converges in probability to a surface that maximizes some functional $Ent^{\diamond}(.)$ which is called the entropy function (of lozenge tiling). We prove the same kind of variational principle in Section 6.4 for the bead model, which is far from simply being a corollary of the existing results on dimers since there is a delicate exchange of limits.

We define the space of admissible functions as the complete space of normalized height functions on the unit square D. As in [CKP01], there exists a functional $Ent(.)$ (see Section 6.3.2) defined on the space of admissible functions that gives the variational principle for beads. More precisely, we have the following theorems:

Theorem 1.3.1. *For any given asymptotic boundary height function h^{∂} defined on ∂D and being constant on $\{x = 0\}$ and $\{x = 1\}$, there is a unique function h_0 among the space of admissible functions that maximizes $Ent(.)$.*

Theorem 1.3.2. *Consider a given asymptotic boundary height function h^{∂} defined on ∂D and being constant on $\{x = 0\}$ and on $\{x = 1\}$. For any $n \in \mathbb{N}^*$, consider the bead model on D with n threads. For any admissible function $h : D \to \mathbb{R}$ such that $Ent(h) > -\infty$, when n tends to infinity, the probability that the normalized surface of a random bead configuration lies within a δ neighborhood of h is proportional to $e^{(Ent(h)+o(1))n^2}$ when $\delta \to 0$.*

Note that Theorems 1.3.1 and 1.3.2 imply a limit shape of the bead model which is the surface h_0 that maximizes the functional $Ent(.)$. We also prove the following result, see Theorem 6.5.1 of Section 6.5.

Theorem 1.3.3. *The limit shape of the bead model h_0 is a properly normalized limit of the limit shapes of the lozenge tilings for the corresponding sequence of domains.*

This theorem proves the commutativity of the following two limits: the limit from a dimer model to a bead model when the height tends to infinity, and the asymptotic limit for the dimer model on an increasing sequence of graphs with given asymptotic boundary condition. This yields a systemical way to explicitly find h_0 via the existing results in [KO07].

As an example, if we consider a bead model on the unit square with the boundary condition given by $h^\partial : \partial([0,1] \times [0,1]) \to \mathbb{R}$,

$$h : (x, y) \mapsto \begin{cases} \frac{1}{4} - \frac{1}{2}|x - \frac{1}{2}| & \text{if } y \leq 0, \\ -\frac{1}{4} + \frac{1}{2}|x - \frac{1}{2}| & \text{if } y > 0, \end{cases}$$

then Figure 1.8 is the expected density (which we will show is the vertical partial derivative of h_0), and Figure 1.9 is a simulation of 256 beads.

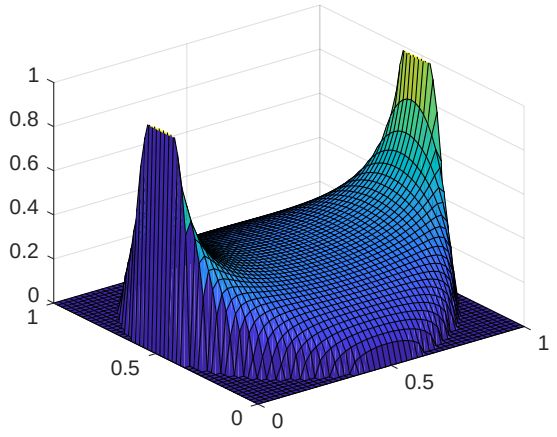

Figure 1.8: The estimated density of beads.

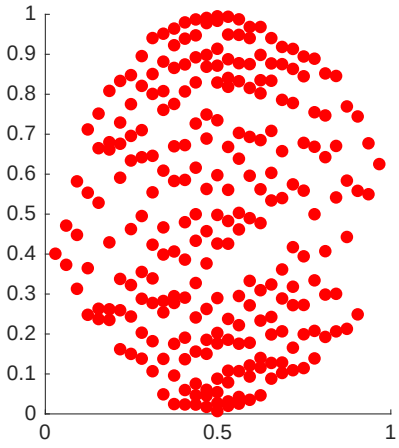

Figure 1.9: A simulation of 256 beads.

There are two significant properties that we can see from Figures 1.8 and 1.9. One is that there is a circle such that outside the circle the theoretical and empirical density of the appearance of a bead converges to 0 when the number of beads and threads tends to infinity. This curve (for other piecewise linear boundary conditions this should be other algebraic curves) is called an *arctic curve*, and the regions outside this curve are called *frozen regions* or *polar regions*.

The second one is that near the points $(\frac{1}{2}, 0)$ and $(\frac{1}{2}, 1)$ the density explodes (this will be more clear if we chose a smaller mesh in Figure 1.8). In fact, by the construction of the measure of the bead model (see Section 5.1.5), for any interval $[a, b] \subset [0, 1]$,

$$\frac{\mathbb{E}\Big(\#\{\text{beads whose vertical coordinate is within}[a,b]\}\Big)}{\#\{\text{all the beads}\}} = [a, b],$$

and the arctic curve corresponding to the boundary condition f is a circle tangent to every side of D (by Proposition 6.5.2), so at $(\frac{1}{2}, 0)$ and $(\frac{1}{2}, 1)$ the density must explode as the length of horizontal slices within the non-frozen region tends to 0.

In Chapters 5 and 6 we also consider the limit shape of a random standard (skew) Young tableau. A *Young diagram* under the French convention is a finite collection of boxes, left aligned, and the lengths of the lines are in non decreasing order from bottom to top. A *skew diagram* is the difference of two Young diagrams if one is a subset of the other. A *standard tableau* of a diagram λ is a filling of the diagram by integers from 1 to $|\lambda|$, which is the number of boxes in the diagram, such that any two different boxes are filled by different numbers and that the numbers in each rows and columns are increasing.

For convenience we turn the diagram by $\frac{\pi}{4}$. This is called the Russian convention. The terminology "column" here will refer to the boxes whose center lie on the same vertical lines. In Section 5.2.2, we define a map from bead configurations with n threads to tableaux with n columns: as the vertical position of the beads take continuous value, almost surely the coordinate of every bead is different from each other, so we can enumerate the beads in order of their vertical position from the lowest to the highest, and we fill the j^{th} box on the i^{th} column of the diagram by the order of the j^{th} bead on the i^{th} thread in a bead configuration.

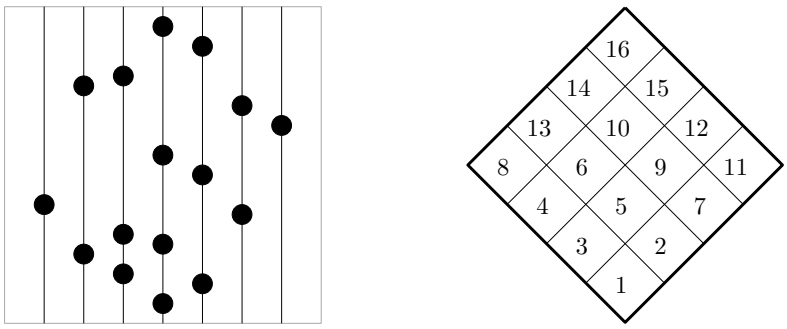

Figure 1.10: An example of mapping a bead configuration to a standard Young tableau.

If we view a random standard Young tableau as a random surface, and we fix a shape of domain but refine its interior and let the number of boxes go to infinity, then Theorem 6.6.1 proves that the random surfaces converge in probability to a surface explicitly determined by h_0, the maximizer of $Ent(.)$ for the corresponding bead model. Figure 1.11 gives a simulation of a square case but the theorem works for a general shape.

This generalizes the results in [PR07] from rectangular shapes to general (skew) shapes.

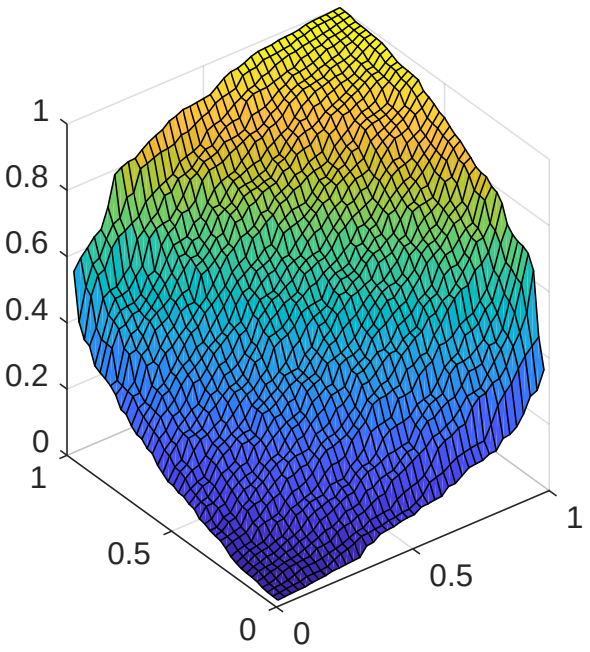

Figure 1.11: The shape of a random standard Young tableau, 40×40.

Chapter 2

Dimer model

In this chapter, we give a brief introduction to the dimer model, from basic definitions to important properties, especially those used in this thesis.

2.1 Definition

Some definitions already appear in the introductory chapter. In this chapter, we introduce the formal definitions and notions.

Let $G = (V, E)$ be a connected graph, where V is the set of vertices and E is the set of edges. A *dimer configuration* M of G is a subset of E such that every vertex $v \in V$ is incident to exactly one edge of M. We also call such a configuration a *perfect matching*. An edge in the configuration is called a *dimer*. We denote the set of all dimer configurations of G by $\mathcal{M}(G)$.

It is clear that for a finite graph G, having an even number of vertices is a necessary condition but not a sufficient condition to have dimer configurations. Throughout the thesis we focus on graphs that admit at least one dimer configuration.

We define a *weight function* $c : E \to \mathbb{R}^+$ by assigning a positive weight to every edge of G. The graph G with a weight function c is called a *weighted graph*. The weight $c(M)$ of a dimer configuration $M \in \mathcal{M}(G)$ is defined to be the product of the weights of the edges present in this configuration, *i.e.*,

$$c(M) = \prod_{e \in M} c(e).$$

The *dimer Boltzmann measure* π defined on $\mathcal{M}(G)$ is a probability measure such that the measure of a configuration M is proportional to its weight

$$\pi(M) = \frac{c(M)}{Z(G)},$$

where $Z(G)$ is the partition function defined by

$$Z(G) = \sum_{M \in \mathcal{M}(G)} c(M).$$

Readers who have basic notions of statistical mechanics will figure out at once that here if we define the energy of a configuration M as follows. The energy of an edge $e \in E$ is defined as $\mathcal{E}(e) = \ln c(e)$, and the energy of a configuration will be the sum of the energy of the edges that are present, *i.e.*,

$$\mathcal{E}(M) = \sum_{e \in M} \mathcal{E}(e) = \ln c(M).$$

Under such setting, the dimer measure is the Boltzmann measure in the framework of statistical mechanics (and this is the reason that this measure is given this name).

Throughout this thesis, we consider a dimer model embedded in a 2-dimensional surface.

2.2 Partition function

2.2.1 General planar case

The first step to understand the dimer model is to calculate the partition function $Z(G)$ explicitly. The first work is due to Kasteleyn [Kas61, Kas67] and independently to Temperley and Fisher [TF61] on planar graphs. The key object is called a *Kasteleyn matrix*.

Before introducing the Kasteleyn matrix, we need the notion of Kasteleyn orientation. A *Kasteleyn orientation* is an orientation of edges such that when traveling clockwise around the boundary of a face, the number of co-oriented edges is odd.

Kasteleyn [Kas67] proved that when the graph G is embedded in the plane, then such an orientation always exists, and this result can be generalized to any connected graph with even number of vertices and embedded in an orientable surface of genus, see [Kas63, GL99, Tes00, CR07].

For u, $v \in V$, we write $u \to v$ if uv is an edge of G and the orientation is from u to v. The *Kasteleyn matrix* K of a weighted graph G associated to a Kasteleyn orientation is a skew-symmetric weighted adjacency matrix defined by

$$K_{u,v} = \begin{cases} c(uv) \text{ if } u \to v, \\ -c(uv) \text{ if } v \leftarrow u, \\ 0 \text{ if } u \text{ and } v \text{ are not adjacent.} \end{cases}$$

To calculate the dimer partition function we need the notion of *Pfaffian*. Consider the following subset Π of the symmetric group S_{2n}:

$$\Pi = \{\sigma : \sigma(2k-1) < \sigma(2k), \sigma(2l-1) < \sigma(2l+1) \text{ for } 1 \leq k \leq n, 1 \leq l \leq n-1\}.$$

This gives a bijection to the pairings of $\{1, 2, ..., n\}$:

$$\{\{\sigma(1), \sigma(2)\}, \{\sigma(3), \sigma(4)\}, ..., \{\sigma(2n-1), \sigma(2n)\}\}.$$

The *Pfaffian* of the $2n \times 2n$ matrix K is defined by

$$\mathrm{Pf}(K) = \sum_{\sigma \in \Pi} \mathrm{sgn}(\sigma) \prod_{k=1}^{n} K_{\sigma(2k-1),\sigma(2k)},$$

and Kasteleyn [Kas61] proves that

$$|\mathrm{Pf}(K)| = Z(G).$$

2.2.2 Bipartite planar case

A graph $G = (V, E)$ is called *bipartite* if we can color the vertices V in black and white in such a way that every black vertex has only white neighbors and vice versa. This kind of graph is of specific interest in the dimer model.

To calculate the partition function of a planar bipartite graph we can use determinants. When doing this, the definition of Kasteleyn orientation is still the same as in the general case, but the Kasteleyn matrix K is a matrix indexed by black vertices in rows and white vertices in columns, defined by:

$$K_{b,w} = \begin{cases} c(bw) & \text{if } b \sim w,\ b \to w \\ -c(bw) & \text{if } b \sim w,\ b \leftarrow w \\ 0 & \text{otherwise.} \end{cases}$$

We have

$$|\det K| = Z(G).$$

To see this, we just need to use the fact that for skew-symmetric matrices, the Pfaffian is a square root of determinant. We denote the Kasteleyn matrix of Section 2.2.1 by K' to differ from that introduced in this section, and by properly labeling rows and columns we have

$$K' = \begin{bmatrix} 0 & K \\ -K^t & 0 \end{bmatrix},$$

so that

$$Z(G) = |\mathrm{Pf}(K')| = \sqrt{|\det K'|} = |\det K|.$$

As a corollary, there is a formula for the marginal probabilities [Ken97]. For any set of edges $\mathfrak{e} \subset E$, $\mathfrak{e} = \{e_1, e_2, ..., e_m\}$, the probability of occurrence of $\mathfrak{e}$ in a random dimer configuration is the sum of the weights of all configurations containing $\mathfrak{e}$ divided by the partition function. If for any i we let b_i and w_i be the black and the white vertex incident to e_i, then the probability of appearance of $\mathfrak{e}$ is equal to

$$\left| K_{b_1,w_1} K_{b_2,w_2} ... K_{b_m,w_m} \frac{\det K_{\mathfrak{e}^c}}{\det K} \right|,$$

where $K_{\mathfrak{e}^c}$ is the submatrix of K without the rows and columns corresponding to the ends of $\mathfrak{e}$. The quotient

$$\frac{\det(K_{\mathfrak{e}^c})}{\det K}$$

is equal to $\det K_{\mathfrak{e}}^{-1}$ times a sign equal to ± 1, where $K_{\mathfrak{e}}^{-1}$ is the submatrix of K^{-1} indexed by vertices corresponding to $\mathfrak{e}$. By checking the sign, we have the following formula of the probability that the set $\mathfrak{e}$ belongs to a random dimer configuration $M \in \mathcal{M}(G)$ [Ken97]:

$$\pi(\mathfrak{e} \subset M) = \left(\prod_{i=1}^{m} K_{b_i,w_i} \right) \det K_{\mathfrak{e}}^{-1}. \tag{2.1}$$

2.2.3 Bipartite toroidal case

The torus is one of the simplest non-trivial two dimensional surfaces, and a variety of results are proved for the bipartite dimer model on the torus, see Section 2.3. In this thesis, among the non planar orientable surfaces we only consider the torus. For the notation of graphs in this thesis, calligraphic letters (like $\mathcal{G}$) symbolize toroidal graphs, and normal letters (like G) symbolize planar ones or both of them (when we talk about something for both planar and toroidal graphs).

Given a toroidal bipartite graph $\mathcal{G}$, we choose a simple curve γ_x (resp. γ_y) on the dual of the graph which winds once horizontally (resp. vertically) around the torus. For every edge crossing γ_x, multiply the corresponding entry of the Kasteleyn matrix by z if its black end is on the left of γ_x and by z^{-1} if the white end is on the left, respectively w or w^{-1} for edges crossing γ_y. Such a modified Kasteleyn matrix is denoted by $K(z, w)$. The *characteristic polynomial* is defined as

$$P(z, w) = \det K(z, w). \tag{2.2}$$

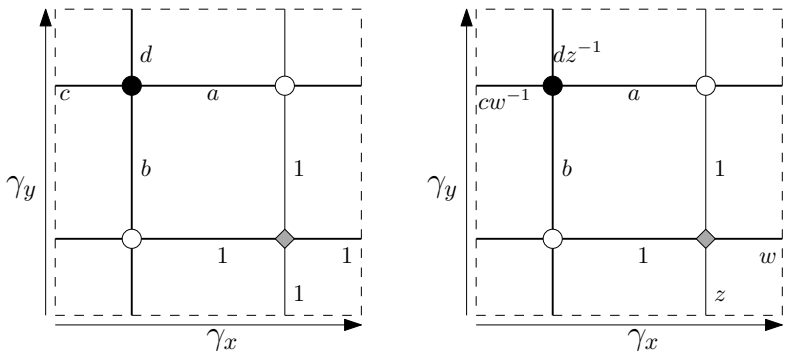

Figure 2.1: An example of adding z and w to a toroidal graph. The opposite sides are identified. This is an example of a double graph, see Chapter 3.

The dimer partition function of a graph on an orientable surface of genus g can be written as a linear combination of 2^{2g} Pfaffians [Kas63, GL99, Tes00, CR07]. For

the torus (case $g = 1$), given θ and τ in $\{0, 1\}$ which is called the parity, let $z = (-1)^\theta$ and $w = (-1)^\tau$ and we denote the corresponding Kasteleyn matrix by $K^{(\theta,\tau)}$, then after choosing a proper Kasteleyn orientation, we have the following equation for the partition function of a toroidal graph $\mathcal{G}$ [Kas63, GL99, Tes00, CR07]:

$$Z(\mathcal{G}) = \frac{1}{2}(-\det K^{(0,0)} + \det K^{(0,1)} + \det K^{(1,0)} + \det K^{(1,1)}). \tag{2.3}$$

2.3 Bipartite dimer model

As mentioned in Section 2.2.2, the bipartite graph is of specific interest when studying the dimer model. In this case there are several interesting properties. In this section we give a brief summary of several properties that are used in this thesis. Most notions here can be found in [KOS06].

2.3.1 Height function

Consider a bipartite graph G on an orientable surface. A unit flow from the white vertices of G to the black vertices is a flow of G of divergence 1 at every white vertex and -1 at every black vertex. Especially, a dimer configuration gives automatically a unit flow that takes value in $\{0, 1\}$.

Fix a reference dimer configuration M_0 and let ω_0 be the corresponding reference unit flow. Then for any unit flow ω corresponding to a dimer configuration M, the difference $\omega - \omega_0$ is a divergence-free flow. Choose a face f_0 of G as the reference face. If G is planar, then for any face f, choose γ as a dual path of G joining f_0 and f, and define the height function $h^{M,M_0}(f)$ as the total flux across γ. Given M, M_0, f and f_0, the height function is well defined and independent of the choice of γ.

When we consider the dimer model on a graph on a general orientable surface, the definition of the height function given above can give a multi-valued function. We only consider the toroidal graphs. A toroidal bipartite graph $\mathcal{G}$ lifts to a $\mathbb{Z}^2-$periodic graph, denoted by G_∞ (so that $\mathcal{G}$ is the quotient of G_∞ by $\mathbb{Z}^2$). Dimer configurations M and M_0 of $\mathcal{G}$ give rise to two periodic dimer configurations of G_∞, denoted by M_∞ and $M_{0,\infty}$. Given f_0, the height function $h^{M_\infty,M_{0,\infty}}$ is well defined. This induces a *height change* $(h_x^{M,M_0}, h_y^{M,M_0})$, which is the difference of the height of two (horizontally or vertically) neighboring copies of the same face. More precisely, if we denote by $\hat{x}$ (resp. $\hat{y}$) the vector that sends a face to its nearest copy on the right of (resp. above) it, then for any dimer configuration $M \in \mathcal{M}(\mathcal{G})$ and any face f, we define

$$h_x^{M,M_0} = h^{M_\infty,M_{0,\infty}}(f + \hat{x}) - h^{M_\infty,M_{0,\infty}}(f),$$

$$h_y^{M,M_0} = h^{M_\infty,M_{0,\infty}}(f + \hat{y}) - h^{M_\infty,M_{0,\infty}}(f).$$

This is independent of the choice of f_0.

2.3.2 Gauge equivalence and magnetic field

Throughout this thesis we take the following convention: for any two adjacent vertices u and v on a graph, uv is the non-directed edge relating them, and (u, v) is a directed one from u to v.

For any graph G, let $\Omega^k(G)$ be the linear space of $k-$forms on G, where $k \in \{0, 1, 2\}$. The $0-$forms are functions on vertices. The $1-$forms are functions f on directed edges such that for any (u, v) and (v, u) being the same edge with opposite orientations we have $f(u, v) = -f(v, u)$. The $2-$forms are that defined on oriented faces. We take d as the standard differential operator.

Consider the energy function $\mathcal{E}$ defined in Section 2.1, where recall that the energy of an edge e is defined as $\mathcal{E}(e) = -\ln c(e)$ and for any dimer configuration M its energy is defined as $\mathcal{E}(M) = \sum_{e \in M} \mathcal{E}(e)$.

Such an energy function $\mathcal{E}$ can be viewed as a $1-$form of G: for every edge $e = wb \in E$, where w is a white vertex and b is a black one, define $\mathcal{E}(w, b) = -\ln c(wb)$ and $\mathcal{E}(b, w) = \ln c(wb)$. Two energy functions $\mathcal{E}_1$ and $\mathcal{E}_2$ are said to be *gauge equivalent* if there exists a function $f \in \Omega^0(G)$ such that

$$\mathcal{E}_1 - \mathcal{E}_2 = df. \tag{2.4}$$

If so, then for every directed edge (w, b), $\mathcal{E}_1(w, b) - \mathcal{E}_2(w, b) = f(b) - f(w)$, so two energies are gauge equivalent if and only if around every cycle the integral is the same. If two energy functions $\mathcal{E}_1$ and $\mathcal{E}_2$ are gauge equivalent and differ by df, then for any dimer configuration M,

$$\mathcal{E}_1(M) - \mathcal{E}_2(M) = \sum_b f(b) - \sum_w f(w),$$

which is independent of M, so they give the same dimer measure.

Given a toroidal graph $\mathcal{G}$ with $|V|$ vertices, $|E|$ edges and $|F|$ faces, the dimension of 1-forms (the energies) is equal to $|E|$, and that of the 0-forms is equal to $|V|$. By Equation (2.4) and by Euler's formula, the degree of freedom of the gauge equivalent classes is equal to

$$|E| - (|V| - 1) = (|F| - 1) + 2. \tag{2.5}$$

The right hand side of Equation (2.5) has an interpretation by homology classes: for any two gauge equivalent 1-forms $\mathcal{E}_1$ and $\mathcal{E}_2$, the property that integral of $\mathcal{E}_1 - \mathcal{E}_2$ is 0 along every cycles is equivalent to that the integral is 0 around every face except the last one (which is automatical 0) and along two other non-trivial cycles. We fix the parts corresponding to faces and parameterize the other two degrees of gauge classes by introducing the *magnetic field* [KOS06]. Denoted by $B = (B_x, B_y) \in \mathbb{R}^2$, the magnetic field is the integral of $\mathcal{E}$ along a cycle γ_x (resp. γ_y) which winds around the torus once horizontally (resp. vertically). In practice, this can be done by the following manipulation of the weight of the edges: for every edge crossing γ_x (resp. γ_y), multiply its weight by $e^{\pm B_x}$ (resp. $e^{\pm B_y}$), where the signs are positive if the black vertex is on the left of γ_x (resp. γ_y) and negative if on the left side (*i.e.* in Figure 2.1 take $z = e^{B_x}$ and $w = e^{B_y}$).

2.3.3 Amoeba

In this section we consider the asymptotic behavior of the dimer measure on toroidal graphs. Again, a toroidal graph $\mathcal{G}$ can be lifted to a $\mathbb{Z}^2-$periodic planar graph G_∞. Its quotient graphs are given by $\mathcal{G}_N = G_\infty/N\mathbb{Z}^2$ so $\mathcal{G}_1 = \mathcal{G}$. We also consider a magnetic field as follows: for every edge of $\mathcal{G}_N$, if its copy in G_∞ crosses γ_x (resp. γ_y), multiply its weight by $e^{\pm B_x}$ (resp. $e^{\pm B_y}$). We remark that this is gauge-equivalent to choosing two curves $\gamma_{x,N}$ and $\gamma_{y,N}$ in $\mathcal{G}_N$ and multiplying the weights of the edges crossing them respectively by e^{NB_x} and e^{NB_y}.

Denote by P_N the characteristic polynomial of $\mathcal{G}_N$. It can be calculated via [KOS06]

$$P_N(z,w) = \prod_{\zeta^N=z}\prod_{\omega^N=w} P(\zeta,\omega),$$

where we recall that P is the characteristic polynomial defined by Equation 2.2.

By Equation (2.3), if we denote by $Z(\mathcal{G}_N)$ the partition function of the dimer model on $\mathcal{G}_N$, then for a properly chosen Kasteleyn orientation,

$$Z(\mathcal{G}_N) = \frac{1}{2}\big(-Z^{(0,0)}(\mathcal{G}_N) + Z^{(0,1)}(\mathcal{G}_N) + Z^{(1,0)}(\mathcal{G}_N) + Z^{(1,1)}(\mathcal{G}_N)\big),$$

where

$$Z^{(\theta,\tau)}(\mathcal{G}_N) = \prod_{\zeta^N=(-1)^\theta}\prod_{\omega^N=(-1)^\tau} P(\zeta,\omega).$$

When N is large, this sum, when taking a logarithm and normalizing by N^2, can be approximated by an integral [KOS06]:

$$\lim_{N\to\infty}\frac{\log Z(\mathcal{G}_N)}{N^2} = \iint_{\mathbb{T}^2}\log P(z,w)\frac{dz}{2\pi iz}\frac{dw}{2\pi iw}, \tag{2.6}$$

and we define this limit as the *free energy per fundamental domain* of the dimer model.

The *Ronkin function* is defined as the following integral:

$$F(x,y) = \iint_{\mathbb{T}^2}\log P(e^x z, e^y w)\frac{dz}{2\pi iz}\frac{dw}{2\pi iw}. \tag{2.7}$$

If we compare this to Equation (2.6) and considering that adding magnetic field is just taking the corresponding values for z and w in the characteristic polynomial, we can see that Equation (2.7) is just the free energy per fundamental domain with a magnetic field (B_x, B_y) if we take x (resp. y) to be the magnetic field B_x (resp. B_y). From now on we use the notation $F(B_x, B_y)$ to denote the free energy with magnetic field (B_x, B_y).

The *amoeba* of a polynomial P is the image of its *spectral curve* $P(z, w) = 0$ under the map

$$(z, w) \to (\log|z|, \log|w|).$$

Figure 2.2 shows the amoeba of the polynomial $P(z, w) = 11+5/w+2w+3/z+z$, which is the characteristic polynomial of the graph corresponding to Figure 2.1 where we take the parameters to be $a = 5, b = 3, c = 2$ and $d = 1$.

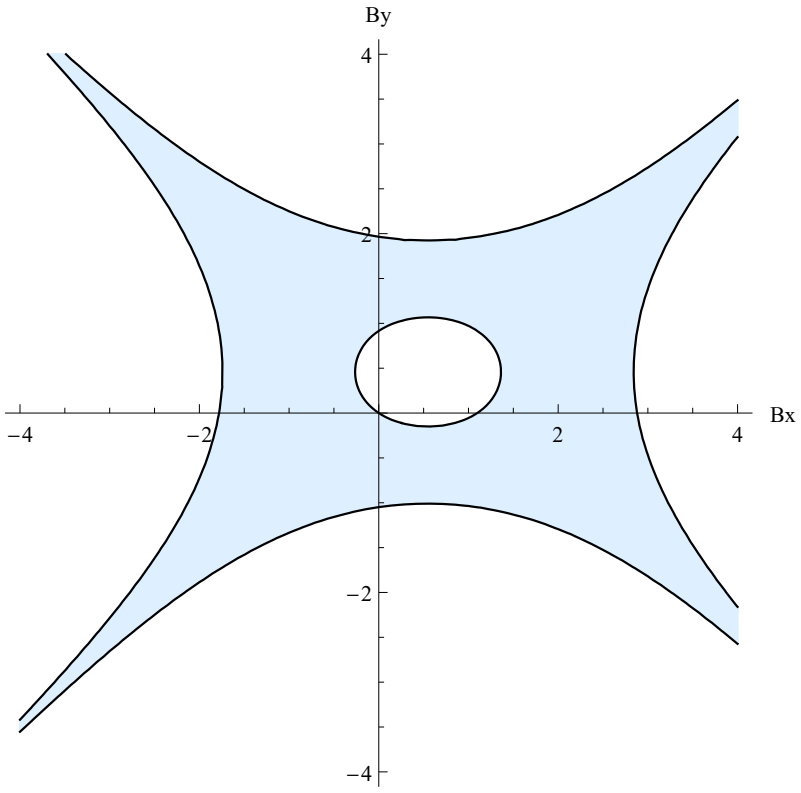

Figure 2.2: The amoeba.

2.3.4 Ergodic Gibbs measure, surface tension and phases

For the dimer model, a probability measure is called a *Gibbs measure* if conditioned to fixing the matching in an annular region, the probability measure of a matching inside the region is independent of that of outside the region, and the probability of any interior matching is proportional to its weight. A measure is *ergodic* if it is invariant and ergodic under the action of $\mathbb{Z}^2$.

For any ergodic dimer Gibbs measure π, let $s = \mathbb{E}(h_x)$ and $t = \mathbb{E}(h_y)$. The pair (s, t) is called the slope of π. Now for any pair $(s, t) \in \mathbb{R}^2$ and any $n \in \mathbb{N}^*$, define $\mathcal{M}_{s,t}(\mathcal{G}_N)$ as the dimer configurations of $\mathcal{G}_N$ whose height change is $(\lfloor ns \rfloor, \lfloor nt \rfloor)$. Denote by $\pi_N(s, t)$ the conditional measure of π on $\mathcal{M}_{s,t}(\mathcal{G}_N)$, then for each (s, t) such that $\mathcal{M}_{s,t}(\mathcal{G}_N)$ is nonempty for sufficiently large N, as $N \to \infty$, the measures $\pi_N(s, t)$ converge to an ergodic Gibbs measure of slope (s, t). Also, the dimer measures of

$\mathcal{G}_N$, denoted by π_N, converge to an ergodic Gibbs measure of some slope (s_0, t_0), which is the limit of $\pi_N(s_0, t_0)$ [She03, KOS06].

The *Newton polygon* of the characteristic polynomial $P(z, w)$, denoted by $N(P)$, is the convex hull in $\mathbb{R}^2$ of the exponents of the monomials in $P(z, w)$. Points lying within the $N(P)$ form the set of possible slopes of the ergodic Gibbs measure. We define

$$Z_{s,t}(\mathcal{G}_N) = \sum_{M \in \mathcal{M}_{s,t}(\mathcal{G}_N)} c(M),$$

and the *surface tension* (or *free energy*) is defined, for any $(s, t) \in N(P)$, by the following formula:

$$\sigma(s, t) = -\lim_{N\to\infty} \frac{1}{N^2} \log Z_{s,t}(\mathcal{G}_N).$$

The entropy function *ent* is defined to be $-\sigma$. The limiting slope (s_0, t_0) is the (unique) slope that maximize the entropy (minimize the surface tension).

Since the free energy $F(B_x, B_y)$ is the limit of the logarithm of the partition function of the dimer measure on $\mathcal{G}_N$ with magnetic field (B_x, B_y) normalized by N^2, we have the following Legendre transform:

$$F(B_x, B_y) = \max_{(s,t)\in N(P)} (-\sigma(s, t) + sB_x + tB_y),$$

and considering the convexity we also have

$$\sigma(s, t) = \max_{(B_x,B_y)\in\mathbb{R}^2} (-F(B_x, B_y) + sB_x + tB_y).$$

By general properties of the Ronkin function of a polynomial, the free energy F is linear on every component of the complement of the amoeba, and strictly convex in the interior of the amoeba. The gradient of the surface of the free energy corresponds to the slope in the Newton polygon, and the facets (the components of the complimentary parts of the amoeba) correspond to the integer points in the Newton polygon. This yields significant different phenomenons on the points in unbounded complementary components of the amoeba, bounded ones, and the region in the interior of amoeba. For (B_x, B_y) lying in the closure of an unbounded complementary component of the amoeba, the dimer measure is said to be in a *frozen phase*. In this case, the height differences are deterministic for some faces. For those lying in the closure of a bounded complementary component of the amoeba, the measure is in a *gaseous phase*, where the height variance is bounded and the edge-edge correlations decay exponentially as the distance of the edges increases to infinity. For points lying in the interior of the amoeba, the height variance is of logarithm order, and the edge-edge correlations decay polynomially.

2.4 A variational principle for the dimer model

In this section we consider dimer configurations of an increasing sequence finite graphs G_n exhausting a periodic bipartite graph denoted by G_∞. Alternatively, we

can think of tilings of a sequence of regions, and typically tiling a finite domain by dominos or lozenges. Simulations show that there exist limit shapes when the sizes of the domains go to infinity while keeping the asymptotic boundary conditions. Proofs and explicit calculations are made for particular cases, for example, tiling an Aztec diamond by dominos [CEP96], tiling a hexagonal domain by lozenges [CLP98]. More recent works on tilings include [Pet14, Pet15, DM15, BK17].

The general principle is given in [CKP01], where the authors give explicit calculations for domino tilings but the results are true for more general cases. This section is a summary of their results.

An equivalent way of thinking of an increasing sequence of graphs G_n is as follows. Consider a fixed domain D with a function h^∂ defined on ∂D (under some constraint to be specified here below). For any $n \in \mathbb{N}^*$, consider a subgraph of the mesh $\frac{1}{n}G_\infty$ such that its boundary is within $O(\frac{1}{n})$ of ∂D and its height function on any face incident to the boundary of the graph (which is fixed by the boundary of the graph up to a constant) is within $O(\frac{1}{n})$ of the value of h^∂ on any point on ∂D of distance $O(\frac{1}{n})$ from that face.

For any $n \in \mathbb{N}^*$, and for any height function on the graph normalized by n, the difference of the heights of any two faces divided by their distance should be within Newton's polygon of the characteristic polynomial. Thus, the normalized height functions are Lipschitz, and in the limit $n \to \infty$ we can approximately view them as surfaces, and the slope (s, t) (since a Lipschitz function is differentiable almost everywhere) should be inside the Newton's polygon whenever it exists. We ask the boundary function h^∂ in the previous paragraph to admit at least one extension h on D such that h verifies the corresponding Lipschitz condition.

Recall that the entropy $ent(s, t)$ of a periodic graph G_∞ is the limit as $n \to \infty$ of the normalized logarithm of the partition function of the dimer configurations of $\mathcal{G}_N = \mathcal{G}_\infty/(N\mathbb{Z})^2$ and of slope (s, t). The following results are proved in [CKP01]:

- There is a unique piecewise differentiable height function h_0 on D which coincides with h^∂ on ∂D and maximizes the entropy $Ent(.)$ defined by

$$Ent(h) = \iint_D ent\left(\frac{\partial h}{\partial x}, \frac{\partial h}{\partial y}\right) dxdy.$$

- For any function $h : D \to \mathbb{R}$ verifying the Lipschitz condition and that $h|_{\partial D}$ is within a δ-neighborhood of h^∂, the partition function of the configurations such that the height function is within a δ-neighborhood of h, after taking logarithm and normalization by n^2, is proportional to

$$Ent(h) + o(1)$$

  as $\delta \to 0$.

Combining the two arguments above, it is clear that when $n \to \infty$, then with probability tending to 1 the normalized height functions of the configurations approximate h_0 which is the maximizer of the entropy function $Ent(.)$.

In Chapter 6 of this thesis we will give a modified version of this variational principle for some scaling limit of a lozenge tiling model.

2.4.1 Solution of the variational principle

The last section shows that the problem of finding the limit shape of dimer configurations of a finite domain can be reduced to a problem of finding the height function h that maximizes the entropy $Ent(h)$ or minimizes the surface tension:

$$\int_D \sigma(\nabla h(x,y))dxdy.$$

A systemical way of doing this is given by [KO07]. In this part of the thesis we give a summary of their results which will be useful in Chapter 6.

Consider a $\mathbb{Z}^2$-periodic bipartite graph G whose characteristic polynomial is P and consider a feasible scaled domain D. In practice we let the polynomial be $P(z,w) = z + w - 1$, which is the dimer characteristic polynomial for the honeycomb lattice, and we suppose that D is a polygon whose boundary is made up of the edges clockwise (or anticlockwise) repeated in the directions of the edges of the honeycomb lattice. So there will be three slopes, and without loss of the generality we take them as ∞, -1 and 1. We note this condition by (†). Especially, those polygons whose edges are in these three directions but not necessarily in the required order can be viewed as polygons satisfying Condition (†) but with certain edges reduced to zero, see Figure 2.3.

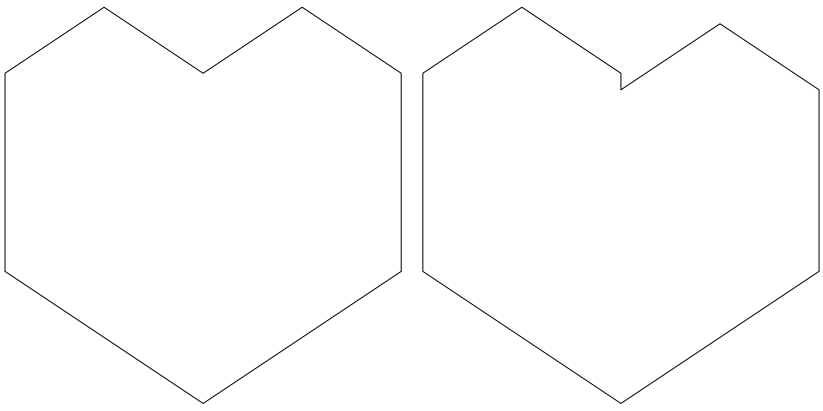

Figure 2.3: A polygon not verifying Condition (†) and a nearby polygon verifying that condition.

The surface tension, as an analytic and strictly convex function in the liquid region, should satisfy the Euler-Lagrange equation in the liquid region:

$$\mathrm{div}(\nabla\sigma \circ \nabla h) = 0.$$

We further more consider a more general version

$$\mathrm{div}(\nabla\sigma \circ \nabla h) = c,$$

where c is a given real constant arising from the volume constrained minimization problem

$$h : h \text{ minimizes } \int_D \sigma(\nabla h(x,y))dxdy + c\int_D h(x,y)dxdy. \tag{2.8}$$

The authors of [KO07] prove that, up to a constant, the solution of (2.8) is given by

$$\nabla h = \frac{1}{\pi}(\arg w, -\arg z), \tag{2.9}$$

where $\arg w$ and $\arg z$ are taken to be on one branch, z and w are two functions $D \to \mathbb{C}$, parameterized by c verifying $P(z,w) = 0$, and furthermore, for $c \neq 0$, there exists an analytic function Q of two variables such that

$$Q(e^{-cx}z, e^{-cy}w) = 0$$

in the liquid region, and when $c = 0$ there is an analytic function Q_0 such that

$$Q_0(z,w) = xzP_z + ywP_w.$$

So the problem of finding the limit shape for every c is reduced to a problem of finding such an analytic function Q which verifies the above system. We refer to the system of P, Q (or Q_0), z and w given above by the symbol ($\diamondsuit$).

In the case that $P(z,w) = z + w - 1$ and D being a feasible simply connected polygon of $3d$ sides, Q is proved to be an algebraic curve of degree d and genus 0. The arctic curve C is shown to be a subset of the locus of the points where the system ($\diamondsuit$) has a double real root given by discriminant $R(e^{-cx}, e^{-cy}) = 0$. The arctic curve C is tangent to every linear piece of the polygon. In the case of the appearance of a non-convex vertex, the position that R meets a piece of the boundary can occur on the extension line. This produces a cusp singularity. A $3d$ sides polygon which verifies Condition (†) should have $d-2$ non-convex corner. This implies that R is of degree $2d-2$.

The above constraint (the real discriminant curve should be tangent to the sides of the boundary) provides $3d$ incidence conditions to the degree d polynomial Q, and the degree of freedom is $3d-1$ (the constraint that the polygon is closed shows that one condition is redundant). This gives a finite set of possibilities.

Among these possibilities it remains to choose the unique one. This can be done by using the following method. When the given constant $c \to \pm\infty$, the solution h^* of (2.8) will tends to those minimizing/maximizing the enclosed volume. For example, for the domain D given in Figure 2.3, such surfaces are as in Figure 2.4.

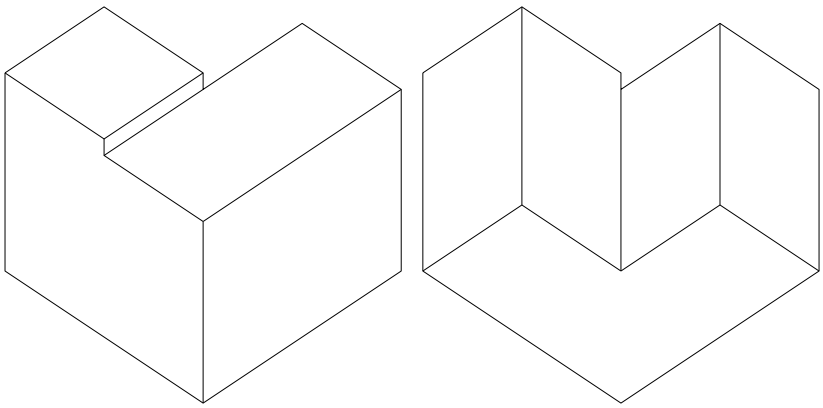

(a) The full surface. (b) The empty surface

Figure 2.4: The limiting surfaces corresponding to $c \to \pm\infty$.

This limiting behavior helps us to eliminate the faulty possibilities of R (and Q).

Here are some other remarks which are also taken from [KO07] and should be good to be included here. If for every vertex of the corner locus (interior edges in the figures above) we add 1 or 2 rays in the directions parallel to the boundary edges, then we get a genus 0 degree d tropical curve. For a general introduction on tropical geometry, we refer the readers to [Mac12].

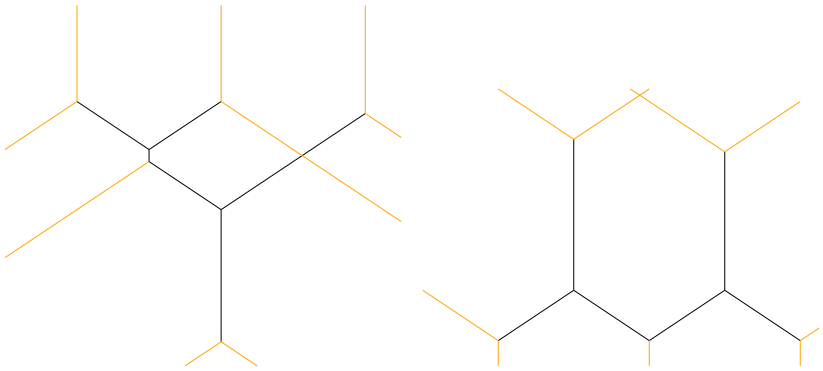

Figure 2.5: The tropical curves corresponding to Figure 2.4. The black edges are the existing corner locus, and the orange rays are newly added.

The tropical curve locally can be viewed as a limit of the amoeba, and the three rays at each vertex in the figures are the limits of the tentacles. The complement of the tropical curve is composed of C^2_{d+2} chambers, corresponding to the lattice points in the Newton's polygon of Q.

Chapter 3

Spanning trees, cycle rooted spanning forests and the dimer model

In this chapter of the thesis, we focus on spanning trees/spanning forests on planar graphs and cycle rooted spanning forests ($CRSF$) on toroidal graphs. These classical mathematical objects are shown to be closely related to the dimer model by Temperley's bijection. More precisely, planar dimer configurations correspond to planar spanning trees, and toroidal dimer configurations correspond to $CRSF$.

Section 3.2 gives a summary of Wilson's algorithm which not only gives a way to efficiently generate random spanning trees but also reveals their intrinsic properties. Section 3.3 gives a summary of [Pem91, BP93], later generalized by [BLPS01], where the authors prove a series of results on the limiting behavior of spanning trees.

We are interested in the following questions: what is the limiting behavior of $CRSF$? Do the same procedures as in [Pem91, BLPS01] still apply? We will answer this in Chapter 4, and readers can view the current chapter as a preliminary introduction.

3.1 Definitions

A *tree* on a given graph G is a connected, contractible union of edges. The tree is called a *spanning tree* if it covers every vertex of G. If every edge is directed and every vertex of G except one has exactly one outgoing edge, then the spanning tree is called an *oriented spanning tree*(OST). The only vertex having no outgoing edge is called the *root* of the tree.

We assign a weight function to this graph. Furthermore, the weight function can be defined on the directed edges, meaning that for any (non-directed) edge $e = uv$, $c(u, v)$ can be different from $c(v, u)$, where we recall that (u, v) is a directed edge from u to v. In particular, if for any edge uv we have $c(u, v) = c(v, u)$, then the

graph is said to be non-directed.

The weight of an oriented spanning tree is the product of the edges present, and the weight of a non-oriented tree is the sum of the weights of every possible orientation (*i.e.* for every possible root). We will consider the weighted measure on oriented or non-oriented spanning trees, where the probability of a configuration is proportional to its weight. In particular, if every edge is equally weighted, then every spanning tree has the same probability of occurrence, and in this case we call the weighted measure as the *uniform measure*.

Similar to the definition of spanning trees, a *cycle-rooted spanning forest* (*CRSF*) of a graph G is a union of edges covering every vertex and every connected component has exactly one cycle which is called *root cycle*. If edges are directed such that every vertex has exactly one outgoing edge, then we call it an *oriented cycle-rooted spanning forest* (*OCRSF*). Clearly, in a *CRSF*, every edge not on the root-cycles is oriented towards one root-cycle.

In this thesis, we consider only the *CRSF* and *OCRSF* on toroidal graphs which furthermore have the following property: the cycles are non contractible on the torus. So the root-cycles in a configuration are all parallel in the sense of homology.

Suppose that F is an *OCRSF* of a toroidal graph $\mathcal{G}$. Then on $\mathcal{G}^*$, non-directed edges that do not cross F form a non-oriented cycle-rooted spanning forest. If we let every edge not on cycles be directed toward the cycle which belongs to the same connected component, and for every cycle we choose an arbitrary orientation, we get an *OCRSF* of $\mathcal{G}^*$. We denote this by F^*, and we say that F and F^* are *dual*. The pair (F, F^*) is an *OCRSF-pair*. Denote the set of *OCRSF*-pairs of $\mathcal{G}$ and $\mathcal{G}^*$ by $\mathcal{F}(\mathcal{G}, \mathcal{G}^*)$. In Section 4.1 we define a weighted measure on *OCRSF* or *CRSF* naturally yielded by Temperley's bijection defined in Section 3.4.

3.2 Wilson's Algorithm

Given an oriented finite planar graph G with weight function c, a random spanning tree of G with probability measure proportional to weights is automatically related, by Wilson's algorithm [Wil96, BLPS01], to a nearest neighbor random walk, which is a Markov chain X_n on G with transition probability given by

$$p_{u,v} = \mathbb{P}(X_{n+1} = v | X_n = u) = \frac{c(u,v)}{\sum_{v' \sim u} c(u,v')}$$

if vertices u and v are adjacent and 0 if not.

Let $p = (v_0, v_1, ..., v_n)$ be a path on G. The *loop erasure* of p is a path $LE(p) = (u_0, u_1, ..., u_m)$, such that $u_0 = v_0$, and for any $j \in \mathbb{N}*$, conditioned on u_j, if k is the largest number such that $v_k = u_j$, then $u_{j+1} = v_{k+1}$.

Wilson's algorithm [Wil96]: for any finite graph G and root r chosen as a vertex of G, the algorithm constructs a growing sequence of trees $\big(T(i)\big)_i$ from $T(0) = r$, and once $T(i)$ is generated, we pick any vertex v not in $T(i)$, start a random walk

X_n starting at v and end it once it hits $T(i)$. The new tree $T(i+1)$ is defined as $T(i)$ plus the loop erasure of the path of X_n. Continue this process until every vertex is in the tree. The constructed spanning tree has a probability proportional to its weight [Wil96, BLPS01].

3.3 Limiting behavior of spanning trees

In [Pem91], Pemantle considers the following problem in $\mathbb{Z}^d$: let $G_1, G_2, ...$ be an increasing sequence of graphs exhausting $\mathbb{Z}^d$, and consider the spanning trees of G_n with uniform measures, $n \in \mathbb{N}^+$. He shows that, when $n \to \infty$, the measures converge to a spanning tree if the dimension d is not bigger than 4, and when d is not less than 5 the measures converge to a measure on spanning forests with an infinite number of connected components.

The convergence of the measures is proved by an analog to electric networks. To study the connectivity, the author uses Wilson's algorithm. The probability that two vertices v_1 and v_2 are connected in $\mathbb{Z}^d$ under the limiting measure is given by

$$\lim_{l\to\infty} \lim_{n\to\infty} \mathbb{P}_n(v_1 \text{ and } v_2 \text{ are connected within a ball of diameter } l), \tag{3.1}$$

where $\mathbb{P}_n$ is the probability for the events on G_n under the uniform spanning tree measure. By Wilson's algorithm, for any $l \in \mathbb{N}^*$ and for any $n \in \mathbb{N}^*$ large, the probability of the right hand side of Equation (3.1) is equal to picking a vertex v_0 on the boundary of G_n, starting a *LERW* at v_1 which ends at v_0, and starting another random walk ending at the first *LERW*, and computing the probability that they meet within a ball of diameter equal to l. In the limit $n \to \infty$, this probability tends to that of a random walk starting from v_2 meeting a *LERW* starting from v_1 within a ball of diameter l. The last probability is shown to be 1 for $d \leq 4$ and strictly less than 1 when $d \geq 5$.

For the limiting measure, in [BP93] the authors prove a transfer impedance theorem, which shows that the uniform spanning tree measure of $\mathbb{Z}^d$ is a determinantal process whose kernels are differences of Green's functions. We will give a similar result for weighted measures of *CRSF* in Section 4.2.5.

3.4 Temperley's bijection

Temperley [Tem74] first introduced a bijection on the square grid between spanning trees and dimer configurations. It was generalized by Burton and Pemantle in [BP93] to unweighted planar graphs. Kenyon, Propp and Wilson [KPW00] generalized this construction to directed weighted planar graphs by providing a measure preserving bijection between oriented, weighted spanning trees of the graph and dimer configurations of its double graph. The construction also applies to graphs on other surfaces. In this section, we give a summary of the construction and its

consequences on both toroidal graphs and on planar graphs. This is for later use in Chapter 4.

3.4.1 Basic structures

Let G be a connected graph embedded in a 2-dimensional surface, and we take G^* as its *dual*, whose vertices correspond to faces of G and two vertices are joined by an edge of G^* if and only if these two faces are neighboring in G (G is also called the *primal*). If we take the union of G and G^*, color their vertices in black (in the figures we use grey diamonds to represent vertices of G^* so that readers can differ vertices of G and G^*), take the intersections of the primal and dual edges as vertices and color them in white, then the new graph we obtain is denoted by G^d and called the *double graph* of G. The graph G^d is *bipartite*: every black vertex of G^d has only white neighbors and vice-versa.

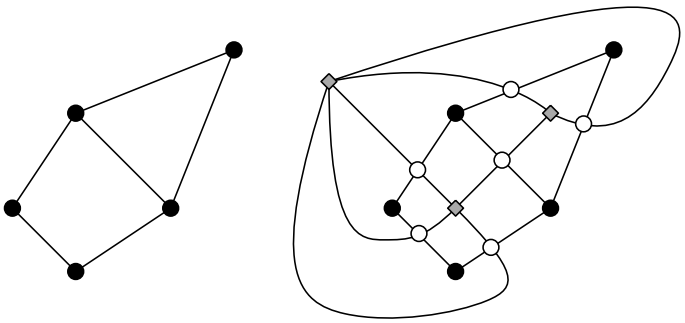

Figure 3.1: Graph G and its double G^d.

Consider weight functions on G, G^* and G^d. Throughout this thesis, we always suppose that G and G^* are directed and G^d is non-directed. There is a natural bijection between the weight functions on G, G^* and those on G^d. For every directed edge (u, v) of G or G^*, on G^d let w be the white vertex between u and v (as in Figure 3.2). For any weight function c on edges of G and G^*, we define a weight function c on edges of G^d (we use the same letter c, and in general there is no ambiguity), where we let $c(uw) = c(u, v)$ and $c(vw) = c(v, u)$. Reciprocally, any weight function on G^d defines a weight function for G and G^* in the same way. This bijection is to be used in the setting of Temperley's bijection in Section 3.4.2.

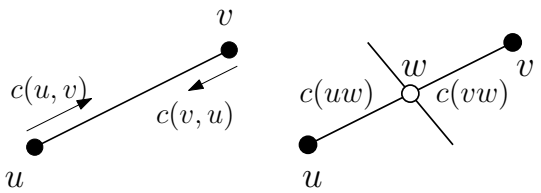

(a) Weights of G. (b) Weights of G^d.

Figure 3.2: Weights.

3.4.2 The bijection

We first consider the bijection on the torus. Given a toroidal graph $\mathcal{G}$, and for any dimer configuration $M \in \mathcal{M}(\mathcal{G}^d)$, we prolong every edge in M by one step (see Figure 3.3) and we get a subset of the edges of $\mathcal{G}$ and $\mathcal{G}^*$. Moreover, we let such edges be directed in the same direction as we prolong them, and denote the set of such directed edges of $\mathcal{G}$ by F and those of $\mathcal{G}^*$ by F^*. It is easy to check that F and F^* form an *OCRSF*-pair.

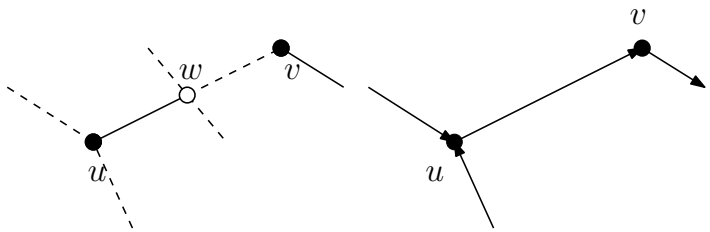

(a) Part of a dimer configuration.

(b) Part of an *OCRSF*.

Figure 3.3: Temperley's bijection.

Conversely, any *OCRSF*-pair (F, F^*) of $\mathcal{G}$ and $\mathcal{G}^*$ induces a dimer configuration $M \in \mathcal{M}(\mathcal{G}^d)$ by the same rule. This gives a bijection between $\mathcal{M}(\mathcal{G}^d)$ and $\mathcal{F}(\mathcal{G}, \mathcal{G}^*)$.

In the case of a planar graph G, choose a vertex of G named v_0 and a face f_0 incident to v_0 and denote by $G^d(v_0, f_0)$ the subgraph of G^d where we remove v_0, f_0 and all edges incident to them. Temperley's bijection is between $\mathcal{M}(G^d(v_0, f_0))$ and *OST*-pairs (T, T^*) of G and G^* rooted on v_0 and f_0.

The weight of (F, F^*) (resp. (T, T^*)) is defined as the product of the weights of all edges present and this gives rise to a weighted measure on *OCRSF*-pair of $\mathcal{G}$ and $\mathcal{G}^*$ (resp. *OST*-pairs of G and G^*). If we take the weight setting as in Figure 3.2, such a bijection is measure preserving.

3.4.3 Height function on the spanning trees, spanning forests and *CRSF*s induced by Temperley's bijection

The height function of the dimer model defined in Section 2.3.1 is one among several equivalent ways of defining the height function. Here we take another definition from [KPW00] which is useful when we consider Temperley's bijection. It induces a height function defined for the spanning trees, spanning forests and *CRSF*.

Consider a graph G embedded in $\mathbb{R}^2$ or the torus as well as its double graph G^d. Every face of G^d is a quadrilateral, and when we say a *diagonal* of a face we mean the one linking two opposite black vertices. We define height functions defined on these diagonals. Given a dimer configuration M, we choose a reference face so the

diagonal of this face has 0 height, then we prolong this to its neighboring diagonals by the turning angle without passing dimers.

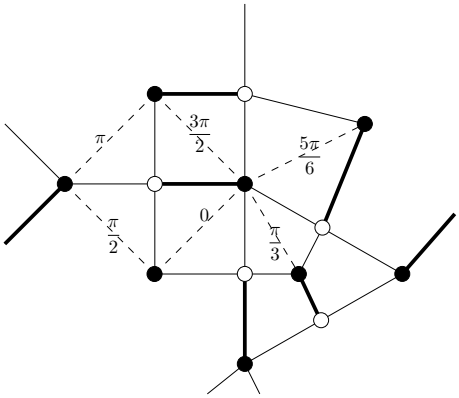

Figure 3.4: Height function of a dimer configuration before normalization by 2π.

If G is planar, this can be prolonged to the whole plane [KPW00]. The height $h^M(.)$ of a face is defined as the height of its diagonal normalized by 2π. Note that the height function so defined depends on the embedding of the graph in the plane. If the graph is toroidal, we write $\mathcal{G}$ in this case, and a configuration $M \in \mathcal{M}(\mathcal{G}^d)$ gives rise to a periodic dimer configuration on G^d_∞ which is the lift of $\mathcal{G}^d$ to the whole plane. The height function of this periodic configuration induces a height change (h^M_x, h^M_y), which is the difference of the height of two (horizontally or vertically) neighboring copies of the same vertex.

Compared to the height function h^{M,M_0} defined in Section 2.3.1, h^M defined as above does not depend on the choice of a reference dimer configuration M_0 but depends on the precise geometric embedding of the graph. Moving a single edge will change the height h^M of its neighboring faces but won't affect the others. In particular, changing the embedding of the graph doesn't affect the height change (h^M_x, h^M_y). Moreover, these two definitions of height functions are related by:

$$h^{(M,M_0)} = h^M - h^{M_0}$$

for any M and M_0. In the remainder of this chapter and Chapter 4, when we speak of height, we use the first definition h^M by default.

If Temperley's bijection maps a dimer configuration M to an OST-pair (T, T^*) or an $OCRSF$-pair (F, F^*), the height function h^M has a natural interpretation using the *winding* of T, which is defined, for a finite directed path on G, as the total angle of the left turns minus the right turns along this path.

A *branch* $\gamma = (v_1, ..., v_{r+1})$ of an oriented tree T is a finite directed path of T co-oriented or anti-oriented with the orientation of T (either every edge v_iv_{i+1} is oriented from v_i to v_{i+1} or from v_{i+1} to v_i).

Denote the white vertex between v_i and v_{i+1} in G^d by w_i. Let $(f_1, ..., f_r)$ be the faces of G^d lying on the left of γ and every f_i is incident to v_iw_i (note that

f_i and f_{i+1} are not neighboring in G^d). For any $i \in \{1, ..., r\}$, define $\alpha^T(f_i)$ as the counterclockwise angle from the vector $v_i e_i$ to the diagonal of f_i renormalized by 2π. Note that for given T, $h^M(f_i) - \alpha^T(f_i)$ only depends on the vertex v_i and doesn't depend on the choice of path (or face).

Theorem 3 in [KPW00] proves that under Temperley's planar bijection, the winding of a branch $\gamma = (v_1, ..., v_r)$ normalized by 2π is equal to

$$\big(h^M(f_r) - \alpha^T(f_r)\big) - \big(h^M(f_1) - \alpha^T(f_1)\big).$$

To simplify notations, we define a height function h^T defined on vertices of G: for any T and $v \in T$, chose a branch passing v, define $h^T(v)$ as $h^M(f) - \alpha^T(f)$ where f is a face incident to v as above. So Theorem 3 in [KPW00] says that going along a branch, the change of h^T is equal to the renormalized winding.

On the torus, Temperley's bijection maps a dimer configuration M of $\mathcal{G}^d$ to an *OCRSF* pair (F, F^*) of $\mathcal{G}$ and $\mathcal{G}^*$. The height change (h_x^M, h_y^M) is determined by the homology class of (F, F^*). This fact is already showed in [DG15]. Here we give another proof because some geometric facts revealed in this proof are useful in the subsequent parts of this thesis (Section 4.2.3).

Suppose that F or F^* has k connected components, each component containing a root-cycle of homology class $\pm(m, n)$, $m, n \in \mathbb{Z}$, where we choose m to be non-negative, and when $m = 0$ we choose n to be positive. Note that m and n are relatively prime. Suppose that there are k_1 (resp. k_2) primal (resp. dual) root-cycles of homology class (m, n), then:

Proposition 3.4.1. [DG15] *If we let M be the dimer configuration corresponding to (F, F^*) by Temperley's bijection, then the height change of M is equal to the signed sum of homology classes of OCRSF-pairs of $\mathcal{G}$ and of $\mathcal{G}^*$. If we take the notation above, then*

$$h_x^M = -n(k - k_1 - k_2),$$
$$h_y^M = m(k - k_1 - k_2).$$

Proof. The graph $\mathcal{G}$ can be lifted to a $\mathbb{Z}^2$-periodic graph G_∞. A dimer configuration M of $\mathcal{G}^d$ gives rise to a $\mathbb{Z}^2$-periodic dimer configuration of G_∞^d. Via Temperley's bijection, this gives a spanning-forest-pair (F, F^*) of G_∞ and G_∞^*. Each of their connected component is a tree, and we call a tree on G_∞ a primal tree, call a tree on G_∞^* a dual tree, and call the only bi-infinite path of a tree its root.

Without loss of generality we only calculate the vertical height change. Choose vertices v_0 and v_1 as two copies of the same vertex of $\mathcal{G}$, and the copy of $\mathcal{G}$ containing v_1 lies above and is neighboring to that containing v_0. We construct a path on G_∞ connecting v_0 and v_1 in the following way (illustrated by Figure 3.5). On G_∞ and G_∞^* there are mk primal trees and mk dual trees between v_0 and v_1. Any edge on the root of a dual tree (e in Figure 3.5) has two neighboring G_∞-vertices (v and v' in the figure), lying on each side of the root. For both of them we follow the branches before we arrive at their roots. This gives a path between roots of two

neighboring primal trees. We also allow walking along the roots of primal trees. Thus, by choosing one edge on every dual tree, we construct a path on G_∞ from v_0 to v_1 with k jumps over the roots of dual trees.

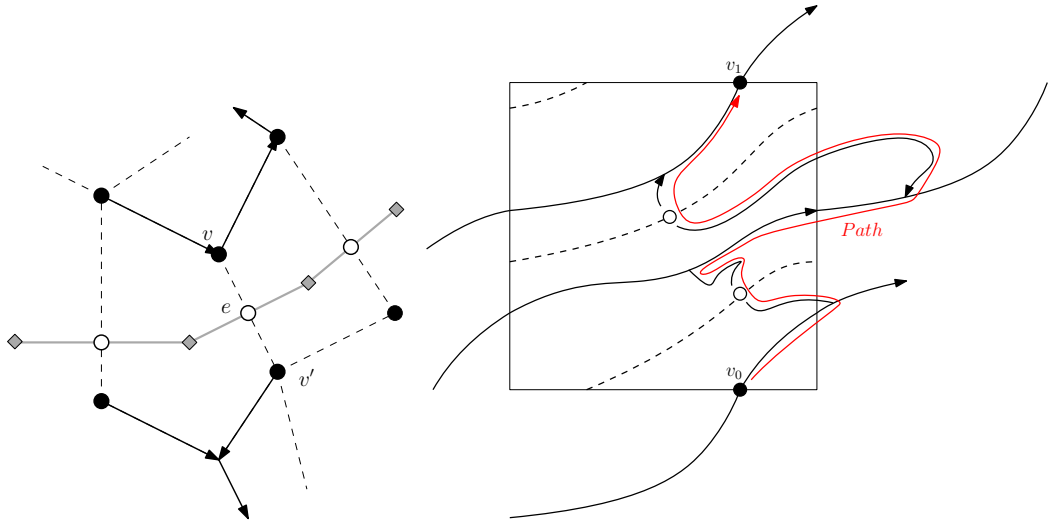

(a) How to choose the neighboring G-vertices of e. The grey path is the root of a dual cycle-rooted tree

(b) How to construct such path.

Figure 3.5: Construction of a periodic path.

When such a path jumps over a dual root, the local height change is the renormalized winding (by adding an imaginary edge between the two ends of the jump) minus 1/2 if it is from right to left over the root, and plus 1/2 if it is from left to right. Walking along a path always co-oriented or anti-oriented gives a height change equal to the renormalized winding. Entering a root, walking along the root and exiting into another branch, the observed orientation is reversed exactly once (from co-orientated to anti-oriented), either at the time of entering the root or at the time of exiting the root. In both cases it can be viewed as joining another path and reversing the orientation. Joining from the right side of another path means a height change equal to the renormalized winding minus 1/2 and from the left side means winding plus 1/2. The proof is geometrical, as illustrated in Figure 3.6.

So we conclude that the total height change from v_0 to v_1 is the renormalized winding plus $\frac{1}{2}(-a+b)$ where a is the number of crossings over the roots of both primal and dual trees from right to left along the path, and respectively b is the number of crossings from left to right. Since such path can be repeated between $v_0+n\hat{y}$ and $v_0+(n+1)\hat{y}$ for any $n \in \mathbb{Z}$ without self-joining, the winding of this path between v_0 and v_1 is 0 and this completes the proof along the y-axis. The proof concerning the height change along the x-axis is similar.

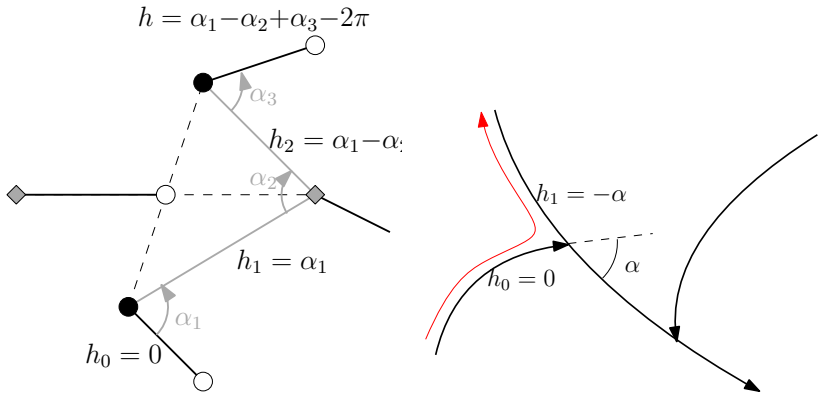

(a) Jump: Winding=$(\alpha_1 - \pi) + (\pi - \alpha_2) - (\pi - \alpha_3) = h + \pi$.

(b) Join: Winding=$\pi - \alpha = h + \pi$.

Figure 3.6: Jumping or joining from the right side of a directed path.

□

Chapter 4

Limiting behavior of *CRSF* measure

Temperley's bijection relates dimer configurations to spanning trees in the planar case and to *CRSF* in the toroidal case (see Section 3.4). We denote by $\pi_{N,B}$ the dimer measure on $\mathcal{G}_N^d$, where B is the magnetic field (Section 2.3.2). When $N \to \infty$ $\pi_{N,B}$ converge to an ergodic Gibbs measure (see Section 2.3.4), denoted by π_B.

The measure $\pi_{N,B}$ gives rise to a measure on primal *OCRSF*, denoted by $\mu_{N,B}$ (see Section 4.1 for complete definitions). The main focus of this chapter is the limiting behavior of $\mu_{N,B}$ when $N \to \infty$, more precisely, the connectivity property and local behaviors of the support of the limiting measure. This is inspired by the work of Pemantle [Pem91], see Section 3.3. We want to get a similar result for the *OCRSF* measures $\mu_{N,B}$.

Our main results are Theorems 4.3.2 and 4.4.3 which can be loosely stated as follows: when the slope of the limiting dimer measure π_B is non-zero, then under μ_B, there are a.s. infinitely many connected components, and if G_∞ is a graph verifying Condition ($\star$) (Definition 4.4.2), then when the slope of the limiting dimer measure π_B is zero, then under μ_B, there is a.s. one connected spanning tree.

Condition ($\star$) is verified by all transient graphs and non-directed graphs. An example is the drifted square grid graph (this name is inherited form [Chh12]), see Example 4.4.6 for definition.

Combining Theorems 4.3.2 and 4.4.3 gives a full picture of the phase diagram of the *OCRSF* measure on graphs verifying Condition ($\star$). The diagram is parameterized by the magnetic field B. When the slope of π_B is not zero, there are a.s. infinitely many trees, and when the slope is zero, there is a.s. only one spanning tree. Zero magnetic field lies in the connected phase. In the case of the drifted square grid graph, an example of the phase diagram is pictured in Figure 4.1.

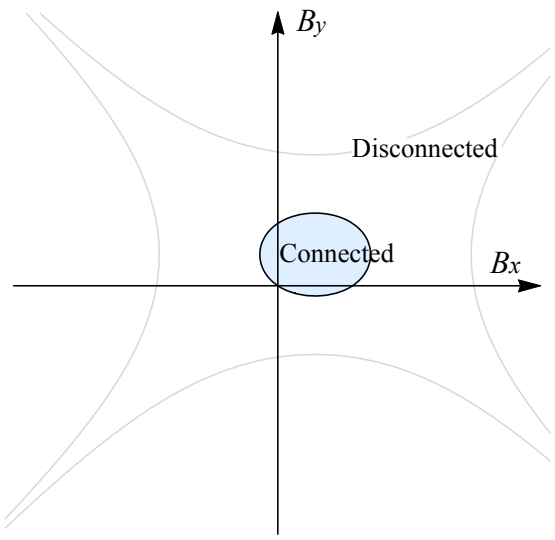

Figure 4.1: Phase diagram of a typical weighting of a drifted square grid graph.

Here is the outline of this chapter. Section 4.1 gives the definition of the *CRSF* measure. Section 4.2.1 introduces the Laplacian with connections, a notion introduced and studied in [Ken11] useful throughout this chapter. Section 4.2.2 relates the Laplacian to the dimer characteristic polynomial, shows that the magnetic field B in the dimer model corresponds to a connection Φ, and as a corollary, gives a modified weighted measure expression of $\mu_{N,B}$. The two following subsections are on matrix relations. Section 4.2.3 deals with the infinite case and relates the Laplacian to the inverse Kasteleyn matrix, and this characterizes the measure $\pi_{N,B}$ according to [KOS06]. Section 4.2.4 handles the infinite case, and Theorem 4.2.3 in this section characterizes μ_B by the Laplacian, which will be used in Section 4.4 to study the topological properties of the configurations under the limiting measure.

4.1 The *CRSF* measure, cases finite and infinite

Consider a directed weighted $\mathbb{Z}^2$-periodic primal graph G_∞, its by-default weight-setting dual graph G_∞^* (every edge is weighted 1) and the double graph G_∞^d generated by G_∞ and G_∞^*. We also take a magnetic field $B = (B_x, B_y) \in \mathbb{R}^2$ on G_∞^d. Recall that adding a magnetic field B means to choose two dual paths γ_x and γ_y in $\mathcal{G}_1^d$ winding once horizontally or vertically around the torus, and for any edge of G_∞^d crossing any copy of γ_x (resp. γ_y), multiply the weight of that edge by $e^{\pm B_x}$ (resp. $e^{\pm B_y}$).

For any $N \in \mathbb{N}^*$, the weight setting above naturally yields a weight on edges of $\mathcal{G}_N^d$. In particular, for the contribution of the magnetic field B in the weights, a gauge equivalent way is to consider $\gamma_{x,N}$ and $\gamma_{y,N}$ as dual paths of $\mathcal{G}_N^d$ winding once horizontally or vertically around the torus, and for any edge of $\mathcal{G}_N^d$ crossing $\gamma_{x,N}$ (resp. $\gamma_{y,N}$), multiply the weight of that edge by $e^{\pm NB_x}$ (resp. $e^{\pm NB_y}$).

For every N, the dimer measure $\pi_{N,B}$ on $\mathcal{G}_N^d$ induces a measure of the *OCRSF*-pairs of $\mathcal{F}(\mathcal{G}_N, \mathcal{G}_N^*)$ by Temperley's bijection. Given an *OCRSF* of $\mathcal{G}_N$, summing over all its duals gives rise to a probability measure on *OCRSF* of $\mathcal{G}_N$. We denote this measure by $\mu_{N,B}$.

The consideration of a magnetic field B follows [KOS06] where the authors get interesting results about the phase transitions using B as parameter. The assumption that $\mathcal{G}_\infty^*$ is an unweighted graph enables us to focus on the objects on the primal graphs which is our main interest.

Here we have two remarks on $\mu_{N,B}$. The magnetic field B on $\mathcal{G}_N^d$ gives rise to a modification of the weights of directed edges of $\mathcal{G}_N$ and $\mathcal{G}_N^*$ by Temperley's bijection. The first remark is that, a priori, this modification is not easy to see directly: readers can check that it changes the weights of those directed edges crossing $\gamma_{x,N}$ or $\gamma_{y,N}$ in one direction but not in the other, and these also depend on the positions of $\gamma_{x,N}$, $\gamma_{y,N}$ and those of the edges. Summing over all duals also complicates the calculation. To understand $\mu_{N,B}$, we prove an explicit formula in Section 4.2.2, showing how the magnetic field influences the measure.

The second remark is that even when $B = (0, 0)$, this measure on primal *OCRSF* is not proportional to weights: the weight of a configuration is multiplied by a factor 2^k where k is the number of its connected components. Compared to a measure where every configuration is equally weighted, the measure $\mu_{N,B}$ favors configurations having more cycles.

In this paper we study the behavior of $\mu_{N,B}$ when $N \to \infty$. In [KOS06], the authors prove that the dimer measures $\pi_{N,B}$ in the limit $N \to \infty$ converge to an ergodic Gibbs measure π_B on dimer configurations of G_∞^d. The measure π_B is a determinantal process whose kernel is determined by an infinite matrix K_∞^{-1} which is the inverse of the infinite Kasteleyn matrix K_∞ of G_∞^d. For any finite set of edges $\mathfrak{e} = \{b_i w_i, i = 1, ..., m\} \subset E_\infty^d$, in a random dimer configuration M of G_∞^d,

$$\pi_B(\mathfrak{e} \subset M) = \left(\prod_{i=1}^{m} K_{b_i,w_i} \right) \det(K_\infty^{-1})_\mathfrak{e}, \tag{4.1}$$

where $(K_\infty^{-1})_\mathfrak{e}$ is the submatrix of K_∞^{-1} indexed by b_i and w_i for $i = 1, ..., m$.

Temperley's bijection directly implies that, when $N \to \infty$, *OCRSF* measures $\mu_{N,B}$ converge weakly to a limiting ergodic Gibbs measure μ_B on configurations of directed edges of G_∞. This measure is a determinantal process whose kernel is determined by a submatrix of K_∞^{-1}. However, the use of the inverse Kasteleyn matrix K_∞^{-1}, is not natural for the *OCRSF* measure. In Theorem 4.2.3 we give a characterization of K_∞^{-1} using the Laplacian, and the characterization of the measure μ_B is given in Proposition 4.2.4, see Section 4.2.4.

4.2 Characterization of the *CRSF* measure

4.2.1 Laplacian with connection

Following [Ken11], for any graph $G = (V, E)$ and to every $v \in V$ and $e \in E$ we assign a space isomorphic to $\mathbb{C}$, denoted by $\mathbb{C}_v$ and $\mathbb{C}_e$. A *connection* Φ on the graph G is the choice for every directed edge $e = uv$ of an isomorphism $\phi_{u,v} : \mathbb{C}_u \to \mathbb{C}_v$ such that $\phi_{u,v} = \phi_{v,u}^{-1}$. This isomorphism is called the *parallel transport* from $\mathbb{C}_u$ to $\mathbb{C}_v$. This is generalized by assigning to every edge $e = uv$ an isomorphism $\phi_{v,e} : \mathbb{C}_v \to \mathbb{C}_e$ with the property that $\phi_{v,e} = \phi_{e,v}^{-1}$ and letting $\phi_{u,v} = \phi_{e,v} \circ \phi_{u,e}$.

On a weighted and directed graph G, the *Laplacian* associated to this connection Φ is the operator $\Delta^\Phi : \mathbb{C}^V \to \mathbb{C}^V$ defined by

$$\Delta^\Phi f(u) = \sum_{v \sim u} c(u, v)(f(u) - \phi_{v,u} f(v)),$$

where the sum is over all vertices adjacent to u. Let $\Lambda^0(G, \Phi)$ be the space of 0-forms and $\Lambda^1(G, \Phi)$ be that of 1-forms. Define $d^\Phi : \Lambda^0(G, \Phi) \to \Lambda^1(G, \Phi)$ and $d^{\Phi,*} : \Lambda^1(G, \Phi) \to \Lambda^0(G, \Phi)$, for any $f \in \Lambda^0(G, \Phi)$, $\omega \in \Lambda^1(G, \Phi)$,

$$(d^\Phi f)(u, v) = \phi_{u,e} f(u) - \phi_{v,e} f(v),$$

$$(d^{\Phi,*}\omega)(u) = \sum_{v \sim u} c(u, v)\phi_{e,u}\omega(u, v),$$

where $e = uv$, then we have the decomposition

$$\Delta^\Phi = d^{\Phi,*} d^\Phi. \tag{4.2}$$

The Laplacian Δ^Φ and the operators d^Φ and $d^{\Phi,*}$ can all be written in matrix form if we fix an orientation of the edges of E, see Section 4.2.3 for more details.

For an oriented cycle $\gamma \subset F$, define the *monodromy* of this cycle as

$$\mathfrak{w}(\gamma) = \prod_{(u,v) \in \gamma} \phi_{u,v}.$$

In [For93], the author proves that for a finite graph $\mathcal{G}$ embedded in the torus,

$$\det \Delta^\Phi = \sum_{F \in OCRSF(\mathcal{G})} \left(\prod_{(u,v) \in F} c(u, v) \prod_{\gamma \subset F} (1 - \mathfrak{w}(\gamma)) \right), \tag{4.3}$$

where the second product is the sum over all directed cycles γ of F.

4.2.2 Toroidal dimer model and Laplacian

Using Equations (4.3) and Proposition 3.4.1, we prove in Proposition 4.2.1 below that the dimer characteristic polynomial of the double graph $\mathcal{G}^d$ arising from a toroidal graph $\mathcal{G}$ is the determinant of a Laplacian with connection. See also [BdT10] where the authors prove this result for non-directed isoradial graphs.

Proposition 4.2.1. *On a toroidal graph $\mathcal{G}$, choose two paths γ_x and γ_y of its dual graph, winding once horizontally and vertically respectively, and choose parallel transport as follows: $\phi_{u,v} = z$ (resp. w) if (u,v) traverses γ_x (resp. γ_y) from left to right, and $\phi_{u,v} = z^{-1}$ (resp. w^{-1}) if it traverses from right to left, otherwise let $\phi = 1$. Consider the modified-weight Kasteleyn matrix K on $\mathcal{G}$ and the Laplacian operator Δ^Φ on $\mathcal{G}$. Then the dimer characteristic polynomial $P(z,w) = \det K(z,w)$ is equal to $\det \Delta^\Phi$.*

Proof. Proposition 3.1 in [KOS06] shows that the characteristic polynomial can be interpreted using the height changes as follows:

$$P(z,w) = \sum_{M \in \mathcal{M}(\mathcal{G}^d)} \Big(\prod_{e \in M} c(e) \Big) z^{-h_x^M} w^{-h_y^M} (-1)^{h_x^M h_y^M + h_x^M + h_y^M}. \tag{4.4}$$

For any $F \in OCRSF(\mathcal{G})$, for (m,n) depending on F as the homology class of F in Proposition 3.4.1, m and n are relatively prime so they can not be both even. Let $a = (k - k_1 - k_2)$ (k, k_1 and k_2 defined as in Proposition 3.4.1 depending on F), then the sign in Equation (4.4) can be simplified to:

$$(-1)^{h_x^M h_y^M + h_x^M + h_y^M} = (-1)^{-nma^2 - na + ma} = (-1)^a.$$

So,

$$\begin{aligned}
P(z,w) &= \sum_{M \in \mathcal{M}(\mathcal{G}^d)} \Big(\prod_{uv \in M} c(uv) \Big) z^{-h_x^M} w^{-h_y^M} (-1)^{h_x^M h_y^M + h_x^M + h_y^M} \\
&= \sum_{(F,F^*) \in \mathcal{F}(\mathcal{G},\mathcal{G}^*)} \Big(\prod_{(u,v) \in F} c(u,v) \Big) z^{-h_x^M} w^{-h_y^M} (-1)^{h_x^M h_y^M + h_x^M + h_y^M} \\
&= \sum_{F \in OCRSF(\mathcal{G})} \Big(\prod_{(u,v) \in F} c(u,v) \Big) \sum_{k_2=0}^{k} \binom{k}{k_2} (-z^n w^{-m})^{k-k_1-k_2} \\
&= \sum_{F \in OCRSF(\mathcal{G})} \Big(\prod_{(u,v) \in F} c(u,v) \Big) (1 - z^{-n} w^m)^{k_1} (1 - z^n w^{-m})^{k-k_1} \qquad (4.5) \\
&= \det \Delta^\Phi,
\end{aligned}$$

which finishes the proof. □

From now on, when we speak of a connection Φ (corresponding to the magnetic field B or the parity (θ, τ), etc.), we mean:

Definition 4.2.2.
(1) On the $\mathbb{Z}^2$-periodic graph G_∞, the connection Φ corresponding to the magnetic field B is the $\mathbb{Z}^2$-periodic connection lifted by that of Proposition 4.2.1 where $z = e^{B_x}$, $w = e^{B_y}$.
(2) On the graph $\mathcal{G}_N$, the connection Φ corresponding to the magnetic field B and the parity (θ, τ) is the connection lifted by that of Proposition 4.2.1 and further

more we choose one dual path $\gamma_{x,N}$ (resp. $\gamma_{y,N}$) winding once horizontally (resp. vertically) and multiply the parallel transport of the directed edges crossing it by $(-1)^\theta$ (resp. $(-1)^\tau$).
(3) For finite planar cases (for example the G_N in Section 4.2.4), we take a trivial connection.

As a corollary of Proposition 4.2.1, if we apply Equation (2.3) to the right hand side of (4.5), and (by using the remark of the gauge equivalence about the magnetic field) we let $z = (-1)^\theta e^{NB_x}$ and $w = (-1)^\tau e^{NB_y}$, then we get the partition function of the dimer measure on $\mathcal{G}_N^d$, *i.e.* that of the *OCRSF* measure on $\mathcal{G}_N$, as a signed sum of 4 terms. Denote this by $Z_{N,B}$, we have

$$Z_{N,B} = \sum_{F \in OCRSF(\mathcal{G})} \Big(\prod_{(u,v)\in F} c(u,v) \Big) (1 + e^{-nNB_x + mNB_y})^{k_1} (1 + e^{nNB_x - mNB_y})^{k-k_1}.$$

By term-term correspondence, we see that $\mu_{N,B}$ is a modified weighted measure on $OCRSF(\mathcal{G})$ where the weight of a configuration F is

$$\Big(\prod_{(u,v)\in F} c(u,v) \Big) (1 + e^{-nNB_x + mNB_y})^{k_1} (1 + e^{nNB_x - mNB_y})^{k-k_1},$$

and the probability of a configuration is just its weight divided by $Z_{N,B}$. This is convenient since when computing the probability it suffices to consider the weights of the primal *OCRSF* of $\mathcal{G}$.

4.2.3 Laplacian and inverse of Kasteleyn matrix on finite graphs

Equation (4.2), as is mentioned, can also be viewed as a matrix multiplication for any connection Φ. We show below that with properly chosen connection Φ, the matrix of the operator $d^{\Phi,*}$ is a part of a Kasteleyn matrix.

Let $G = (V, E)$ be a finite graph, where we suppose that G is either planar or toroidal. Fix any orientation of E and this generates an orientation on edges of $G^* = (V^*, E^*)$ in the following way: for any oriented edge (u, v) of E, denote by $u^* \in V^*$ the dual vertex on the left of (u, v) (*i.e.* the face incident to (u, v) and lying on its left) and by $v^* \in V^*$ the one on the right. The dual edge $u^*v^* \in E^*$ is taken to be directed as (u^*, v^*). The orientation of edges of E and that of E^* generated as above give rise to an orientation of the edges of G^d, which is a Kasteleyn orientation. To see this, we note that every simple face of G^d is a quadrilateral and it is easy to verify the 4 possible cases.

Now consider the connection Φ defined as in Definition 4.2.2. Then for the fixed orientation of E, consider the matrix form of d^Φ and $d^{\Phi,*}$, where the rows of $d^{\Phi,*}$ and columns of d^Φ are indexed by the vertices of G, and the rows of d^Φ and columns

of $d^{\Phi,*}$ are indexed by the edges E with given direction. We can also define the operators $d^{\Phi,*}_{dual}$ and d^{Φ}_{dual} as analog of $d^{\Phi,*}$ and d^{Φ} on the dual graph G^*. It is not hard to verify that the matrix

$$K = \begin{pmatrix} d^{\Phi,*} \\ d^{\Phi,*}_{dual} \end{pmatrix}$$

is a Kasteleyn matrix whose rows are indexed by vertices of G and G^* and whose columns can either be viewed as directed edges or as white vertices of G^d.

Similarly we define the adjacency matrix

$$M = \begin{pmatrix} d^{\Phi} & d^{\Phi}_{dual} \end{pmatrix}.$$

Let $v \in G$ and $v^* \in G^*$ be opposite black vertices in any quadrilateral of G^d, and denote the white vertices in this quadrilateral by e_1 and e_2. Without loss of generality we suppose that dual edges are oriented from v^* to e_1 and e_2, so the primal edges are respectively oriented from e_1 to v and from v to e_2. Note that $c(v^*e_1) = c(v^*e_2) = 1$ by the settings of this chapter, we have

$$\begin{pmatrix} d^{\Phi,*}_{dual} & d^{\Phi} \end{pmatrix}_{v^*,v} = \phi_{e_1,v^*}\phi_{v,e_1} - \phi_{e_2,v^*}\phi_{v,e_2} = 0,$$

and in other cases of v and v^* the entries of $d^{\Phi,*}_{dual}\ d^{\Phi}$ is trivially 0.

Thus, we can write a matrix equation:

$$KM = \begin{pmatrix} d^{\Phi,*} \\ d^{\Phi,*}_{dual} \end{pmatrix} \begin{pmatrix} d^{\Phi} & d^{\Phi}_{dual} \end{pmatrix} = \begin{pmatrix} \Delta^{\Phi} & \star \\ 0 & \Delta^{\Phi}_{dual} \end{pmatrix}. \tag{4.6}$$

Formally, by taking the inverse of K (when invertible) we have:

$$K^{-1} \begin{pmatrix} \Delta^{\Phi} & \star \\ 0 & \Delta^{\Phi}_{dual} \end{pmatrix} = M. \tag{4.7}$$

Equation (4.7) gives a useful characterization of K^{-1} (Theorem 4.2.3) for studying the limiting behavior of *OCRSF* (Section 4.2.4).

4.2.4 Infinite Laplacian and inverse of Kasteleyn matrix

Denote the Kasteleyn matrix of $\mathcal{G}^d_N$ by K_N and recall that the Kasteleyn matrix of G^d_∞ is denoted by K_∞. Same convention for other matrices (Δ, M, *etc.*). As mentioned in Section 4.1, in this section we characterize K^{-1}_∞ by the Laplacian.

Equation (4.6) holds for K_∞, Δ_∞ and M_∞ and so does Equation (4.7). By construction of K_N, here the first half columns of K^{-1}_∞, denoted by $(K^{-1}_\infty)^V$, are indexed by V, vertices of G_∞, and the second half are by those of G^*_∞. We are only interested in the first half (primal *OCRSF*), fully described by $(K^{-1}_\infty)^V$. We may write

$$K^{-1}_\infty = \begin{pmatrix} (K^{-1}_\infty)^V & (K^{-1}_\infty)^{V^*} \end{pmatrix}$$

and then by verifying the block product version of (4.7) we have

$$(K_\infty^{-1})^V \Delta_\infty^\Phi = d_\infty^\Phi.$$

Fixing a row in this equation means fixing some edge e (*i.e.* choosing a white vertex). Denote by $(K_\infty^{-1})_e^V$ and $(d_\infty^\Phi)_e$ the corresponding row vectors of $(K_\infty^{-1})^V$ and d_∞^Φ.

Theorem 4.2.3 below gives a description of $(K_\infty^{-1})^V$ by a statement of existence and uniqueness. A similar argument can be found in [BdT10].

A vertex u of G_∞^d can be written in the form $(x, y; v)$, where $(x, y) \in \mathbb{Z}^2$, $v \in \mathcal{G}_1^d$. Define $\mathcal{C}_0(\mathbb{Z}^2)$ as the space of $\mathcal{G}_1^d$-vector-valued functions decaying at infinity, and define $\mathcal{C}_0^B(\mathbb{Z}^2)$ as its (magnetic field B) modified version:

$$\mathcal{C}_0^B(\mathbb{Z}^2) := \{f : \mathbb{Z}^2 \to \mathcal{G}_1^d : (x, y) \mapsto e^{xB_y + yB_x} f(x, y) \in \mathcal{C}_0(\mathbb{Z}^2)\}.$$

Theorem 4.2.3. *The matrix $(K_\infty^{-1})^V$ is the unique infinite matrix A such that every row $A_e \in \mathcal{C}_0^B(\mathbb{Z}^2)$ and $A\Delta_\infty^\Phi = d_\infty^\Phi$.*

Proof. To prove the uniqueness here we use Fourier transform. The space of rapidly decaying $\mathcal{G}_1^d$-vector-valued functions is

$$\mathcal{S}(\mathbb{Z}^2) := \{f : \mathbb{Z}^2 \to \mathcal{G}_1^d : \forall (m, n) \in \mathbb{Z}^2, \lim_{\|(x,y)\| \to \infty} \|x^m y^n f(x, y)\| = 0\},$$

and its B-modified version:

$$\mathcal{S}^B(\mathbb{Z}^2) := \{f : \mathbb{Z}^2 \to \mathcal{G}_1^d : e^{xB_y + yB_x} f(x, y) \in \mathcal{S}(\mathbb{Z}^2)\}.$$

Also denote by $\mathcal{S}(\mathbb{T}^2)$ the space of $\mathcal{G}_1^d$-vector-valued smooth function on the torus.

The Fourier transform of a $\mathcal{G}_1^d$-vector-valued function f, when it exists, is

$$\widehat{f}(z, w) = \sum_{(x,y) \in \mathbb{Z}^2} f(x, y) w^x z^y, \ (z, w) \in \mathbb{T}^2,$$

and we define the Fourier transform with magnetic field B as

$$\widehat{f}^B(z, w) = \sum_{(x,y) \in \mathbb{Z}^2} f(x, y)(we^{B_y})^x (ze^{B_x})^y, \ (z, w) \in \mathbb{T}^2.$$

The Fourier transform gives a bijection between $\mathcal{S}(\mathbb{Z}^2)$ and $\mathcal{S}(\mathbb{T}^2)$. Denote by $\langle\ ,\ \rangle_{\mathbb{Z}^2}$ (resp. $\langle\ ,\ \rangle_{\mathbb{T}^2}$) the duality bracket between between $\mathcal{S}(\mathbb{Z}^2)$ and its dual $\mathcal{S}'(\mathbb{Z}^2)$ (resp. between $\mathcal{S}(\mathbb{T}^2)$ and its dual $\mathcal{S}'(\mathbb{T}^2)$). The Fourier transform extends as a bijection from $\mathcal{S}'(\mathbb{Z}^2)$ to $\mathcal{S}'(\mathbb{T}^2)$ by duality.

The Laplacian acting on the right side is:

$$f\Delta_\infty^\Phi(u) = \sum_{u' \sim u} c(u'u)[f(u) - \phi_{uu'} f(u')],$$

where the parallel transport is

$$\phi_{u,u'} = \phi_{(x,y;v),(x',y';v')} = e^{B_y(x'-x)+B_x(y'-y)}.$$

Thus,

$$\begin{aligned}\widehat{f\Delta_\infty^\Phi}^B &= \sum_{(x,y)\in\mathbb{Z}^2} (we^{B_y})^x (ze^{B_x})^y \sum_{u'\sim u} c(u'u)[f(u) - e^{B_y(x'-x)+B_x(y'-y)} f(u')] \\ &= \sum_{(x,y)\in\mathbb{Z}^2} w^x z^y \sum_{u'\sim u} c(u'u)[e^{xB_y+yB_x} f(u) - e^{x'B_y+y'B_x} f(u')] \\ &= \widehat{g_f\Delta_\infty},\end{aligned}$$

where $g_f(x,y;v) = e^{xB_y+yB_x} f(x,y;v)$ and Δ_∞ is the Laplacian with trivial connection. By definition we see that when $f \in \mathcal{C}_0^B(\mathbb{Z}^2)$, then $g_f \in \mathcal{C}_0(\mathbb{Z}^2)$, and the action of Δ_∞ preserves the space $\mathcal{C}_0(\mathbb{Z}^2)$.

To prove the uniqueness it suffices to show that the only solution of $f\Delta_\infty^\Phi = 0$ in $\mathcal{C}_0^B(\mathbb{Z}^2)$ is 0. Then its Fourier transform with B, which is equal to $\widehat{g_f\Delta_\infty}$, is also 0. Their Fourier transforms (with or without B) are well defined, and for any test function $h \in \mathcal{S}(\mathbb{T}^2)$,

$$0 = \langle \widehat{g_f\Delta_\infty}, h\rangle_{\mathbb{T}^2} = \langle g_f\Delta_\infty, \check{h}\rangle_{\mathbb{Z}^2} = \langle g_f, \Delta_\infty\check{h}\rangle_{\mathbb{Z}^2} = \langle \widehat{g_f}, \widehat{\Delta_\infty} h\rangle_{\mathbb{T}^2}.$$

The second and fourth equalities are by Parseval's theorem, the fourth equality is also by the fact that Δ_∞ acts on $\check{h}$ as a convolution rather than a product. The third equality is well defined as $g_f \in \mathcal{C}_0(\mathbb{Z}^2) \subset \mathcal{S}'(\mathbb{Z}^2)$, and $\widehat{g_f}$ in the forth equality is in $\mathcal{S}'(\mathbb{T}^2)$ defined by duality. Since $\widehat{\Delta_\infty}$ is invertible except at $(1,1)$, the above calculations show that for all $\psi \in \mathcal{S}(\mathbb{T}^2)$ such that $\hat{\psi}$ has support contained in $\mathbb{T}^2\backslash\{(1,1)\}$, let h be $\widehat{\Delta_\infty}^{-1}\psi \in \mathcal{S}(\mathbb{T}^2)$, so the support of $\widehat{g_f}$ is contained in $\{(1,1)\}$. For $g_f \in \mathcal{C}_0(\mathbb{Z}^2)$, the only possibility is $g_f = 0$, so $f = 0$.

To prove the existence, knowing that $(K_\infty^{-1})^V$ exists and verifies $(K_\infty^{-1})^V\Delta^\Phi = d$, we should also prove that every row $(K_\infty^{-1})_e^V$ is in the space $\mathcal{C}_0^B(\mathbb{Z}^2)$. By definition it is equivalent to proving that $g_{(K_\infty^{-1})_e^V} \in \mathcal{C}_0(\mathbb{Z}^2)$, and we have

$$\left(\widehat{g_{(K_\infty^{-1})_e^V}\Delta_\infty}\right) = \left(\widehat{(K_\infty^{-1})_e^V\Delta_\infty^\Phi}\right)^B = \widehat{d_e}^B = \widehat{g_{d_e}}.$$

In the last term $g_{d_e} = e^{B_yx+B_xy}d_e^0$, d_e^0 is the matrix form of d where the magnetic field B is 0. Thus, in the case that e satisfies $x(e) = y(e) = 0$ (*i.e.* the edge e is in the copy $x = y = 0$), $(K_\infty^{-1})_e^V \in \mathcal{C}_0(\mathbb{Z}^2)$ by the same proof as in Proposition 5 of [BdT10], where the crucial fact is that Proposition 4.2.1 gives a characterization of the zeros of $\det K(z,w)$ on the torus $\mathbb{T}^2$. By translation invariance it is true for all e. □

As a corollary of Theorem 4.2.3 and the results of [KOS06, BdT10], we give the following characterization of the measure μ_B. Note that the notions in Proposition 4.2.4 are all interpreted via operators on the primal graph. However, so as not to introduce too many notations, we use notations similar to those of Equation (4.1) (which considers the dimer model on the double graph).

Denote by $K_{u,e}$ the entry of $d_\infty^{\Phi,*}$ corresponding to the vertex u and edge e. By construction of $d_\infty^{\Phi,*}$, $K_{u,e}$ is equal to $\pm c_B(u,v)$, where the sign depends on the orientation and the subscript B of c means that the weight $c(u,v)$ is modified by the magnetic field B.

Proposition 4.2.4. *When $N \to \infty$, OCRSF measures $\mu_{N,B}$ converge weakly to a limiting ergodic Gibbs measure μ_B on configurations of directed edges of G_∞. For any finite set of oriented edges $\mathbf{e} = \{(u_i, v_i), i = 1, ..., m\}$, if for every i we denote by e_i the non-directed edge $u_i v_i$, then in a random configuration F,*

$$\mu_B(\mathbf{e} \subset F) = \left(\prod_{i=1}^{m} K_{u_i,e_i} \right) \det(K_\infty^{-1})_{\mathbf{e}}^V, \tag{4.8}$$

where $(K_\infty^{-1})_{\mathbf{e}}^V$ is the submatrix of $(K_\infty^{-1})^V$ indexed by u_i and e_i for $i = 1, ..., m$, $(K_\infty^{-1})^V$ characterized by Theorem 4.2.3.

4.2.5 Transfer impedance theorem

In this section we give a brief discussion on the measures on non-oriented edges of the *CRSF* of G_∞. We prove a transfer impedance theorem which gives a kernel of the non-oriented-edge measure, and this measure shares an obvious similarity with that of spanning trees proved in [BP93]. This indicates that in the case of a square grid with equal weighted edges (the case considered in [BP93]), the limiting measure of *CRSF* is supported on spanning trees. This inspires our Section 4.4.

Recall that oriented edges of *OCRSF* under the limiting measure μ_B is characterized by Equation (4.8). By entering K_{u_i,e_i} into columns of $(K_\infty^{-1})^V$, we can rewrite the right hand side of Equation (4.8) as a single determinant: under the convention $e_i = u_i v_i$, the element in the determinantal kernel corresponding to (e_i, u_j) is

$$K_{u_j,e_j} \left(K_\infty^{-1}\right)_{e_i,u_j}^V.$$

Consider the probability of non-directed edges of E, which is a binomial sum over directed edges. Such probability measure is a determinantal process with an edge-edge matrix kernel, and the element corresponding to (e_i, e_j) is

$$K_{u_j,e_j} \left(K_\infty^{-1}\right)_{e_i,u_j}^V + K_{v_j,e_j} \left(K_\infty^{-1}\right)_{e_i,v_j}^V. \tag{4.9}$$

We note that when the magnetic field is 0 and the weights of edges are all equal to 1, formally (4.7) says that $(K_\infty^{-1})^V$ is the difference of two Green's functions

g, and by construction the sign of K_{u_j,e_j} is different from that of K_{v_j,e_j}. We can rewrite (4.9) as

$$(g(v_i,u_j)-g(u_i,u_j))-(g(v_i,v_j)-g(u_i,v_j))\,,$$

although only differences of g make sense.

This result is the same as the kernel of the probability measure on uniform spanning trees on the equal-weighted square lattice studied in [BP93]. Thus for $G_\infty=\mathbb{Z}^2$ with equal weight-setting, the measures on *OCRSF* of $\mathcal{G}_N$ converge weakly to the uniform measure on spanning trees of $\mathbb{Z}^2$.

4.3 Non-zero slope

In Section 4.2.5, by comparing to the results of [BP93], we showed that in the simplest case (square lattice whose edges are equally weighted), under the limiting measure there is a.s. exactly one connected component. A natural question is to understand the number of connected components in more general cases. In this section, we prove that when the slope of the limiting measure is non-zero, then there are a.s. infinitely many connected components, and in Section 4.4 we prove that under Condition ($\star$) to be specified, zero slope means exactly one connected component.

Consider the $\mathbb{Z}^2$-periodic planar graph G_∞ and a magnetic field B. Following [Pem91], for two given vertices v_1 and v_2 in G_∞, and for any $N\in\mathbb{N}$ such that $\mathcal{G}_N$ contains v_1 and v_2, we consider the event in $\mathcal{G}_N$ that v_1 and v_2 are connected within a ball B_L by *OCRSF* of the toroidal graph $\mathcal{G}_N$ (we ask that the size N of the torus is larger than the diameter of B_L so that B_L doesn't superpose with itself). The probability that, under the limiting measure μ_B, v_1 and v_2 are connected is equal to:

$$\lim_{L\to\infty}\lim_{N\to\infty}\mu_{N,B}[v_1\leftrightarrow v_2 \text{ within } B_L].$$

The measure on *OCRSF*-pairs of the torus gives rise to a measure on their roots (oriented cycles). Proposition 3.4.1 proves that for any simple closed curve γ_x (resp. γ_y) that winds once horizontally (resp. vertically), the signed sum of the crossings of the oriented cycles on such a curve is equal to the horizontal (resp. vertical) height change. We have the following Lemma.

Lemma 4.3.1. *For (F,F^*) an OCRSF pair on a toroidal graph $\mathcal{G}$, we omit the branches and look at the cycles. For any vertices v_1 and v_2, choose a path γ on $\mathcal{G}$ that links v_1 and v_2. Then for any simply connected region containing v_1 and v_2, these vertices are not connected within the region if the absolute value of the signed sum of the number of cycles of (F,F^*) passing γ between v_1 and v_2 is not less than two.*

Proof. For any simply connected finite region on the torus, if two vertices lie on different side of a dual cycle, then they are not connected within the region. If the

signed sum of the cycles passing γ between these vertices is not less than two, then there should be at least one dual cycle passing γ between these vertices. □

The following theorem is the main result of this section. Recall that for the dimer model on $\mathcal{G}_N$, when $N \to \infty$, the average height change under $\pi_{N,B}$ converges to the slope (s,t) of the Gibbs measure π_B [KOS06].

Theorem 4.3.2. *If the slope (s,t) of the limiting dimer measure π_B is non-zero, then under the limiting OCRSF measure μ_B there are a.s. infinitely many connected components.*

Proof. We suppose that $t > 0$. On G_∞ we choose v_1 arbitrarily and choose v_2 being a copy of v_1 lying k pieces above v_1 (we write $v_2 = v_1 + k\hat{y}$). Choose γ_y as a periodic path on G_∞ (so on the path there are only the white vertices and the primal black vertices of G_∞^d), winding vertically and passing v_1 and v_2. Let $M-1$ be the number of black vertices on γ_y between v_1 and $v_1 + \hat{y}$, so there are $kM-1$ black vertices and kM white vertices on γ_y between v_1 and v_2.

For any ball B_L that contains v_1 and v_2, and for any N large enough such that B_L is contained in $\mathcal{G}_N$ as a simply connected set, Lemma 4.1 says that the probability that v_1 and v_2 are not connected is bounded from below by the probability that the signed sum of the cycles passing through γ between them are strictly bigger than 1 or strictly less than -1.

For any N, and any *OCRSF* of $\mathcal{G}_N$, the total height change h_y along the y-axis is the total signed sum of primal cycles and dual cycles that pass through the once-vertically winding curve γ_y. So for v_1 and v_2, the expected height difference $h_y(v_1, v_2)$ is the expected signed sum of the number of crossings of the cycles between v_1 and v_2.

As N goes to infinity, $\mathbb{E}[h_y(v_1,v_2)] \to kt$. So $\forall \alpha > 0$ small, when N is large, we have $\mathbb{E}[h_y(v_1,v_2)] \geq kt - \alpha$. As there are at most $2kM-1$ vacancies that allow the cycles to pass through, the expectation of the signed sum can be written as:

$$p_{-2kM+1}(-2kM+1) + ... + p_{-1}(-1) + p_1 + ... + p_{2kM-1}(2kM-1),$$

where p_i is the probability that the signed sum is i. And if $|i| \geq 2$, then there are at least two cycles passing between v_1 and v_2.

By assumption t is positive. We want to maximize $p_{-1} + p_0 + p_1$ under the constraints

$$\sum_{i=-2kM+1}^{2kM-1} p_i i \geq kt - \alpha, \quad \sum_{i=-2kM+1}^{2kM-1} p_i = 1.$$

If $p_{-1} + p_0 + p_1$ is equal to p, then their contribution to the expectation is at most p, and the remaining terms contribute at most $(1-p)(2kM-1)$. So we have

$$p + (1-p)(2kM-1) \geq kt - \alpha,$$

which turns to be

$$p(2kM-2) \leq 2kM - kt - 1 + \alpha.$$

Choose k bigger than $1/M$ and $1/t$, α sufficiently small, then $p < \frac{2kM-1-kt+\alpha}{2kM-2}$, which is less than 1, and this is bigger than the probability that v_1 and v_2 is not connected. Especially, we remark that this upper bound when N is large enough doesn't depend on L. As L tends to infinity, the probability that v_1 and v_2 are connected is less than 1, so the probability that there is a unique connected component is less than 1.

By the same method we can generalize this result to finite subset of vertices $v_1, ..., v_k \in V$. The probability that any two of them is connected is less than 1, so the probability that there are at most $k-1$ connected components is less than 1.

Since the measure is ergodic, and since the event that there are at most $k-1$ components is translation-invariant, the probability that there are at most $k-1$ connected components is 0, and the proof is complete. □

4.4 Zero slope

The following lemma is an important observation for a graph G_∞^d under our setting.

Lemma 4.4.1. *In the phase diagram of the dimer measure on G_∞^d, the point $B = (0,0)$ always corresponds to a zero slope.*

Proof. When $B = (0,0)$, $(z,w) = (e^0, e^0) = (1,1)$ is always a real zero of the characteristic polynomial $\det K(z,w) = \det \Delta^\Phi$, so either $B = (0,0)$ lies on the boundary of the amoeba (when $(1,1)$ is a single root) or in the interior of the amoeba (when $(1,1)$ is a double root). In either case, it corresponds to an integer point in the Newton polygon.

If the graph G_∞ has a symmetric weight setting (i.e. $c(u,v) = c(v,u)$ for all edges uv), then the Laplacian Δ^Φ is symmetric in z and z^{-1} (resp. in w and w^{-1}). Since $\det K(z,w) = \det \Delta^\Phi$, the amoeba is symmetric with respect to the origin and so is the Newton polygon, and $B = (0,0)$ corresponds to $(s,t) = (0,0)$. For this symmetric Laplacian, $(1,1)$ is a double real root, so $B = (0,0)$ lies in the interior of the amoeba (a liquid phase). Also, as an interior integer point, $(s,t) = (0,0)$ corresponds either to a liquid phase or to a gaseous phase.

In general, any weight setting can be obtained from the symmetric weight setting via continuous deformation. Along this deformation, for any fixed magnetic field B the slope (s,t) changes continuously, while the point $B = (0,0)$ always corresponds to an integer point (s,t). Thus $B = (0,0)$ always corresponds to $(s,t) = (0,0)$. This finishes the proof. □

Note that same slope means same limiting measure. To study the case where the slope is zero, we just need to study the case where the magnetic field is zero, and we write μ_N instead of $\mu_{N,B}$ and μ instead of μ_B. The advantage is that $B = (0,0)$ enables us to approach μ by another sequence of measures m_N but on finite planar graphs. The later one has a random-walk interpretation, which gives some tools to study connectivity.

Similarly, in the following part we omit the connection Φ (which is trivial when $B = (0, 0)$) of the Laplacian Δ^Φ to simplify the notation.

Let the finite graphs $(G_N)_N$ form an exhausting sequence of G_∞ with a *wired boundary condition*, which means gluing every vertex on the boundary into one single vertex. A spanning tree of G_N rooted at the boundary vertex denoted by r_N is called a *wired spanning trees* (*WST*) [Pem91, Häg95, BLPS01]. We denote this weighted wired spanning tree measure by m_N.

In [BLPS01], the authors prove the existence of a weak limit of the measures of *WST* on non-directed weighted graphs, also called *networks*. Such name is given because of its natural relation to electrical networks. Graphs arising from dimer models are directed and weighted. We show that the same approach still works.

Let G_N^* be the dual of G_N and let G_N^d be the double graph. Choose an arbitrary vertex in G_N^* incident to r_N, denoted by r_N^*, and let T^* be the dual of T rooted at r_N^*. Recall that Temperley's bijection gives a measure preserving bijection between dimer configurations of $G_N^d \setminus \{r_N, r_N^*\}$ and *OST*-pairs (T, T^*), T rooted at r_N and T^* rooted at r_N^*. Here the weight of T^* is always 1 and every T has only one dual T^*, so m_N is the same measure as the *OST*-pairs measure (the dimer measure).

Similar to what we have in the toroidal case, the oriented-edge-measure of the *OST* of G_N rooted at r_N forms a determinantal measure. If we denote by $\tilde{K}_N$ the Kasteleyn matrix of $G_N^d \setminus \{r_N, r_N^*\}$, then the measure is described by $(\tilde{K}_N^{-1})^V$, the submatrix indexed by vertices of G_N.

Here the matrix relation (4.2) writes $\Delta_N = d_N^* d_N$. We rearrange the columns and rows in such a way that the first half of the black vertices are indexed by the vertices of G_N. Removing r_N and r_N^* corresponds to deleting the corresponding rows and columns in the matrices. These modified matrices are denoted by symbols with tilde:

$$\begin{pmatrix} \widetilde{d}_N^* \\ \widetilde{d}_{dual\ N}^* \end{pmatrix} \begin{pmatrix} \widetilde{d}_N & \widetilde{d}_{dual\ N} \end{pmatrix} = \begin{pmatrix} \widetilde{\Delta}_N & \star \\ 0 & \widetilde{\Delta}_{dual\ N} \end{pmatrix}.$$

Removing r_N and r_N^* leaves $\widetilde{\Delta}_N$ and $\widetilde{\Delta}_{dual\ N}$ invertible. The matrix $\begin{pmatrix} \tilde{d}_N^* \\ \tilde{d}_{dual\ N}^* \end{pmatrix}$ is exactly the Kasteleyn matrix $\tilde{K}_N$. So $(\tilde{K}_N^{-1})^V$ is the only matrix A_N which satisfies

$$A_N \widetilde{\Delta}_N = \widetilde{d}_N.$$

Let D_N be a diagonal matrix indexed by $u \in G_N \setminus \{r_N\}$, and $(D_N)u, u = \sum_{v \sim u} c(u, v)$. Then

$$\left(D_N^{-1} \widetilde{\Delta}_N\right)_{u,v} = \begin{cases} 1 & v = u \\ -c(u, v) / \sum_{v' \sim u} c(u, v') & v \neq u. \end{cases}$$

When $v \neq u$, the $(u, v)^{th}$ entry is the transition probability of the random walk from u to v. Write

$$p_{u,v} = c(u, v) / \sum_{v \sim u} c(u, v).$$

The only matrix P_N satisfying $P_N D_N^{-1} \widetilde{\Delta}_N = \widetilde{d}_N$ is $(\tilde{K}_N^{-1})^V D_N$. Meanwhile, there is a natural solution of this equation given by the Green's function. For the white vertex w associated to the directed edge (v_1, v_2) (see Figure 4.2), and for any vertex v, if we define $X_a^{G_N}$ as the random walk on G_N starting at a and killed at r_N, then

$$\left(P_N\right)_{w,v} = \mathbb{E}\left[\#X_{v_2}^{G_N} \text{ visits } v - \#X_{v_1}^{G_N} \text{ visits } v\right]. \tag{4.10}$$

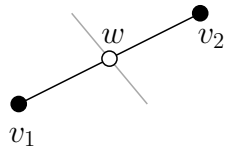

Figure 4.2: v_1,v_2 and w.

Definition 4.4.2. If the right hand side of (4.10) converges when $N \to \infty$ and decays to zero when the distance between w and v tends to infinity, we say that the graph G_∞ verifies *Condition* $(\star)$.

Theorem 4.4.3. *When Condition* $(\star)$ *is verified, as* N *goes to infinity,* m_N *converges to a measure* m *on spanning trees of* G_∞*. This is the same measure as* μ*, the weak limit of* μ_N*.*

Condition $(\star)$ is true for a big class of graphs. See the following propositions. We postpone the proof of Theorem 4.4.3 after these propositions.

Proposition 4.4.4. *If the graph* G_∞ *is transient, then Condition* $(\star)$ *is verified.*

Proof. We have

$$\mathbb{E}\left[\#X_{v_2}^{G_N} \text{ visits } v\right] = \mathbb{P}\left(X_{v_2}^{G_N} \text{ visits } v\right) \mathbb{E}\left[\#X_v^{G_N} \text{ visits } v\right].$$

In the transient $\mathbb{Z}^2$ case, the second factor on the right hand side converges when $N \to \infty$ and is bounded. The first factor also converges when $N \to \infty$, and it tends to zero when the distance between v_2 and v tends to infinity, since in scaling the random walk γ behaves like a drift of order n plus a term of variance $\sqrt{n}$. For a fixed-size ball, the probability that such a path visits it decays to zero as the distance between the ball and the origin tends to infinity. □

Proposition 4.4.5. *If the graph is non-directed, then Condition* $(\star)$ *is verified.*

For non directed graph, such properties are proved in [BLPS01].

Example 4.4.6. *The drifted grid graph.*

Here we look at an example: the drifted square grid graph, which is a square lattice with drifted weight setting: every vertex has four incident edges with conductances being a, b, c and d clockwise, see Figure 4.3. Its dual is the square lattice with edges weighted 1. The fundamental domain of its double graph is the same as the example in Figure 2.1.

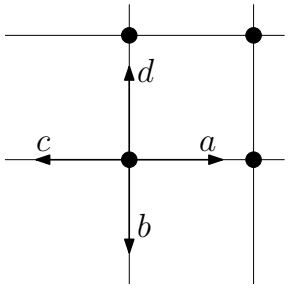

Figure 4.3: Drifted square grid.

The phase diagram of the dimer model on its double graph with typical weighting is as in Figure 4.1 (black and grey curves give the amoeba). There is only one possible bounded gaseous region for any value of (a, b, c, d) such that $a \neq c$ or $b \neq d$, otherwise such region vanishes. In Figure 4.1 the gaseous region is in light blue.

If the random walk associated is recurrent, then $a = c$ and $b = d$, so Proposition 4.4.5 applies. Otherwise this is a transient graph and Proposition 4.4.4 applies. So the drifted square grid graph always satisfies Condition $(\star)$.

Proof of Theorem 4.4.3. When Condition $(\star)$ is verified, any entry of P_N converges when $N \to \infty$. Denote its limit by P_∞. Measures $(m_N)_N$ converge to a limiting measure m. The entry of P decays to 0 as the distance between two vertices tends to infinity. Let $A_\infty = P_\infty D_\infty^{-1}$ where D_∞ is the infinite diagonal matrix as analogue of D_N. It determines m and satisfies the equation $A_\infty \Delta_\infty = d_\infty$. Each row vector of the matrix A_∞ can be viewed as a function on the vertices of G_∞.

Theorem 4.2.3 says that $(K_\infty^{-1})^V$, the matrix determines μ, is the unique matrix verifying this equation and decays at infinity. This proves that $m = \mu$. To finish the proof, we just need to prove that the measure m is supported by spanning trees. This is Lemma 4.4.7 below.

Lemma 4.4.7. *The measure m is supported on spanning trees of G_∞.*

Proof. In [Pem91], the author shows that spanning trees of equal weighted square grid converge to trees of $\mathbb{Z}^2$ if and only if independent simple random walk and loop erased random walk intersect infinitely often a.s. The same argument still applies to other cases. This is also known to the authors of [LPS03] in their Proposition 3.4.1. Here in our case where the weight function is defined on directed edges, there is nothing new.

Theorem 1.1 in [LPS03] shows that, for two independent transient Markov chains X^1 and X^2 on the same graph and having the same transition probabilities, if the path of X^1 and that of X^2 intersect infinitely a.s., then $LE(X^1)$ and X^2 intersect infinitely a.s. too.

In our case, in scaling the random walk $X_n^{1,2}$ behaves like a drift term of order n plus a term of variance $\sqrt{n}$. The paths of two independent random walk meets infinitely a.s. as the time tends to infinity. This finishes the proof. □

Remark: Here we choose wired spanning tree measures m_N to approach μ. However, we conjecture that the local behavior of the spanning tree finally does not depend on the choice of root r_N on the boundary of G_N, *i.e.* we choose the root vertex simply to be a vertex on the boundary of G_N instead of gluing the boundary, and when $N \to \infty$ this always converges to the same measure no matter where the root is. Readers can imagine the following situation, where we construct the spanning tree by starting the first *LERW* at some boundary vertex in the direction of the drift of the graph, and the *LERW* is killed at the chosen boundary vertex r_N. Denote this path by γ_1. If γ_1 isn't dense anywhere, then for any window far away from γ_1, continuing the construction of the spanning tree is as if to construct a spanning tree rooted at γ_1, which is a big object so a random walk has a big probability to meet it before too long, so we can expect that the local behavior of such trees will only depend on the property of the random walk and not r_N.

However, it will be interesting to see what is the behavior of the first branch, i.e. a *LERW* in a finite domain killed at a single boundary vertex.that meets every open set in the limit), then for vertices far from this branch, starting a second

Our result is true for any graph satisfying Condition ($\star$), among which the drifted square grid graph is an interesting example. Proposition 5.4 works for all transient graphs. So the main difficulty for getting such results as Theorem 5.3 on general $\mathbb{Z}^2$-periodic graphs is that we don't know how to prove that the difference of the Green's function for recurrent random walk on directed graphs killed at wired boundary converges when the size of the graph tends to infinity and decays when the distance of the vertices tends to infinity. We conjecture that this is true, and we note that without boundary conditions, the decay of the difference of the Green's function can be found in some references, for example, [KU08].

4.5 Phase diagram

Combining the results in Section 4.3 and Section 4.4, we can give a full picture of the phase diagram for graphs verifying Condition ($\star$). The diagram is parameterized by the magnetic field B. When the slope of π_B is not zero, there are a.s. infinitely many trees, and when the slope is zero, there is a.s. only one spanning tree. Zero magnetic field lies in the connected phase. In the case of the drifted square grid graph, this can be pictured as in Figure 4.1.

The bounded closed set corresponding to a $(0, 0)$ slope (the region in light blue)

corresponds to the phase where there is a.s. exactly one connected component (a spanning tree). Outside this set there are a.s. infinitely many connected components (a spanning forest). This bounded set corresponds to a gaseous phase in the dimer model (as in Figure 4.1 and Figure 4.4) or reduces to a single point in the liquid phase.

We give another example to show the existence of multiple gaseous phase but among them there is only one corresponding to a connected phase: for the same G_∞ we take $\mathcal{G}_2$ as its fundamental domain and for each of its four vertices we independently assign an arbitrary weighting, the phase diagram is as Figure 4.4.

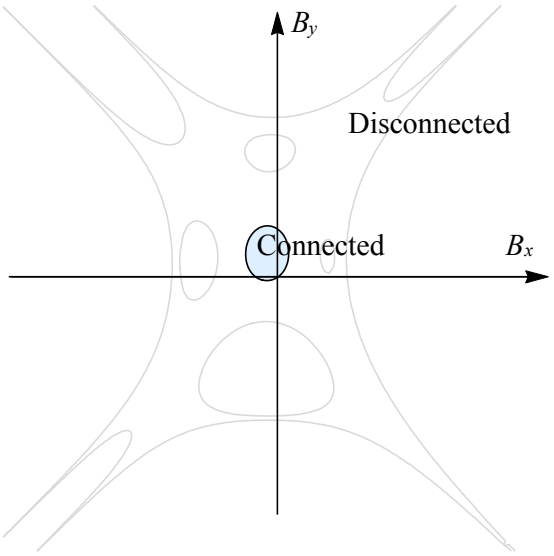

Figure 4.4: Phase diagram of a square grid graph with fundamental domain 2×2.

There are also some interesting properties other than connectivity. Some are just repetitions of the results on the dimer model, see [KOS06]. In the liquid phase, the oriented edge-edge correlations decay polynomially and the variances of the height functions grow at a logarithm order. In the gaseous phases, the oriented edge-edge correlations decay exponentially, and the variances of the height functions are bounded. In the frozen phase, some of the height differences are deterministic.

4.6 Remarks and open questions

When we talk about the height, we mean the height function h^M rather than $\tilde{h}^{(M,M_0)}$. The zero height change has a specific role in our problem. Note that $(0,0)$ slope is an integer point in Newton polygon, if the weights are arbitrarily chosen, this is likely to correspond to a gaseous phase, and the origin $B = (0,0)$ lies on its boundary.

Measure corresponding to slope $(0,0)$ gives spanning trees whose branches are described by $LERW$. When slope is not $(0,0)$, there are bi-infinite bands. Inside

such bands there are free spanning forests rooted at boundaries of bands, which are bi-infinite paths. It is interesting to see what such paths are.

When the slope is zero and Condition ($\star$) is verified, the toroidal dimer measure on $\mathcal{G}_N$ and the wired-spanning-tree measure on G_N converge to the same limiting measure. By this fact we may conclude that their asymptotic entropies are the same. In fact, [CKP01] states that the asymptotic entropy of a region depends loosely on the boundary height function. For spanning-tree measures on G_N, the boundary height function is given by the winding of a $LERW$ killed at boundary, and by geometric intuition this is about zero when renormalized by N.

Chapter 5

Bead model and standard Young tableaux

The *bead model* is a random point field on $\mathbb{Z} \times \mathbb{R}$ or a subset of it. A bead configuration is composed of a collection of parallel vertical threads. On each thread there is a collection of points which we call the *beads*. We furthermore ask an interlacing relation on the vertical positions of the beads (see Section 5.1 for the formal definition). Figure 5.1 shows a typical local configuration.

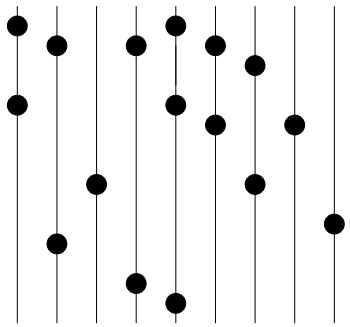

Figure 5.1: A local view of a bead configuration.

Boutillier [Bou09] considers this model on the infinite plane and constructs a family of ergodic Gibbs measures. This measure is constructed as a limit of the dimer model measures on a bipartite graph when some weights degenerate, in particular the hexagon lattice which is equivalent to lozenge tilings. The author proves that under this measure the beads form a determinantal point process whose marginal is the sine process.

In this chapter, we consider the bead model on finite planar simply connected domains and on the torus, and we take the uniform measure on configurations. We describe the general setting of a bead model (Section 5.1.1), define the height function (Section 5.1.3), precisely define the boundary conditions considered in this thesis (Section 5.1.4) and define the uniform measure of the bead model (Section 5.1.5). We also show that the bead model in such cases can be viewed as a limit of the

dimer model (Section 5.1.2 and 5.1.6).

Young diagrams and standard Young tableaux are classical combinatorics objects which describe the irreducible representations of the symmetric and general linear groups. Some problems such as the values of the characters or its decomposition into irreducible representations can be solved by using the exact formulas proved for Young diagrams and tableaux.

In the second part of this chapter we give the definition of (skew) Young diagrams and tableaux (Section 5.1.2). In Section 5.2.2, we show that every Young diagram (which can be skew) corresponds to one specific bead model. We also show that there is a map from bead configurations to standard tableaux of the given diagram, and the map is measure preserving when considering the uniform measure.

5.1 Presentation of the bead model

5.1.1 General setting of a bead configuration

A general bead configuration is a random collection of points on the whole of $\mathbb{Z} \times \mathbb{R}$ or a subset of it, which we denote by $\mathbf{B}$. Furthermore, we ask that the positions of the beads present in a configuration respect the following geometric restrictions:

- The beads are interlacing: for two consecutive beads on a thread, on each of its neighboring thread there is exactly one bead whose vertical position is between them.

- The configuration is locally finite.

In this thesis we focus on the case where the number of threads and that of beads are large but finite, so the locally finite property is automatically satisfied.

Denote by (i, y) the coordinate of a bead. We suppose that there are n threads for some $n \in \mathbb{Z}$. Without loss of generality we suppose that the threads are $\{i = 1, 2, ..., n\}$. For the vertical coordinates y of the beads, we always suppose that y takes value in $[0, 1]$.

As mentioned in the beginning of this chapter, we consider the bead model on finite, planar, simply connected domains and on the torus. Here below we make this more precise:

- *The case of a finite planar simply connected domain.* Consider a planar simply connected domain $R \subset]0, n + 1[\times[0, 1]$. A bead configuration on the domain R means that the coordinates of the beads (i, y) take value in $R \cap (\mathbb{Z} \times [0, 1])$.

- *The case of a torus.* We suppose that $(i, y) \in (\mathbb{Z}/n\mathbb{Z}) \times (\mathbb{R}/\mathbb{Z})$, so we can writes $i \in \{1, ...n\}$ in the sense of modulo n and $y \in [0, 1[$ in the sense of modulo 1.

Among the simply planar domains we are particularly interested in the rectangular case where $R = [1, n] \times [0, 1]$, but due to some technical reasons we will also consider the case that R is a right triangle.

5.1.2 Bead configurations as limit of lozenge tilings: a first view

The bead model can be viewed as a limit of lozenge tilings [Bou09], which is equivalent to the dimer model on the hexagonal lattice. Throughout Chapters 5 and 6 we consider the following three types of lozenges:

- $\diamond$, generated by the vectors $(1, -\frac{1}{2})$ and $(1, \frac{1}{2})$,
- $\triangleright$, generated by the vectors $(1, -\frac{1}{2})$ and $(0, 1)$,
- $\triangleleft$, generated by the vectors $(1, \frac{1}{2})$ and $(0, 1)$.

In a lozenge tiling, any vertical line where the centers of horizontal tiles $\diamond$ locate is considered as a thread, and consider the highest points of horizontal lozenges in a tiling as particles, then such particles on threads automatically verify the interlacing property. The vertical positions of the particles take discrete values, but if we let the vertical size of the domain or that of the torus tend to infinity and then vertically scale the domain into $[0, 1]$ or $\mathbb{R}/\mathbb{Z}$, the step length tends to zero, and the vertical positions of the particles take continuous values.

In the limit where the step size tends to 0, the strict inequalities between the vertical coordinates which give the interlacing property (in the case of torus we can locally compare them) can turn to be non-strict, but under the measure we study (to be defined in Section 5.1.5) this possibility is of negligible probability.

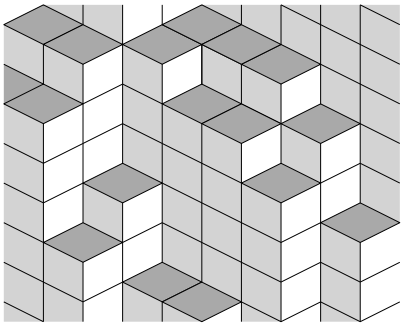

Figure 5.2: A lozenge tiling corresponding to the bead configuration in Figure 5.1.

5.1.3 Height function

We define the height function of the bead model in this section. So as to make this more intuitive, we first define the height function of lozenge tilings and then introduce the definition on bead configurations as an analogue. We first consider the case of a simply connected domain and then consider that of torus.

Throughout Chapters 5 and 6 we use the following definition of the height function H for lozenge tilings. For a horizontal lozenge $\diamond$, the upper vertex is 1 higher than the lower vertex, and the other two are equal to the average. For $\square$ or $\square$, vertices along the same vertical edge have the same height, and going right-up or left-up one step will raise the height by $\frac{1}{2}$.

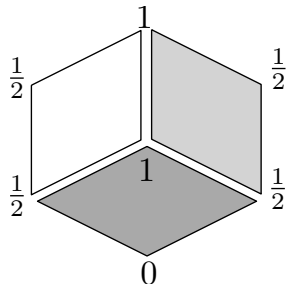

Figure 5.3: Discrete height function H.

By properties of the height function of the dimer model (Section 2.3.1), for every simply connected domain tileable by lozenges, if we fix the height of a given vertex on the boundary, then for every tiling, the definition above gives a unique height for every vertex (as vertex of a lozenge) in the tiling. It is clear that the heights of the vertices on the boundary of the tiled domain do not depend on the tiling.

We consider the height function of the bead model as the limit of the above height functions which is defined on vertices when the vertical step size tends to 0. In this limit, the vertices become a finite subset of the set of threads $\{1, 2, ..., n\} \times [0, 1]$. We have the following natural definition, in which we define the height function on the threads. We still use the same letter H as that of the lozenge tilings. Normally this won't cause ambiguity.

Definition 5.1.1. Consider a finite planar simply connected domain $R \subset]0, n+1[\times[0, 1]$. Given a bead configuration $\mathbf{B}$ of the domain R, the *height function* $H = H^{\mathbf{B}}$ (for convenience we omit $\mathbf{B}$) is the function

$$H : R \cap (\mathbb{Z} \times [0, 1]) \to \mathbb{R}$$

unique up to a constant which verifies the following conditions. The constant is fixed once we fixe the height of any point of $R \cap (\mathbb{Z} \times [0, 1])$.

- The function H is up-continuous, *i.e.*, for any point $(i_0, y_0) \in D$,

$$\lim_{y \to y_0^+} H(i_0, y) = H(i_0, y_0).$$

- For any $i \in \{1, ..., n\}$, and for any $y_1, y_2 \in [0, 1]$, $y_1 < y_2$, $H(i, y_2) - H(i, y_1)$ is equal to the number of beads on the i^{th} thread between y_1 and y_2.
- If there is a bead at some point (i_0, y_0), then on the neighboring threads $i = i_0 \pm 1$, we have

$$\lim_{y \to y_0^-} H(i_0 \pm 1, y) = H(i_0, y_0) - \frac{1}{2}.$$

The definition of the height function of the bead model on the torus is an analogue of that on a simply connected region. In the toroidal case, the coordinates of beads take values in $(\mathbb{Z}/n\mathbb{Z}) \times (\mathbb{R}/\mathbb{Z})$. Any toroidal bead configuration lifts to a configuration on $\mathbb{Z} \times \mathbb{R}$, and there exists a unique (up to a constant) un-normalized height function defined on the whole plane that corresponds to this configuration. This height function is n-periodic in x and 1-periodic in y, so this defines a unique (up to a constant) multivalued height function H defined on $(\mathbb{Z}/n\mathbb{Z}) \times (\mathbb{R}/\mathbb{Z})$, or equivalently (without considering the topology) defined on $\{1, 2..., n\} \times [0, 1[$.

5.1.4 Boundary conditions and periodic conditions

The way to define the boundary conditions may seem a little bit artificial. We first give an intuitive explanation: for a bead model in a simply connected region R, the interlacing property yields a collection of inequalities between the vertical coordinates of some pairs of beads on neighboring threads. For almost every bead, given the position of every other bead, the position of the underlying bead is restricted by four inequalities, but those near the boundary of R may have less restrictions. We consider the boundary condition as a collection of supplementary restrictions for these beads.

We begin by defining the fixed boundary conditions.

Definition 5.1.2. For any planar simply connected domain $R \subset]0, n + 1[\times[0, 1]$, the bead model on it is said to have *fixed boundary condition* if, given a fixed exterior bead configuration $\mathbf{B}^{ext}$ on $(\mathbb{Z} \times \mathbb{R})\backslash R$, the union of any bead configuration of R and $\mathbf{B}^{ext}$ is a bead configuration of $\mathbb{Z} \times \mathbb{R}$.

A fixed boundary condition means fixing the number of beads on every thread $i \in \{1, 2, ..., n\}$ and giving a collection of inequalities on the vertical coordinates of the beads inside R. It is uniquely determined by the exterior bead configurations $\mathbf{B}^{ext}$ on $(\mathbb{Z} \times \mathbb{R})\backslash R$ modulo an equivalence relation: if two exterior configurations give the same restriction on the vertical coordinates of the beads inside R, then they are equivalent.

In some cases it is easier to describe the boundary condition by fixing the height function on the boundary. For example, it is simple to verify that when $R = [1, n] \times [0, 1]$, the following definition of a fixed boundary condition is reduced to Definition 5.1.2.

Definition 5.1.3. For the bead model on $R = [1, n] \times [0, 1]$, a function

$$H^{\partial} : (\{0, n+1\} \times [0, 1]) \cup (\{1, 2, ..., n\} \times \{0, 1\}) \to \mathbb{R}$$

is called *boundary height function* if

- H^{∂} takes value in $\frac{1}{2}\mathbb{Z}$ up to a constant.
- Restricted to $\{0\} \times [0, 1]$ or $\{n+1\} \times [0, 1]$, H^{∂} viewed as a function of y is non-decreasing, piecewise constant and every jump is equal to 1.
- For every $i \in \{0, 1, ..., n+1\}$, $H^{\partial}(i, 1) - H^{\partial}(i, 0) \in \mathbb{N}$.
- For every $i \in \{0, 1, ..., n\}$, $H^{\partial}(i+1, 1) - H^{\partial}(i, 1)$ and $H^{\partial}(i+1, 0) - H^{\partial}(i, 0)$ take values in $\{\pm\frac{1}{2}\}$.

A bead model on R is said to have *fixed boundary condition given by* H^{∂} if every bead configurations $\mathbf{B}$ can be extended to a bead configuration of $\{0, ...n+1\} \times [0, 1]$, and the height function of the extended configuration coincides with H^{∂} where H^{∂} is defined.

Clearly, the number of beads is fixed by the height function, and it is equal to

$$\sum_{i=1}^{n} \big(H^{\partial}(i, 1) - H^{\partial}(i, 0)\big).$$

It is not hard to adapt the above definition into a more general shape of R. Define the neighborhood of a bead model on R as the following polygon P, where

$$P = \bigcup_{(i,y) \in R \cap (\mathbb{Z} \times \mathbb{R})} ([i-1, i+1] \times \{y\}) = R \cap (\mathbb{Z} \times \mathbb{R}) + [-1, 1] \times \{0\},$$

see Figure 5.4 for an example of polygon P. There the boundary function H^{∂} is defined on

$$\partial P \cap (\mathbb{Z} \times [0, 1]).$$

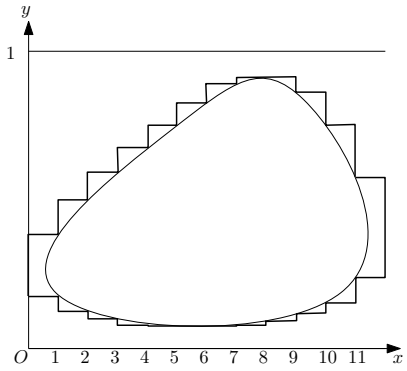

Figure 5.4: An example of polygon P.

We end this part by the following definition.

Definition 5.1.4. Let $R \subset]0, n+1[\times[0,1]$ be a simply connected domain, and let $\mathcal{U}$ be a subset of fixed boundary conditions of the bead model on R. The bead model is said to have the *$\mathcal{U}$-boundary condition* if it contains all the configurations with fixed boundary conditions taken from $\mathcal{U}$.

Especially, if $\mathcal{U}$ has only one element, the $\mathcal{U}$-boundary condition is just a fixed boundary condition, and if $\mathcal{U}$ contains all possible fixed boundary conditions, we say that the bead model has free boundary conditions.

Now consider the toroidal case. A toroidal bead configuration gives rise to a configuration in $\mathbb{Z} \times \mathbb{R}$, n-periodic in i and 1-periodic in y. As in the dimer model, for any $(i_0, y_0) \in \mathbb{Z} \times \mathbb{R}$, define the horizontal height change as

$$H_x = H(i_0 + n, y_0) - H(i_0, y_0),$$

and the vertical height change as

$$H_y = H(i_0, y_0 + 1) - H(i_0, y_0).$$

It is not hard to see that when the number of beads is not 0, (H_x, H_y) takes value in

$$\left\{-\frac{n}{2}+1, -\frac{n}{2}+2, ..., \frac{n}{2}-2, \frac{n}{2}-1\right\} \times \mathbb{N}^*,$$

independent of the choice of (i_0, y_0).

Definition 5.1.5. For every given pair

$$(a, b) \in \left\{-\frac{n}{2}+1, -\frac{n}{2}+2, ..., \frac{n}{2}-2, \frac{n}{2}-1\right\} \times \mathbb{N}^*,$$

we say that a toroidal model has *periodic boundary condition* (a, b) if its height change (H_x, H_y) is equal to (a, b).

Clearly, the number of beads is fixed by the periodic conditions and equal to $nH_y = nb$.

5.1.5 The uniform measure of the bead model

Consider a bead model with fixed boundary condition or periodic condition, which fixes the number of beads in the model. Denote the number of beads by N. The vertical coordinates can be viewed as a subset of $[0,1]^N$ or $\mathbb{T}^N$ (the N-dimensional torus). Moreover, the fixed boundary condition is equivalent to a collection of inequalities, so the set of the vertical coordinates is a convex set. The meaning of inequality is not clear for the toroidal case, but it is not hard to verify that the periodic condition also gives a convex subset of $\mathbb{T}^N$. In both cases, it makes sense to talk about the Lebesgue measure of the set of the vertical coordinates. Thus, we can define the uniform bead measure:

Definition 5.1.6. For a fixed, resp. periodic, boundary condition of the bead model with N beads, the *uniform bead measure* is the uniform probability measure of the vertical coordinates on the convex set determined by the fixed, resp. periodic, boundary condition, viewed as a subspace of $[0,1]^N$, resp. $\mathbb{T}^N$, equipped with the Lebesgue measure.

In particular, under the uniform measure, the event that any two beads have the same vertical coordinate is a subspace of the convex of coordinates with lower dimension. So with probability 1, the vertical coordinates of the beads are all different.

5.1.6 Bead configuration as limit of lozenge tilings: a second view

Now that we have defined the fixed and periodic conditions of a bead model and the uniform measure, the argument that "the bead model is a limit of the lozenge tiling model" in Section 5.1.2 can be described in a more detailed way. As usual, we respectively discuss the case of a simply connected planar domain and that of torus.

To simplify the discussion, we suppose that the simply connected planar domain is $R = [1,n] \times [0,1]$ where n as usual is the number of threads. Given a boundary condition H^∂ as in Definition 5.1.3, for any $l \in \mathbb{N}^*$ big enough, we construct a very tall polygon R_{l,H^∂} tileable by lozenges as follows.

We first construct two piecewise linear paths p_0 and p_1. The path p_0 is a piecewise linear continuous path defined on $[0,n+1]$, which is a linear extension of $H^\partial(x,0) - H^\partial(0,0)$ on every interval $x \in [i,i+1]$, $i \in \{0,1,...,n\}$. Define analogously p_1 on $[0,n+1]$ as a piecewise linear extension of $H^\partial(x,1) - H^\partial(0,1) + l$. The paths

$$p_0, \quad p_1, \quad \{0\} \times [0,l],$$

$$\{n+1\} \times [H^\partial(n+1,0) - H^\partial(0,0), H^\partial(n+1,1) - H^\partial(0,1) + l]$$

enclose a region of $\mathbb{R}^2$ when l is big enough so that p_0 and p_1 do not intersect. The paths p_0 and p_1 correspond to the upper and lower boundary conditions of R, and we still need to remove some tiny triangles from this region so that it corresponds to the left and right boundary condition.

For any $j \in \mathbb{N}$, define Δ_j^0 as the triangle defined by the three vertices

$$(0,j),\ (0,j+1),\ (1,j+\frac{1}{2})$$

and for any $j' \in \mathbb{N}$ define $\Delta_{j'}^1$ as the triangle defined by

$$(n+1, H^\partial(n+1,0) - H^\partial(0,0) + j'), \quad (n+1, H^\partial(n+1,0) - H^\partial(0,0) + j' + 1),$$

$$(n, H^\partial(n+1,0) - H^\partial(0,0) + j' + \frac{1}{2}).$$

Suppose that the jumps of $H^\partial(0,y)$ (resp. $H^\partial(n+1,y)$) are at $(0,y_k)$ (resp. $(n+1,y_{k'})$), we remove the triangles $\Delta^0_{\lfloor ly_k\rfloor}$ and $\Delta^1_{\lfloor ly_{k'}\rfloor}$ (when l is large enough, these triangles are all different) from the region defined above, and we define R_{l,H^∂} as the new domain. A removed triangle is called a *crack* on the left or on the right boundary of R_{l,H^∂}. It is not hard to check that R_{l,H^∂} is tileable.

For some reason that will be clear in Chapter 6, we are particularly interested in the case where there are no cracks, *i.e.* the function H^∂ restricted to $i=0$ or on $i=n+1$ is constant. This domain is tileable in the following way: consider the case $l=0$, the region R_{0,H^∂} is tileable and only tileable by all $\diamond$. Now for $l>0$, the region $R_{l,H^\partial}\backslash R_{0,H^\partial}$ is enclosed by two pairs of parallel paths, and it is easy to see that this difference is tileable by $\diagup$ and $\diagdown$.

Figure 5.5 gives an illustration of a bead model of 9 threads and boundary condition H^∂. On the left, the grey region is R_{0,H^∂}, tiled in the only possible way. It is enclosed in a bigger polygon R_{7,H^∂}, which can be tiled by $\diagup$ and $\diagdown$. On the right is a general tiling. Readers can think of a pile of boxes in $\mathbb{R}^3$ and a lozenge tiling is its projection on $\mathbb{R}^2$ in the direction $(1,1,1)$. The height function H on the vertices is given by the projection of the pile in the direction $(1,1,0)$ (the up-down direction may be contradictory to the intuition). The number of horizontal lozenges in a tiling is the projection of this pile on $\mathbb{R}^2$ in the direction $(0,0,1)$, so it is independent of the exact pile of boxes and l (the height of that pile).

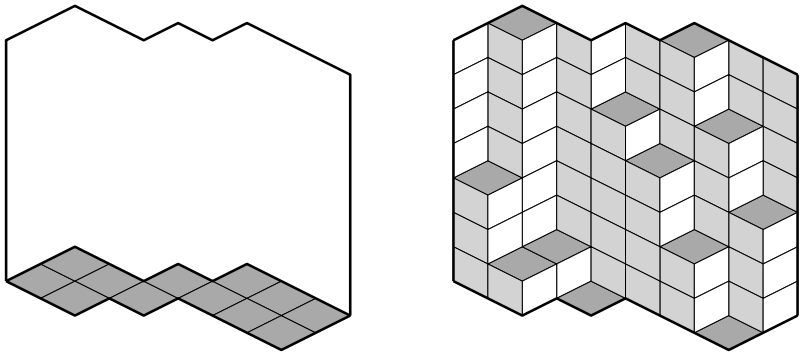

Figure 5.5: Tiling R_{0,H^∂} and R_{7,H^∂}.

If we consider the uniform measure on the tilings, it is not hard to check that when $l\to\infty$, the joint Dirac measure of the positions of the horizontal lozenges $\diamond$ in a uniform tiling of R_{l,H^∂} and vertically normalized by l converges weakly to that of the uniform bead measure with boundary condition H^∂.

The torus is much simpler. We consider $T_{l,n}$ as a torus of size $n\times l$ where l is big enough. Its height change (H_x,H_y) can take value in

$$\left\{-\frac{n}{2}+1,-\frac{n}{2}+2,...,\frac{n}{2}-2,\frac{n}{2}-1\right\}\times\mathbb{N}^*\cup\left\{(\pm\frac{n}{2},0)\right\},$$

where $(\pm\frac{n}{2}, 0)$ correspond to the cases that there are only ◸ or ◹, so they should not be taken into consideration. If we fix (H_x, H_y), then the number of ◇ is fixed and equal to nH_y. When $l \to \infty$ the joint Dirac measure of the positions of ◇ in a uniform tiling of $T_{l,n}$ and vertically normalized by l converges weakly to that of the uniform bead measure with periodic condition (H_x, H_y).

5.2 Standard Young tableaux and bead model

5.2.1 Young diagrams and Young tableaux

A *Young diagram* is a finite collection of boxes, left aligned, and the lengths of the lines are in non decreasing order from bottom to top. It is named in honor of Young who constructs the irreducible representations of the symmetric groups S_n [You28, You30]. It is also called a *Ferrers diagram* if we replace the boxes by dots. Note that in the definition above we use the French convention. In the English convention, the lines are placed non decreasing from top to bottom, and in the Russian convention the diagram is turned by 45°, see Figure 5.6.

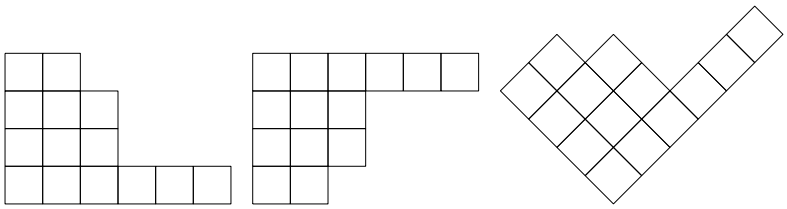

(a) French (b) English (c) Russian

Figure 5.6: Three conventions for the Young diagrams.

The diagrams containing n boxes give integer partitions of n, which are sequences of non decreasing integers that sum up to n. The *conjugate* of a Young diagram λ is defined as the transpose of the diagram, and we denote it by $\lambda^\perp$. The number of boxes of λ is denoted by $|\lambda|$ and called the *dimension* of the diagram. If $|\lambda| = n$, we write $\lambda \vdash n$.

Given two Young diagrams μ and η, if η is contained in μ as its bottom-left most part under the French convention (we write $\eta \leq \mu$ in this case), then their difference is called a *skew Young diagram* $\mu\backslash\eta$. A skew diagram can also be simply denoted by a single Greek letter, for example we let $\lambda = \mu\backslash\eta$.

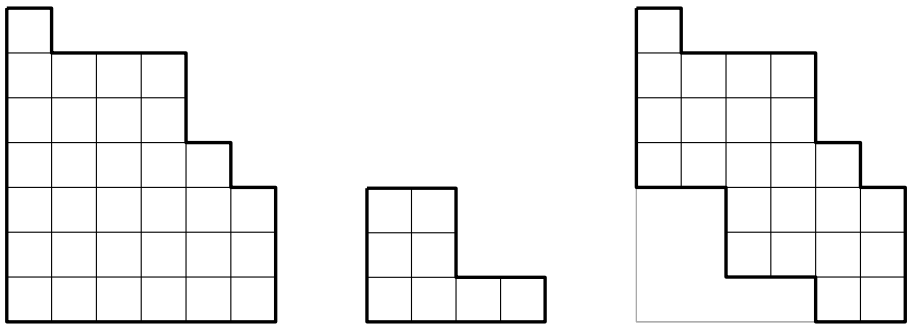

(a) Diagram μ (b) Diagram η (c) Diagram $\lambda = \mu \backslash \eta$

Figure 5.7: An example of skew Young diagrams.

A *Young tableau* of a Young diagram or a *skew Young tableau* of a skew Young diagram is obtained by filling the boxes of the corresponding diagram with integer numbers given in an alphabet as a subset of $\mathbb{N}^*$. Denote the diagram by λ. If we take the alphabet to be $\{1, 2, ..., |\lambda|\}$ and fill the diagram in such a way that the numbers in each row and column (under the French convention) are increasing, then such a tableau is called *standard*. If in the tableau the numbers of each row is non-decreasing but those of each column are strictly increasing, then the tableau is called *semi-standard* (in the semi-standard case we have no specific restriction on the choice of the alphabet).

5.2.2 A map from the bead configurations to the standard Young tableaux

In Section 5.1.6 we have considered a specific case with fixed boundary conditions of the bead model, where the domain is taken to be $R = [1, n] \times [0, 1]$, and the boundary function H^∂ restricted on $i = 0$ and $i = n + 1$ is constant. In Figure 5.5, we give an example of a lozenge tiling corresponding to this kind of boundary condition, and we see that R_{0,H^∂} is a skew Young diagram under the Russian convention if we view every horizontal lozenge in the tiling of R_{0,H^∂} as a box. We generalize this observation.

For every (skew) Young diagram λ written under the Russian convention, let n be the number of columns (*i.e.* the number of possible horizontal positions that a box may be located at). Consider a bead model defined in the region $[1, n] \times [0, 1]$ with a boundary function H^∂ such that H^∂ is constant if restricted on $i = 0$ and $i = n + 1$, and the path p_0 (resp. p_1) constructed as in Section 5.1.6 is exactly the lower (resp. upper) boundary of the Young diagram (vertically scaled by 2).

There is a natural way to encode the boxes of the Young diagram with the beads in the corresponding bead model: the j^{th} bead on the i^{th} thread naturally corresponds to the j^{th} box on the i^{th} column of the (skew) Young diagram under the Russian convention. In particular, the number of beads is equal to $|\lambda|$.

For any bead configuration, let $y_{i,j}$ be the vertical coordinate of the j^{th} bead on

the i^{th} thread. We sort them in a non-decreasing order:

$$y_{i_1,j_1} \leq y_{i_2,j_2} \leq ... \leq y_{i_{|\lambda|},j_{|\lambda|}}.$$

As under the uniform measure, the probability that any two coordinates coincide is equal to 0, with probability 1 we can rewrite the inequalities above as

$$y_{i_1,j_1} < y_{i_2,j_2} < ... < y_{i_{|\lambda|},j_{|\lambda|}}. \tag{5.1}$$

For the given diagram λ, define $\mathcal{T}_\lambda$ as the set of standard tableaux of λ and $\mathcal{B}_\lambda$ as the space of bead configurations with same constraint. Any inequality on the vertical coordinates of a pair of beads on neighboring threads interprets itself to be an inequality relation between the ranks of neighboring boxes, which is exactly the inequality relation of the neighboring entries in the definition of a standard Young tableau. So conditioned to that all vertical coordinates $y_{i,j}$ are different, if we define the following map $\mathcal{Y}$ as:

$$\begin{aligned} \mathcal{Y}: \quad \mathcal{B}_\lambda &\to \mathcal{T}_\lambda, \\ \mathbf{B} &\mapsto T, \end{aligned}$$

where $T = \mathcal{Y}(\mathbf{B})$ is a filling of λ such that $T(i_k, j_k) = k$ for any $k \leq |\lambda|$ (define $T(i,j)$ as the number in the cell (i,j) of T). Then for every configuration $\mathbf{B} \in \mathcal{B}_\lambda$, $T = \mathcal{Y}(\mathbf{B})$ is a tableau whose entries are all different and verify the constraint of a Young tableau, thus $T \in \mathcal{T}_\lambda$.

In short, the map $\mathcal{Y}$ just turns the continuous coordinates y to its total rank among all the coordinates. If we take the uniform measure of the bead model, the measure induced by $\mathcal{Y}$ on the standard (skew) tableaux is the uniform measure. In fact, for any $T \in \mathcal{T}_\lambda$, the induced probability measure is by definition proportional to the Lebesgue measure of its preimage $\mathcal{Y}^{-1}(T)$, *i.e.*, the volume of the simplex

$$0 < y_{i_1,j_1} < y_{i_2,j_2} < ... < y_{i_{|\lambda|},j_{|\lambda|}} < 1,$$

which is always equal to $\frac{1}{|\lambda|!}$ for any T. Thus the induced measure is uniform.

The fact that the map $\mathcal{Y}$ from $\mathcal{B}_\lambda$ to $\mathcal{T}_\lambda$ preserves uniform measure and that this gives a way to study $\mathcal{T}_\lambda$ is known to the authors of [BR10]. They enumerate the standard Young tableaux of a diagonal strip (see Figure 5.8), a particular type of skew shapes. Their work is based on [Elk03], which studies the case where the strip is of width 2 (the width means the maximal number of boxes on the same column under the Russian convention) so Inequalities (5.1) can be written as a series of inequalities like

$$y_{1,1} > y_{2,1} < y_{3,1} > y_{4,1} < ...$$

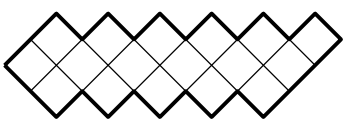

Figure 5.8: A diagonal strip of width 3.

Chapter 6

A variational principle of the bead model and limit shape of random standard Young Tableaux

It is known by [CKP01] (see also Section 2.4) that for the dimer model, when the size of the domain tends to infinity while the normalized boundary condition tends to a fixed asymptotic function, the normalized random surface converges in probability to the surface that maximizes a functional called entropy. As the bead model is some kind of limit of the dimer measure, we can expect that the results of the dimer model also apply to the bead model in some way.

The limit shape of standard Young tableaux with given asymptotic shape of diagram is studied in [PR07] and [Ś06] via different approaches. In [PR07], the authors consider a rectangular shape and use the hook formula to establish a variational principle, while in [Ś06] the author consider a tableau of a (not skew) Young diagram as a subrepresentation of the symmetric group. We summarize these results in Appendix A.

By the map constructed in Section 5.2.2 from the uniform bead configurations to standard (skew) Young tableaux, once we have proved the existence of a limit shape for the bead model, it is natural to think of the existence of the limit shape of standard tableaux as corollary of the corresponding results in the bead model.

Since it is already very interesting, and also due to some technical reasons, in this chapter we will mainly consider the bead model corresponding to a (skew) Young diagram, which means with fixed boundary condition constant on the left and right side, see Sections 5.1.6 and 5.2.2. Consider a sequence of such bead models whose numbers of threads and beads tend to infinity. If their normalized boundary functions have an asymptotic limit, then we prove that the normalized height function under the uniform norm converges in probability to the unique surface that maximize a functional $Ent(.)$ called the entropy function. With the help of the results on the bead model, in Section 6.6, we generalize the results of the limit shape random Young tableaux of [PR07] and [Ś06] to a more general shape, notably containing

also the skew shapes.

Here is an outline of this chapter. In Section 6.1, we define the (adjusted) combinatorial entropy $S(.)$ of the bead model. The definition may appear not natural, but we prove that it is some kind of limit of that of the dimer model to have the good order in the limit.

In [CKP01] the authors compare planar dimer configurations having some slope with those on the torus having the same slope. Using the same idea, in Section 6.2, we consider the toroidal bead model and compute its free energy and the local entropy function $ent(.,.)$. We postpone the proof of the relation between the local entropy function ent and the combinatorial entropy S to Section 6.4.

Sections 6.3 and 6.4 can be viewed as an adaption of the ideas of [CKP01] and [CEP96] to the bead model. We prove that there is a functional $Ent(.)$ defined on the space of surfaces (to be precised), and there is a variational principle there. The large deviation property (Theorem 6.4.10) particularly yields that when the size of the bead model is big, the random surface converges to the maximizer of the functional Ent (Theorem 6.4.15).

Please pay attention to the different uses of the same terminology "entropy" in this chapter:

- the adjusted combinatorial entropy S of the bead model, see Section 6.1.
- the local entropy function ent as a function of the slope, see Section 6.2.2.
- the entropy function Ent as a functional on the space of admissible functions, see Section 6.3.2.

As the bead model is a limit of the dimer model, it is natural to consider the following question: is the limit shape of the bead model a limit of the limit shapes of the dimer model? We give a positive answer to this question. Theorem 6.5.1 of Section 6.5 proves the commutative diagram (6.39). Authors of [KO07] provide a way to find the limit shape of the dimer model, especially for that of the hexagon lattice on domains with an asymptotic boundary condition piecewise linear in the direction of the edges of the hexagons. By the commutative diagram, their result implies directly a way to find the limit shape of the bead model. We give an example at the end of Section 6.5.

In Section 6.6, we apply the results on the bead model to random standard Young tableaux with a given asymptotic shape. We prove a surface version (Theorem 6.6.1) and a contour line version (Theorem 6.6.2) of convergence of the tableaux. In Section 6.6.2, we consider a jump process encoding the standard Young tableaux, originally proposed in [Rom12] for square tableaux and prove the existence of an arctic curve for a general piecewise shape.

6.1 Entropy of the bead model

Our first task is to define the combinatorial entropy. Once defined, we will use the letter S to denote it.

First consider the classical case where a random variable X takes a countable number of possible different values (or states) with p_i be the corresponding probability. For example, we can consider the dimer model. In this case, the *combinatorial entropy* is defined as

$$S(X) = \sum_i -p_i \ln p_i,$$

and if every state has the same probability, then

$$S(X) = \ln Z,$$

where Z is the number of states, known as the "partition function".

One significant difference between the bead model and the dimer model is that rather than considering the "number" of dimer configurations in a state, here we should consider the volume of similar bead configurations. Moreover, in practice we will adjust it by adding an additional term to let the entropy be of the good order. We give the definition here below.

Definition 6.1.1. Consider a bead model with fixed number of beads. Let N be the number of beads and n be that of threads. Consider a random bead configuration as a random vector X taking values in $[0,1]^N$, where every component of X is the vertical coordinates of the corresponding bead (in the toroidal case the coordinates are in the sense of modulo 1).

For any point $\mathbf{y} = (y_1, y_2, ..., y_N) \in [0,1]^N$, define $\rho(\mathbf{y})$ as the *density of the bead measure* $\mathbb{P}$ at the point $\mathbf{y}$ with respect to the Lebesgue measure of $[0,1]^N$ whenever it exists, *i.e.*,

$$\rho(\mathbf{y}) = \lim_{\varepsilon \to 0} \frac{\mathbb{P}(X \in \prod_{i=1}^N [y_i - \varepsilon, y_i + \varepsilon])}{(2\varepsilon)^N}$$

whenever this limit exists.

If we consider the uniform bead measure, and if we define V as the N-dimensional Lebesgue measure of the convex set of coordinates, then

$$\rho(\mathbf{y}) = \begin{cases} \frac{1}{V} & \text{if } h \text{ is an inner point of the convex set of the admissible coordinates,} \\ 0 & \text{otherwise,} \end{cases}$$

and the undefined points are negligible.

We use the same letter S to denote the adjusted combinatorial entropy of the bead model.

Definition 6.1.2. If the density ρ is well defined almost everywhere, then for the bead model with a fixed boundary condition or periodic condition, we define the

(adjusted) combinatorial entropy S associated to the random variable X of the bead model as

$$S(X) = \int_{[0,1]^N} -\rho(\mathbf{y}) \ln \rho(\mathbf{y}) dy_1 ... dy_N + N \ln n,$$

where N is the number of beads and n is the number of threads.

The term $N \ln n$ may seem not natural, but soon we will see that this term helps to adjust the entropy so that it is of a proper order if we consider a sequence of bead models where $n \to \infty$ and N is of order n^2.

In particular, if we consider the uniform measure, we have

$$S(X) = \ln V + N \ln n.$$

The following lemma is a general result for entropies.

Lemma 6.1.3. *Suppose* $E = \{E_1, E_2, ...\}$ *is a countable partition of the state space, and* I_E *is a random variable that tells* X *is in which* E_i*, and* X_i *is the variable equipped with the conditional law of* X *restricted on* E_i*. We have*

$$S(X) = S(I_E) + \sum_i \mathbb{P}(X \in E_i) S(X_i). \tag{6.1}$$

The proof is straightforward.

We want to remark that the decomposition (6.1) allows us to define the entropy S for a union of conditions that not necessarily have the same number of beads once we have defined the probability of taking different number of beads N:

Definition 6.1.4. For a random bead configuration X that with probability p_i to be in the state of N_i beads, define

$$S(X) = -\sum_i p_i \ln p_i + \sum_i p_i S(X_i),$$

where X_i is the random configuration equipped with the induced probability measure conditioning to have N_i beads.

The following proposition proves that the entropy of the bead model under the uniform measure is the limit of the entropies of the corresponding lozenge tiling models. This discrete approximation is useful in the remaining part of this chapter.

Consider a bead model with n threads and N beads, with a fixed boundary condition H^∂ or a given periodic condition (H_x, H_y). Consider the corresponding lozenge tiling model, where for l sufficiently large we tile a simply connected domain R_{l,H^∂} or a toroidal region $T_{l,n}$. In each of the cases, we define $Z_{l,n}$ as the partition function of the lozenge tilings of the region, and V as the volume of the convex set in $[0,1]^N$ or $(\mathbb{R}/\mathbb{Z})^N$ formed by the vertical coordinates of the beads.

Proposition 6.1.5. *For either a fixed boundary condition H^∂ or a given periodic condition (H_x, H_y), we have the following relation between $Z_{l,n}$ and V:*

$$\ln V = \lim_{l\to\infty} \big(\ln Z_{l,n} - N \ln l\big). \tag{6.2}$$

In particular, if we let $l = mn$, then for fixed n and N, $l \to \infty$ is equivalent to $m \to \infty$, and we have that the entropy of the bead model is equal to

$$S(X) = \lim_{m\to\infty} \big(\ln Z_{mn,n} - N \ln m\big). \tag{6.3}$$

Proof. Consider the convex set of the vertical coordinates of the beads. For any $l \in \mathbb{N}^*$ big enough, $Z_{l,n}$ is approximately equal to the number of points on the lattice $\big(\frac{1}{l}\mathbb{Z}\big)^2$ inside the convex set, so we have

$$\lim_{l\to\infty} \frac{Z_{l,n}}{l^N} = V,$$

and by taking logarithm we get Equation (6.2) in the proposition. Replacing l by mn, we obtain Equation (6.3). □

We now explain why the combinatorial entropy S defined in Definition 6.1.2 is adjusted by $N \ln n$, and why we use the substitution of l by mn in Proposition 6.1.5. As mentioned, we are interested in the asymptotic behavior of the bead model, *i.e.* in the limit $n \to \infty$. If the boundary function H^∂ of the bead model has an asymptotic limit when $n \to \infty$, then N is asymptotically proportional to n^2. We write $H^\partial = H^\partial(n)$ and $N = N(n)$ to emphasize their dependances on n.

For every given m and n, consider $R_{mn,H^\partial(n)}$ as in Section 5.1.6. Since we fix the asymptotic shape of $H^\partial(n)$ in the remaining part of this thesis, from now on we simply write $R_{mn,n}$ instead of $R_{mn,H^\partial(n)}$ to simplify the notation. Consider

$$\frac{\ln Z_{mn,n} - N(n) \ln m}{n^2}. \tag{6.4}$$

If we fix m and let $n \to \infty$ (we pretend to forget that m should be chosen large enough depending on n), the boundary condition of $R_{mn,n}$ has an asymptotic limit, so by [CKP01, KOS06], (6.4) converges when m is fixed and $n \to \infty$. Meanwhile, Proposition 6.1.5 proves that (6.4) converges to $\frac{S(X)}{n^2}$ when $m \to \infty$ for fixed n.

For this reason, it is natural to ask the following questions:

- In (6.4), can we take the limit $m \to \infty$ first and then the limit $n \to \infty$?
- If this limit exists, does it have a good order?
- Can we exchange the order of the limits in m and in n?

We give a positive answer to each of them in Sections 6.4 and 6.5, but before that we want to give some discussion.

We first give an intuitive explanation for the first and the second questions in a specific case. When the boundary condition of the bead model corresponds to a square Young diagram (Section 5.2.2), then $N = \frac{(n+1)^2}{4}$. The volume V is equal to the number of possible total ranking of the vertical coordinates (which is the number of standard Young tableaux for a $\frac{n+1}{2} \times \frac{n+1}{2}$ square diagram) times the volume of the convex set of the coordinates totally ranked (which is equal to $\frac{1}{N!}$). Thus, by the hook formula (Appendix A.1.1), we have

$$\begin{aligned}
\frac{S(X)}{n^2} &= \frac{\ln V + N(n)\ln n}{n^2} \\
&= \frac{1}{n^2}\left(\ln\left(\frac{N(n)!}{\prod_{1\le i,j\le\frac{n+1}{2}}(i+j+1)}\frac{1}{N(n)!}\right) + N(n)\ln n\right) \\
&= \frac{1}{n^2}\left(\sum_{1\le i,j\le\frac{n+1}{2}} \ln\left(\frac{n}{i+j+1}\right)\right) \\
&\simeq \frac{1}{4}\iint_{x,y\in[0,1]} \ln\frac{1}{x+y}dxdy.
\end{aligned}$$

This double integral also appears in [PR07], which studies the limit shape of a random square Young tableaux using hook formula, see Appendix A.1.2.

For the third question, we show why a priori it is not obvious that we can exchange the order of the limits in n and in m. In fact, in the proof of Proposition 6.1.5 we use an approximation of the volume of a convex set of dimension $N(n) = O(n^2)$ by a mesh of size $\frac{1}{mn}$, and this approximation is not uniform in m and n for whatever type of convex set. For example, if we consider a simplex

$$0 \le y_1 \le y_2 ... \le y_{N(n)} \le 1,$$

the volume of this simplex is $\frac{1}{N(n)!}$, while the number of lattice points of a $(\mathbb{Z}/mn)^{N(n)}$ mesh inside this simplex is equal to the number of choosing $N(n)+1$ non-negative ordered integers that sum to mn, which is equal to $\binom{mn+N(n)}{N(n)}$. Thus, the approximation has a relative error of order

$$\begin{aligned}
&\binom{mn+N(n)}{N(n)}\left(\frac{1}{mn}\right)^{N(n)}\left(\frac{1}{N(n)!}\right)^{-1} - 1 \\
=\ &\left(1+\frac{1}{mn}\right)\left(1+\frac{2}{mn}\right)...\left(1+\frac{N(n)}{mn}\right) - 1.
\end{aligned}$$

We see that as in Proposition 6.1.5, for fixed n, the relative error tends to 0 when $m \to \infty$, while this is not uniform in n.

6.2 Free energy and local entropy function of the bead model

In this section, we consider a sequence of toroidal bead models with given asymptotic periodic condition (which means that the height change (H_x, H_y) is proportional to the number of threads n), and we calculate its entropy when the size of the torus tends to infinity. In the computation we mainly use the discrete approximation given by Proposition 6.1.5.

In [Bou09], the author defines a family of ergodic Gibbs bead measures which are limits of the ergodic Gibbs measures of the dimer model on the hexagonal lattice when some weights degenerate. We begin by considering this parameterized weight setting of the dimer model, then apply a Legendre transform on the adjusted partition function of the dimer model to obtain the local entropy function *ent*. The proof of that *ent* is equal to the normalized combinatorial entropy S is postponed to Theorem 6.4.10 of Section 6.4.

6.2.1 Free energy

Throughout this section, suppose that a lozenge ◇ has weight a, ◹ has weight b and ◺ has weight c, see Figure 6.1.

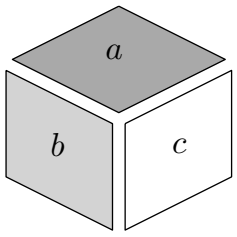

Figure 6.1: The lozenges respectively weighted a, b and c.

Consider a fundamental domain as Figure 6.2. The characteristic polynomial is

$$a^2 z - (b + cw)^2 / w.$$

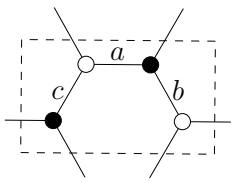

Figure 6.2: The fundamental domain.

The advantage of taking this domain is that it has an obvious horizontal-vertical decomposition. We consider $\mathcal{G}_{mn,n}$ as a toroidal graph which is $mn \times n$ this fundamental domain. The dimer model on $\mathcal{G}_{mn,n}$ corresponds to a toroidal lozenge tiling

model defined in Section 5.1.6 where we use the substitution of l by mn. But pay attention, $\mathcal{G}_{mn,n}$ corresponds to $T_{mn,2n}$ rather than $T_{mn,n}$.

We take two parameters $\alpha \in \mathbb{R}^+$, $\gamma \in]-1,1[$, and let $a = \alpha/m$, $b = e^{\alpha\gamma/m}$, $c = 1$. The author of [Bou09] proves that the ergodic Gibbs dimer measure under such setting, which is to first take $n \to \infty$ for a dimer model on $\mathcal{G}_{mn,n}$, converges to an ergodic Gibbs measure on the configurations of the beads on threads when $m \to \infty$, and the limiting measure is parameterized with respect to α and γ. We will take the reverse order, *i.e.*, we first take $m \to \infty$ and then $n \to \infty$.

Denote the dimer partition function of $\mathcal{G}_{mn,n}$ by $Z_{mn,n}(\alpha,\gamma)$. The set of dimer configurations is denoted by $\mathcal{M} = \mathcal{M}(\mathcal{G}_{mn,n})$. Let N_a (resp. N_b and N_c) be the number of edges with weight a (resp. b and c), then the partition function is

$$Z_{mn,n}(\alpha,\gamma) = \sum_{M\in\mathcal{M}} a^{N_a(M)} b^{N_b(M)} c^{N_c(M)} = \sum_{M\in\mathcal{M}} (\alpha/m)^{N_a(M)} e^{\alpha\gamma N_b(M)/m}.$$

To simplify the notation we denote the weight of a configuration $(\alpha/m)^{N_a(M)} e^{\alpha\gamma N_b(M)/m}$ by $w(M)$.

Here the order of $\ln Z_{mn,n}(\alpha,\gamma)$ is n^2 (while for fixed a, b and c the logarithm of the partition function should be of order mn^2). In fact, if we differentiate $\ln Z_{mn,n}(\alpha,\gamma)$ with respect to γ or α, we get:

$$\begin{aligned}
\frac{\partial \ln Z_{mn,n}(\alpha,\gamma)}{\partial\gamma} &= \frac{1}{Z_{mn,n}(\alpha,\gamma)} \frac{\partial Z_{mn,n}(\alpha,\gamma)}{\partial\gamma} = \frac{\sum_{M\in\mathcal{M}} \alpha N_b(M) w(M)}{m\sum_{M\in\mathcal{M}} w(M)} = \frac{\alpha\mathbb{E}[N_b]}{m},\\
\frac{\partial \ln Z_{mn,n}(\alpha,\gamma)}{\partial\alpha} &= \frac{1}{Z_{mn,n}(\alpha,\gamma)} \frac{\partial Z_{mn,n}(\alpha,\gamma)}{\partial\alpha} = \frac{\sum_{M\in\mathcal{M}} \left(\frac{1}{\alpha} N_a(M) + \gamma/m N_b(M)\right) w(M)}{\sum_{M\in\mathcal{M}} w(M)}\\
&= \frac{1}{\alpha}\mathbb{E}[N_a] + \frac{\gamma}{m}\mathbb{E}[N_b].
\end{aligned}$$

When divided by n^2, we get

$$\frac{\partial}{\partial\gamma}\frac{\ln Z_{mn,n}(\alpha,\gamma)}{n^2} = \alpha\frac{\mathbb{E}[N_b]}{mn^2}. \tag{6.5}$$

$$\frac{\partial}{\partial\alpha}\frac{\ln Z_{mn,n}(\alpha,\gamma)}{n^2} = \frac{1}{\alpha}\frac{\mathbb{E}[N_a]}{n^2} + \gamma\frac{\mathbb{E}[N_b]}{mn^2}. \tag{6.6}$$

Since we expect that the number of edges a is of order n^2 and that of edges b and c is of order mn^2, Equations (6.5) and (6.6) show that $\ln Z_{mn,n}(\alpha,\gamma)$ normalized by n^2 is of the good order. The aim of this section is to compute the limit of $\frac{\ln Z_{mn,n}(\alpha,\gamma)}{n^2}$, where we first take $m \to \infty$ and then $n \to \infty$.

Proposition 6.2.1. *For any given $n \in \mathbb{N}^*$, when $m \to \infty$, $Z_{mn,n}(\alpha,\gamma)$ converges.*

Assuming Proposition 6.2.1, we define the partition function of the bead model of the torus of size n and of parameters α and γ as

$$\widetilde{Z}_n(\alpha,\gamma) = \lim_{m\to\infty} Z_{mn,n}(\alpha,\gamma).$$

Proposition 6.2.2. *When $n \to \infty$, $\ln \widetilde{Z}_n(\alpha, \gamma)$ is of order n^2, and*

$$\lim_{n\to\infty} \frac{\ln \widetilde{Z}_n(\alpha,\gamma)}{n^2} = \frac{2\alpha}{\pi}\big(\gamma \arccos(-\gamma) + \sqrt{1-\gamma^2}\big).$$

This limit is called the free energy of the bead model with parameters α and γ per fundamental domain. This value depends on the choice of fundamental domain.

Proof of Propositions 6.2.1 and 6.2.2. Fix the parameters α and γ so we can simply write $Z_{mn,n}$ and $\tilde{Z}_n$ (this notation is only limited to this proof because the notation $Z_{mn,n}$ is already used for the partition function of lozenge tilings of $R_{mn,n}$ or $T_{mn,n}$). The characteristic polynomial is

$$\det \hat{K}(z,w) = a^2 z - (b+cw)^2/w = (\alpha/m)^2 z - (e^{\alpha\gamma/m} + w)^2/w. \tag{6.7}$$

The partition function $Z_{mn,n}$ can be written as a linear combination of 4 terms $Z^{(\theta,\tau)}_{mn,n}$, where $\theta, \tau \in \{0,1\}$, and the term $Z^{(\theta,\tau)}_{mn,n}$ is defined by

$$Z^{(\theta,\tau)}_{mn,n} = \prod_{\substack{z^n=(-1)^\theta,\\ w^{mn}=(-1)^\tau}} \det \hat{K}(z,w) = \prod_{\substack{z^n=(-1)^\theta,\\ u^n=(-1)^\tau}} \prod_{w^m=u} \big((\alpha/m)^2 z - (e^{\alpha\gamma/m}+w)^2/w\big).$$

In the linear combination, the coefficient for every term is either $\frac{1}{2}$ or $-\frac{1}{2}$, where three terms have positive signs and one has negative sign. See Equation (2.3) of Section 2.2.3.

Taking logarithm, we have

$$\ln Z^{(\theta\tau)}_{mn,n} = \sum_{\substack{z^n=(-1)^\theta,\\ u^n=(-1)^\tau}} \sum_{w^m=u} \ln\big((\alpha/m)^2 z - (e^{\alpha\gamma/m}+w)^2/w\big). \tag{6.8}$$

We rewrite (6.7) as

$$-(w-w_1)(w-w_2)/w, \tag{6.9}$$

where w_1 and w_2 are two roots of the polynomial (6.7) given by

$$w_{1,2} = -1 + \frac{\alpha}{m}(-\gamma \pm \sqrt{-z}) + o\left(\frac{1}{m}\right), \tag{6.10}$$

which are close to -1 when m is large.

For given parameters α and γ, parity $(\theta,\tau) \in \{0,1\}^2$, and $n \in \mathbb{Z}$, for fixed $z \in S^1$, we first calculate the sum over m. As in the dimer model, we hope to approximate this sum by an integral. However, as we have stated, now the sum is of order 1 so the integral (which approximates the sum divided by m) is of order $1/m$. So rather than to compare the sum divided by m to the integral as usual, we compare the sum to m times the integral. As a result, the difference between them is something a priori not negligible and should be determined precisely.

For every (θ,τ), the term $Z_{mn,n}^{(\theta,\tau)}$ is a real number, so $\ln Z_{mn,n}^{(\theta,\tau)}$ is either real or purely imaginary. Since the partition function $Z_{mn,n}$ satisfies

$$Z_{mn,n}^{(\theta,\tau)} \leq Z_{mn,n} \leq 2 \max_{(\theta,\tau)} Z_{mn,n}^{(\theta,\tau)},$$

we can just consider the case where $\ln Z_{mn,n}^{(\theta,\tau)}$ is real. Especially, we can just consider it real part.

For every (θ,τ), by (6.8), the real part of the logarithm $\ln Z_{mn,n}^{(\theta,\tau)}$ can be written as a sum over z, u and w. Consider first the sum over w, which by (6.9) can be rewritten as

$$\sum_{w^m=u} \big(\mathfrak{Re}\ln(-1) + \mathfrak{Re}\ln(w-w_1) + \mathfrak{Re}\ln(w-w_2) - \mathfrak{Re}\ln w\big).$$

Since $\ln(-1)$ and $\ln w$ are purely imaginary, the above sum is always equal to

$$\sum_{w^m=u} \big(\mathfrak{Re}\ln(w-w_1) + \mathfrak{Re}\ln(w-w_2)\big). \tag{6.11}$$

We need to compare this to the following value, which is an integral over the unit circle $S^1 = \{w \in \mathbb{C} : |w| = 1\}$:

$$\mathfrak{Re}\Big(m\int_{S^1} \big(\ln(w-w_1) + \ln(w-w_2)\big)\frac{dw}{(2\pi i)w}\Big). \tag{6.12}$$

We calculate the integral (6.12) first. Its value depends on whether the root w_1 and w_2 are inside or outside of the unit circle S^1. If a root is inside the unit circle S^1, we denote this root by w_{in}, and by the fact that $\ln w$ is purely imaginary we have

$$\mathfrak{Re}\Big(m\int_{S^1} \ln(w-w_{in})\frac{dw}{(2\pi i)w}\Big) = \mathfrak{Re}\Big(m\int_{S^1} \ln\big(1-\frac{w_{in}}{w}\big)\frac{dw}{(2\pi i)w}\Big).$$

Since $\big|\frac{w_{in}}{w}\big| < 1$, we can develop $\ln\big(1-\frac{w_{in}}{w}\big)$ into a power series of $\frac{w_{in}}{w}$, whose powers in w are not bigger than -1. The contour integral of any term in this series times $\frac{dw}{(2\pi i)w}$ around S^1 is 0, so for an root inside S^1 we have

$$\mathfrak{Re}\Big(m\int_{S^1} \ln(w-w_{in})\frac{dw}{(2\pi i)w}\Big) = 0.$$

If a root is outside S^1, denote it by w_{out}, we have

$$\mathfrak{Re}\Big(m\int_{S^1} \ln(w-w_{out})\frac{dw}{(2\pi i)w}\Big) = \mathfrak{Re}\Big(m\ln w_{out} + m\int_{S^1} \ln\big(1-\frac{w}{w_{out}}\big)\frac{dw}{(2\pi i)w}\Big).$$

Again, we develop the logarithm $\ln\big(1-\frac{w}{w_{out}}\big)$ into a power series of $\frac{w}{w_{out}}$ with powers in w bigger than 1, so the contour integral is 0.

In conclusion, if we use the indicator function $\mathbb{1}_{out}$ to tell whether a root $w_{1,2}$ is outside S^1, then the integral (6.12) is equal to

$$m \sum_{j=1,2} \mathfrak{Re}\big(\mathbb{1}_{out} \ln(w_j)\big). \tag{6.13}$$

When m is large, the roots w_1 and w_2 are both close to -1, so whether a root is inside or outside the unit circle mainly depends on its real part. When $m \to \infty$, we just need to check whether $\mathfrak{Re}(-\alpha\gamma \pm \alpha\sqrt{-z})$ is positive or negative, and when it is negative, the root w_j is outside S^1, and in the logarithm of $\ln(w_j)$, the only term of order $\frac{1}{m}$ is $\alpha\gamma \mp \alpha\mathfrak{Re}\sqrt{-z}$. Thus, when $m \to \infty$, (6.12) tends to

$$\sum_{+,-} \big(\alpha(\gamma \mp \mathfrak{Re}\sqrt{-z})\big)_+, \tag{6.14}$$

where $(x)_+$ is defined to be $\max\{x, 0\}$.

Summing this term for $u \in S^1$, $u^n = (-1)^\tau$ just multiply it by n. Summing this for $z \in S^1$, $z^n = (-1)^\theta$ and divided by n can be approximated by an integral over S^1:

$$\begin{aligned}
&\int_{S^1} \big(\sum_{+,-} \alpha \left(\gamma \mp \mathfrak{Re}\sqrt{-z}\right)_+ \big) \frac{dz}{(2\pi i)z} \\
= &\int_0^{2\pi} \frac{\alpha}{2\pi} \left(\Big(\gamma + \cos\big(-\theta/2\big)\Big)_+ + \Big(\gamma - \cos\big(-\theta/2\big)\Big)_+ \right) d\theta \\
= &\int_0^{2\pi} \frac{\alpha}{\pi} (\gamma + \cos(\theta))_+ d\theta = \frac{2}{\pi}\big(\alpha\gamma \arccos(-\gamma) + \alpha\sqrt{1-\gamma^2}\big),
\end{aligned} \tag{6.15}$$

and the error term between the sum over u and z and the integral (6.15) is negligible.

Now we consider the difference between (6.11) and (6.12). It suffices to consider the difference between terms of w_1, and the argument for w_2 is similar. We use Euler-Maclaurin formula, and to simplify the notation we denote by f the function

$$f(x; w_1) = \ln(e^{i(\frac{2\pi x + \mathrm{Arg} u}{m})} - w_1),$$

then our problem is reduced to estimating the real part of

$$\sum_{k=1}^{m} f(k; w_1) - \int_0^m f(x; w_1) dx. \tag{6.16}$$

A little remark is that here the function $f(.; w_1)$ is taken in the class C^∞. Both the sum and the integral in (6.16) differ from the original ones but only by imaginary constants, which causes no effect.

Apply the Euler-Maclaurin formula to (6.16) to order two, then we have

$$\begin{aligned}
&\sum_{k=1}^{m} f(k;w_1) - \int_0^m f(x;w_1)dx \\
=\ & \frac{1}{2}\big(f(m;w_1) - f(0;w_1)\big) + 1/12\big(f'(m;w_1) - f'(0;w_1)\big) - \int_0^m \frac{1}{2} f''(x;w_1) B_2(x - \lfloor x \rfloor)dx \\
=\ & \mathbb{1}_{w_1 \in D}\pi i - R(w_1),
\end{aligned}$$

where the first term is imaginary and the second term $R(w_1)$ is the remainder term of the Euler-Maclaurin formula,

$$R(w_1) = \int_0^m \frac{1}{2} f''(x) B_2(x - \lfloor x \rfloor)dx, \tag{6.17}$$

where B_2 is the Bernoulli polynomial of order 2 and f'' is equal to

$$f''(x;w_1) = \frac{e^{i(\frac{2\pi x + \mathrm{Arg}u}{m})} w_1}{\left(e^{i(\frac{2\pi x + \mathrm{Arg}u}{m})} - w_1\right)^2} \left(\frac{2\pi}{m}\right)^2.$$

The remainder term $R(w_1)$ is a priori not negligible. We will split the unit circle S^1 into the following three parts and respectively consider (6.16) there. If we let $w = e^{i(\frac{2\pi x + \mathrm{Arg}u}{m})}$, then considering the following partition of S_1 is equivalent to considering a partition of $x \in [0, m]$:

$$\begin{aligned}
S_{\mathrm{I}} &:= \left\{ w \in S_1 : |w+1| > C_1 \frac{\ln m}{\sqrt{m}} \right\} \\
S_{\mathrm{II}} &:= \left\{ w \in S_1 : C_1 \frac{\ln m}{\sqrt{m}} > |w+1| > C_2 \frac{\ln m}{m^{3/4}} \right\} \\
S_{\mathrm{III}} &:= \left\{ w \in S_1 : |w+1| < C_2 \frac{\ln m}{m^{3/4}} \right\}.
\end{aligned}$$

Here C_1 is an arbitrary positive real number and C_2 is a positive real number small enough. When m is sufficiently large, on S_{I}, $f'' = O(\frac{1}{m(\ln m)^2})$, so its contribution in the remainder term $R(w_1)$ (an integral over S_{I}) tends to 0 when $m \to \infty$. On S_{II}, $f'' = O(\frac{1}{\sqrt{m}(\ln m)^2})$. The length of S_{II} is $\frac{\ln m}{\sqrt{m}}$ so the terms in total is of order $\sqrt{m}\ln m$, so its contribution in $R(w_1)$ also tends to 0.

To calculate the difference on S_{III}, we approximate the sum and integral on the arc S_{III} respectively by the sum and integral on a line segment passing w_1 orthogonal to the $x-$axis whose length is of order $C_2\frac{\ln m}{m^{3/4}}$. In fact, if $w_1 \in D$, this is a part of a chord passing w_1, whose length is $O\left(\frac{1}{\sqrt{m}}\right)$.

Without loss of generality we suppose that m is even, let $x' = x - m/2$, so near -1 we have

$$e^{i(\frac{2\pi x + \mathrm{Arg}u}{m})} = -e^{i(\frac{2\pi x' + \mathrm{Arg}u}{m})} = -1 - \frac{2\pi x' + \mathrm{Arg}u}{m} i + \frac{1}{2}\frac{(2\pi x' + \mathrm{Arg}u)^2}{m^2} + o\left(\frac{1}{m^2}\right),$$

where $|x'| < C_2 m^{1/4} \ln m$. We have

$$\ln(-e^{i(\frac{2\pi x' + \mathrm{Arg}u}{m})} - w_1) - \ln(-1 - \frac{2\pi x' + \mathrm{Arg}u}{m} i - w_1) = O\left(\frac{\ln m}{m^{3/4}}\right).$$

This difference, if summed over $\{k \in \mathbb{Z},\ |k| < C_2 m^{1/4} \ln m\}$ or integrated over $\{|x| < C_2 m^{1/4} \ln m\}$, tends to zero when $m \to \infty$. Consider the sum

$$\sum_{k=-A}^{A-1} \ln(-1 - \frac{2\pi k + \mathrm{Arg}u}{m} i - w_1) = \sum_{k=-A}^{A-1} \Big(- \ln m + \ln\big(\alpha\gamma \mp \alpha\sqrt{-z} - (2\pi k + \mathrm{Arg}u)i\big)\Big),$$

and the integral

$$\int_{-A}^{A} \ln(-1 - \frac{2\pi x' + \mathrm{Arg}u}{m} i - w_1) dx' = \int_{-A}^{A} \Big(- \ln m + \ln\big(\alpha\gamma \mp \alpha\sqrt{-z} - (2\pi x' + \mathrm{Arg}u)i\big)\Big) dx'.$$

Their difference is independent of m. Let

$$g(x') = \ln\big(\alpha\gamma \mp \alpha\sqrt{-z} - (2\pi x' + \mathrm{Arg}u)i\big),$$

and apply the Euler-Maclaurin formula to g, we get

$$\begin{aligned} & \sum_{k=-A}^{A-1} g(k) - \int_{-A}^{A} g(x') dx' \\ = \ & \frac{1}{2}\big(g(A) - g(-A)\big) + \frac{1}{12}\big(g'(A) - g'(-A)\big) \\ - \ & \frac{1}{2}\int_{-A}^{A} \frac{-4\pi^2}{(\alpha\gamma \mp \sqrt{-z} - (2\pi x' + \mathrm{Arg}u)i)^2} B(x' - \lfloor x' \rfloor) dx'. \end{aligned}$$

For A large, the first term is close to $\frac{\pi}{2}i$ so its real part is close to 0, and the second term is close to 0. Considering the property of $\int \frac{dx}{(z+xi)^2}$, it is clear that the third part (the remainder term of Euler Maclaurin formula) is converging. Moreover, $\forall \varepsilon > 0$, there exits $C(\varepsilon) \in \mathbb{N}^*$ such that outside $[-C(\varepsilon), C(\varepsilon)]$, uniformly on u and z, the remainder term is less than ε. Note that we have proved the convergence of (6.16) when $m \to \infty$, and we still need to prove that it can be arbitrarily small when $n \to \infty$.

For any given ε, we consider the difference of the finite sum $\sum_{k=-C(\varepsilon)}^{C(\varepsilon)-1} g(k)$ and the integral $\int_{-C(\varepsilon)}^{C(\varepsilon)} g(x') dx'$.

We calculate the sum first. Fix $k \in \mathbb{Z} \cap [-C(\varepsilon), C(\varepsilon) - 1]$, the sum of $g(k)$ over $z : z^n = 1$ divided by n is approximated by

$$\ln \alpha + \int_{S^1} \ln\big(\gamma \mp \sqrt{-z} - \frac{2\pi k + \mathrm{Arg}u}{\alpha} i\big) \frac{dz}{(2\pi i) z}$$

within $o(1)$ as function of n. Let $s = s(k, u) = \gamma - \frac{2\pi k + \mathrm{Arg}u}{\alpha} i$. We consider the sum of those corresponding to w_1 and w_2,

$$\int_{S^1} \ln(s + \sqrt{-z}) \frac{dz}{(2\pi i) z} + \int_{S^1} \ln(s - \sqrt{-z}) \frac{dz}{(2\pi i) z}, \tag{6.18}$$

and by taking $\sqrt{-z} = Z$, $Z \in S^1$, Arg$Z$ from $\frac{\pi}{2}$ to $\frac{3\pi}{2}$, (6.18) is equal to

$$\int_{S^1} \ln(s+Z)\frac{2dZ}{(2\pi i)Z} + C,$$

where C is imaginary so we don't need to consider. By a power expansion similar to what we used for w, we have

$$\mathfrak{Re}\Big(\int_{S^1} \ln(s+Z)\frac{2dZ}{(2\pi i)Z}\Big) = 2\mathfrak{Re}(\mathbb{1}_{s\notin D}\ln s).$$

We now approximate the sum over u divided by n. Again this term can be approximated by an integral over u. Note that in fact if we glue the interval of $2\pi k - \text{Arg}u$ for every $k \in [-C(\varepsilon), C(\varepsilon)-1]$, this gives exactly a continuous interval of $[-2\pi C(\varepsilon), 2\pi C(\varepsilon)]$, and the double sum of g over u and z is equal to

$$2\mathfrak{Re}\Big(\int_{-2\pi C(\varepsilon)}^{2\pi C(\varepsilon)} \mathbb{1}_{(\gamma-\frac{y}{\alpha}i)\notin D}\ln(\gamma - \frac{y}{\alpha}i)dy\Big).$$

If we do the same thing for the double integral of g over u and z, this gives exactly the same form. We see that integral over z and u makes disappear the difference between the sum and the integral of g.

By taking $\varepsilon \to 0$, we have proved the proposition.

□

As a corollary, by (6.5) and (6.6), we get an estimate of the numbers of the different types of edges:

$$\mathbb{E}\left(\frac{N_a}{n^2}\right) = \frac{2\alpha}{\pi}\sqrt{1-\gamma^2},\ \mathbb{E}\left(\frac{N_b}{mn^2}\right) = \frac{2}{\pi}\arccos(-\gamma),\ \mathbb{E}\left(\frac{N_c}{mn^2}\right) = \frac{2}{\pi}\arccos(\gamma).$$

The following proposition allows us to take the limit $m, n \to \infty$ in an arbitrary way.

Proposition 6.2.3. *The limit $m \to \infty$ and the limit $n \to \infty$ can be exchanged when calculating the partition function, i.e.,*

$$\lim_{m\to\infty}\lim_{n\to\infty}\frac{\ln Z_{mn,n}(\alpha,\gamma)}{n^2} = \lim_{n\to\infty}\frac{\ln \widetilde{Z}_n(\alpha,\gamma)}{n^2}.$$

Moreover, this convergence is uniform for any compact of parameters K such that α and $\frac{\alpha}{\sqrt{1-\gamma^2}}$ are bounded in K.

This proposition says that the free energy of the bead model is some kind of limit of that of the dimer model on the hexagonal lattice.

Proof. We prove this by computation. Consider the dimer model on the $mn \times n$ torus whose fundamental domain is given by Figure 6.2 where $a, b, c \in \mathbb{R}^+$. This is two times another frequently used fundamental domain, given by Figure 6.3.

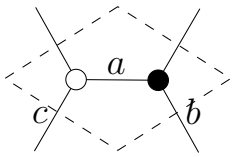

Figure 6.3: Another fundamental domain.

For this fundamental domain and for fixed m, a, b, c, the free energy of lozenge tilings, denoted by $F_\diamond$, is known [CKP01, Ken09] to be

$$F_\diamond(a,b,c) = \frac{1}{\pi}(\mathcal{L}(\theta_a) + \mathcal{L}(\theta_b) + \mathcal{L}(\theta_c) + \theta_a \ln a + \theta_b \ln b + \theta_c \ln c)$$

if three edges of length a, b and c form a triangle and in this case θ_a, θ_b and θ_c are the angles opposite the edges a, b and c in the triangle, and $\mathcal{L}$ is the Lobachevsky function defined by

$$\mathcal{L}(\theta) = -\int_0^\theta \ln|2\sin t|dt.$$

In particular, for all $\theta \in [0,\pi]$, $\mathcal{L}(\theta) + \mathcal{L}(\pi-\theta) = \mathcal{L}(\pi) = 0$.

If we take $a = \alpha/m$, $b = e^{\alpha\gamma/m}$, $c = 1$, and define $F_\diamond^m(\alpha,\gamma) = F_\diamond(\alpha/m, e^{\alpha\gamma/m}, 1)$, then in the triangle,

$$\begin{aligned}
\theta_a &= \frac{\alpha}{m}\sqrt{1-\gamma^2} + o\left(\frac{1}{m}\right),\\
\theta_b &= \arccos(-\gamma) - \frac{\alpha(1-2\gamma^2)}{2m\sqrt{1-\gamma^2}} + o\left(\frac{1}{m}\right),\\
\theta_c &= \arccos(\gamma) - \frac{\alpha}{2m\sqrt{1-\gamma^2}} + o\left(\frac{1}{m}\right),
\end{aligned}$$

and when $m \to \infty$ the $o\left(\frac{1}{m}\right)$ are uniformly converging to zero on any compact where α and $\frac{\alpha}{\sqrt{1-\gamma^2}}$ are bounded.

We have

$$\begin{aligned}
\mathcal{L}(\theta_a) &= -\theta_a \ln 2 + \theta_a - \theta_a \ln\theta_a + o\left(\frac{1}{m}\right),\\
\mathcal{L}(\theta_b) + \mathcal{L}(\theta_c) &= \int_{\arccos(\gamma)-\frac{\alpha}{2m\sqrt{1-\gamma^2}}+o\left(\frac{1}{m}\right)}^{\arccos(\gamma)+\frac{\alpha(1-2\gamma^2)}{2m\sqrt{1-\gamma^2}}+o\left(\frac{1}{m}\right)} \ln|2\sin t|dt\\
&= \frac{\alpha}{m}\ln(2\sqrt{1-\gamma^2})\sqrt{1-\gamma^2} + o\left(\frac{1}{m}\right),
\end{aligned}$$

so we have

$$\begin{aligned}
\theta_b \ln b &= \frac{\alpha\gamma}{m}\arccos(-\gamma) + o\left(\frac{1}{m}\right),\\
\theta_c \ln c &= 0,\\
F_\diamond^m &= \frac{1}{\pi m}(\alpha\gamma\arccos(-\gamma) + \alpha\sqrt{1-\gamma^2}) + o\left(\frac{1}{m}\right) = \frac{1}{2m}F + o\left(\frac{1}{m}\right),
\end{aligned}$$

where F is the value we have computed in Proposition 6.2.2. Here all the $o\left(\frac{1}{m}\right)$ are uniform on any set that α and $\frac{\alpha}{\sqrt{1-\gamma^2}}$ are bounded. In particular, we have

$$\lim_{m\to\infty} 2mF_{\diamond}^{m} = \frac{2}{\pi}\big(\alpha\gamma\arccos(-\gamma) + \alpha\sqrt{1-\gamma^2}\big),$$

which is the same value as in Proposition 6.2.2, and the convergence is uniform on any region that α and $\frac{\alpha}{\sqrt{1-\gamma^2}}$ bounded.

We remark that the coefficient 2 is just caused by the choice of different fundamental domains. □

6.2.2 Surface tension, local entropy function

We now turn to the uniform measure on the periodic bead model with given height change, which corresponds to the uniform bead measure with given periodic boundary condition introduced in Section 5.1.4. Take the definition of height function of Section 5.1.3, and let N_a, N_b and N_c respectively be the number of ◇, ◺ and ◰ in a tiling of $T_{mn,n}$, then the height change (H_x, H_y) is given by

$$N_a = nH_y,\ \ N_b - N_c = -2mnH_x,\ \ N_a + N_b + N_c = mn^2.$$

Recall that $T_{mn,n}$ corresponds to $\mathcal{G}_{mn,n/2}$ (without loss of generality we suppose that n is even). If we fix the height change (H_x, H_y) and define $Z_{mn,n}^{H_x,H_y}$ as the partition function for a uniform tiling of $T_{mn,n}$, then the partition function of $\mathcal{G}_{mn,n/2}$ with parameters α, γ is given by

$$Z_{mn,n/2}(\alpha,\gamma) \;=\; \sum_{H_x,H_y} Z_{mn,n}^{H_x,H_y}\left(\frac{1}{m}\right)^{nH_y} e^{n^2\left(\ln\alpha\frac{H_y}{n}+\alpha\gamma(-\frac{H_x}{n}+\frac{1}{2})+o(1)\right)}, \quad (6.19)$$

where $o(1)$ is in m. Recall that in Proposition 6.1.5 we proved that for given (H_x, H_y), the term

$$Z_{mn,n}^{H_x,H_y}\left(\frac{1}{m}\right)^{nH_y}$$

converges when $m \to \infty$. Later in Section 6.4 we prove that moreover the logarithm of this limit value divided by n^2 converges when $n \to \infty$ and the limits depends and is continuous on the average slope $(\frac{H_x}{n}, \frac{H_y}{n})$, which by construction should be included in $[-\frac{1}{n}] \times [0, +\infty]$. The case where $\frac{H_y}{n} = \infty$ (*i.e.* H_y is beyond the order $O(n)$) is possible, but this has a negligible contribution because otherwise the right hand side of (6.19) explodes if we take an α bigger than 1, which is not the case.

Following the idea of [KOS06], for $(s,t) \in [-\frac{1}{2}, \frac{1}{2}] \times [0, \infty[$, and for any m, n, consider the lozenge tilings of $T_{mn,n}$ of height change

$$(H_x, H_y) = (\lfloor ns \rfloor, \lfloor nt \rfloor),$$

and by the discussion above we can define the surface tension as

$$\sigma(s,t) = -\lim_{n\to\infty}\lim_{m\to\infty}\left(\frac{\ln Z_{mn,n}^{\lfloor ns\rfloor,\lfloor nt\rfloor}}{n^2} - t\ln m\right).$$

If we consider a fundamental domain as in Figure 6.3 (which is half of that of Figure 6.2), and consider the free energy per fundamental domain which is equal to

$$F(\alpha,\gamma) = \lim_{n\to\infty}\lim_{m\to\infty}\frac{\ln Z_{mn,n}(\alpha,\gamma)}{n^2} = \frac{1}{\pi}\big(\alpha\gamma\arccos(-\gamma) + \alpha\sqrt{1-\gamma^2}\big),$$

(it is half of the limit in Proposition 6.2.2), then equation (6.19) implies that

$$F(\alpha,\gamma) = \max_{s,t}\big(-\sigma(s,t) + \ln\alpha t + \alpha\gamma(\frac{1}{2}-s)\big).$$

Let $A = \ln\alpha$, $B = -\alpha\gamma$, then we get that

$$\alpha = e^A,\ \gamma = -\frac{B}{e^A}. \tag{6.20}$$

Replace α and γ by A and B, and define

$$\widetilde{F}(A,B) = F(\alpha,\gamma) - \frac{\alpha\gamma}{2} = \frac{1}{\pi}\big(-B\arccos(\frac{B}{e^A}) + \sqrt{e^{2A}-B^2}\big) + \frac{B}{2}.$$

Its Hessian matrix is positive-definite so $\widetilde{F}$ is strictly convex. Since the σ as a limit of strictly convex function (the surface tension in the dimer model) is convex, $\widetilde{F}$ and $\sigma(s,t)$ are Legendre duals, so we have

$$\begin{aligned}\sigma(s,t) &= \max_{A,B}\big(-\widetilde{F}(A,B) + At + Bs\big)\\ &= -\left(1+\ln\left(\frac{\cos(\pi s)}{\pi t}\right)\right)t.\end{aligned}$$

Define the local entropy *ent* of the bead model as $-\sigma$. More precisely,

Definition 6.2.4. For any slope $(s,t) \in [-\frac{1}{2},\frac{1}{2}]\times[0,\infty]$, define the *local entropy function* $ent(s,t)$ of the bead model as the following function:

$$ent(s,t) = \begin{cases} 0 & \text{if } t = 0,\\ -\infty & \text{if } s = \pm\frac{1}{2},\ t\neq 0,\\ \left(1+\ln\left(\frac{\cos(\pi s)}{\pi t}\right)\right)t & \text{otherwise.}\end{cases}$$

The function $ent(s,t)$ is concave in s and t and strictly concave on any domain where $t > 0$.

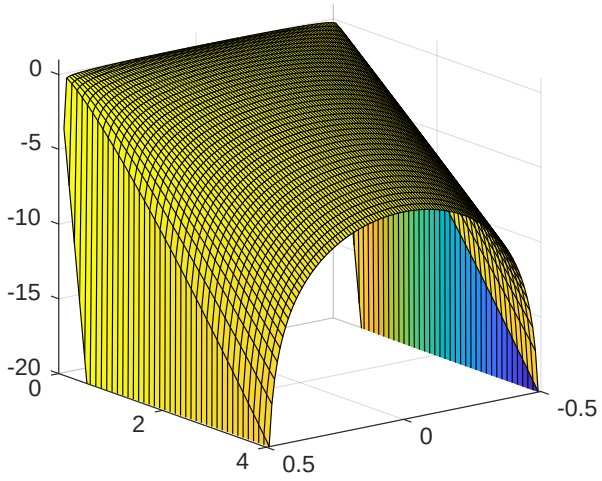

Figure 6.4: The local entropy function as a function of slope.

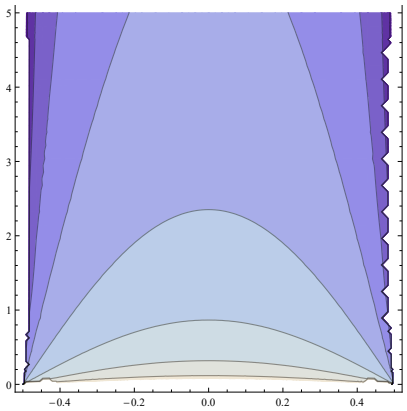

Figure 6.5: Contour lines of the local entropy function.

In Section 6.3, we consider the problem of maximizing (roughly speaking) the integral of *ent* over D where t will be taken to be $\frac{\partial h}{\partial y}$ and $s = \frac{\partial h}{\partial x}$. For later use, we here take a look at the expression of the local entropy $ent(s,t)$ (Definition 6.2.4):

$$\left(1 + \ln\left(\frac{\cos(\pi s)}{\pi t}\right)\right) t,$$

The integral of any constant times $\frac{\partial h}{\partial y}$ on D is fixed by the boundary condition. Also, $-u \ln u \leq \frac{1}{e}$. So maximizing the integral of *ent* is equivalent to maximizing the integral of

$$\ln\left(\frac{\cos(\pi s)}{t}\right) t - \frac{1}{e},$$

which is non-positive and we call it the *active part* of $ent(s,t)$. In Section 6.3, without loss of generality, sometimes we consider the active part and assume that ent is bounded above by 0 for the sake of simplification.

Meanwhile, it is good to remark that $ent(s,t)$ tends to $-\infty$ when t to infinity or when s tends to $\pm\frac{1}{2}$ while t not tends to 0 fast enough.

We end this section by an analog of Proposition 6.2.3 for entropy. Denote by $ent^\diamond$ the entropy of the dimer model on the honeycomb lattice.

Proposition 6.2.5. *For any $(s,t) \in [-\frac{1}{2},\frac{1}{2}] \times [0,+\infty[$, the entropy function of the bead model $ent(s,t)$ is the following limit of that of the dimer model on the honeycomb lattice:*

$$ent(s,t) = \lim_{m\to\infty} m\ ent^\diamond(s,t/m) - \ln mt. \tag{6.21}$$

Also, we have the following properties concerning the convergence:
(a) *for any compact set of possible slopes that doesn't contain points where $s = \pm\frac{1}{2}$, the above convergence (6.21) is uniform.*
(b) *for any $\varepsilon > 0$, there exists $\delta < 0$ and $M \in \mathbb{N}^*$ such that for all possible slopes (s,t) such that $t \le \delta$ and for all $m \ge M$, we have*

$$m\ ent^\diamond(s,t/m) - \ln mt < \varepsilon.$$

Note that in (b) we just claim an arbitrarily small upper bound and the lower bound is in fact $-\infty$.

Proof. The surface tensions are Legendre transforms of the free energy, so the convergence of the entropy function is implied by the convergence of $F_\diamond^m$ in the liquid region proved in Proposition 6.2.3 altogether with other necessary properties. But to make this more clear we choose to give a direct proof.

By [CKP01, Ken09], the dimer entropy of slope (s,t) is

$$ent^\diamond(s,t) = \frac{1}{\pi}\big(\mathcal{L}(\pi t) + \mathcal{L}(\pi(\frac{1}{2} - s - \frac{t}{2})) + \mathcal{L}(\pi(\frac{1}{2} + s - \frac{t}{2}))\big),$$

so

$$m\ ent^\diamond(s,\frac{t}{m}) = -\frac{m}{\pi}\int_0^{\pi\frac{t}{m}} \ln|2\sin t|dt + \frac{m}{\pi}\int_{\pi(\frac{1}{2}-s-\frac{t}{2m})}^{\pi(\frac{1}{2}-s+\frac{t}{2m})} \ln|2\sin t|dt. \tag{6.22}$$

The first term of (6.22) is equal to

$$\big(1 + \ln m - \ln 2 - \ln\pi - \ln t\big)t + o(1)$$

where the $o(1)$ tends to 0 when $m \to \infty$ and this is uniform on any set where t is bounded.

For the second term of (6.22), for any (s,t), when m is big this is equal to

$$\ln|2\sin(\pi(\frac{1}{2}-s))|t+o(1), \tag{6.23}$$

so we have proved the pointwise convergence in the lemma:

$$m\ ent^{\diamond}(s,t/m)-\ln mt=\left(1+\ln\left(\frac{\cos(\pi s)}{\pi t}\right)\right)t+o(1)=ent(s,t)+o(1).$$

Clearly, the convergence (6.23) is uniform on any compact set of slopes that excludes the points where $s=\pm\frac{1}{2}$, which finish the proof of (a). The convergence is not uniform on a bounded set containing $(\pm\frac{1}{2},0)$, as for all m the function $ent_m^{\diamond}$ is continuous on any possible point of slopes, while ent is not continuous at $(\pm\frac{1}{2},0)$.

To prove (b), we have

$$\begin{aligned}&m\ ent^{\diamond}(s,t/m)-\ln mt\\&=\left[-\frac{m}{\pi}\int_0^{\pi\frac{t}{m}}\ln|2\sin t|dt+(-\ln m+\ln 2)t\right]+\frac{m}{\pi}\int_{\pi(\frac{1}{2}-s-\frac{t}{2m})}^{\pi(\frac{1}{2}-s+\frac{t}{2m})}\ln|\sin t|dt.\end{aligned}$$

For any $\delta>0$, the term in the bracket converges uniformly to $(1-\ln\pi-\ln t)t$ on the set $t\le\delta$ when $m\to\infty$ and $(1-\ln\pi-\ln t)t$ converges to 0 when $t\to 0$, so it suffices to choose a δ small enough and M large enough so that for all $m>M$ this term is less than ε. Meanwhile, the second term is always negative. Thus we have finished the proof. □

6.3 Entropy-maximizing problem

Our main aim is to establish a variational principle for the bead model as in [CKP01]. This mainly consists of three parts: giving an entropy function, proving that there exists a unique maximizer and proving that there is a large deviation type behavior around that maximizer. In this section we focus on the first two parts, *i.e.* raise a functional Ent and prove that there exists a unique maximizer of it.

Since the bead model is just some kind of limit of that of the dimer, there are a lot of similarities between our case and that in [CKP01]. It is natural to think of defining a global entropy function $Ent(h)$ as the integral of $ent\circ\nabla h$ on some domain with given boundary condition, where h is the normalized height function. However, some delicate differences make the proof in the case of the bead model not a trivial and direct corollary of the dimer model. As we will see, the most remarkable difference is the unboundness of ent.

We consider a bead model normalized into the unit square $D=[0,1]\times[0,1]$, define a normalized height function h and define the space of admissible functions $\mathcal{H}$ in Section 6.3.1. In Section 6.3.2 we define the functional Ent on the admissible functions, and in Section 6.3.3 we prove that there is a unique admissible function that maximizes the entropy Ent.

6.3.1 Bead model normalized into unit square

We normalize the bead configuration into the unit square $D = [0,1]\times[0,1]$. Consider a bead model with n threads as in Section 5.1 but take the threads as

$$\left\{\left(x = \frac{i-1}{n-1}, y\right) : i = 1,2,...,n,\ y \in [0,1]\right\},$$

and we normalize the bead height function H defined in Section 5.1.3 by $n-1$. Moreover, we extend this function to the whole of D in a piecewise linear way.

Definition 6.3.1. Given a bead configuration $\mathbf{B}$ on threads $x \in \left\{\frac{i-1}{n-1}, i = 1,2,...,n\right\}$, $y \in [0,1]$, the *normalized height function* $h = h^{\mathbf{B}}$ (again for convenience we omit $\mathbf{B}$) is defined as

$$h(x,y) = \frac{1}{n-1} H\big((n-1)x+1, y\big)$$

along every thread

$$\left\{\frac{i-1}{n-1}, i = 1,2,...,n,\right\} \times [0,1],$$

then extended to the whole unit square D in the following way: for every $y \in [0,1]$, the height function $x \mapsto h(x,y)$ viewed as a function of x is taken to be the piecewise linear extension of $h(\frac{i-1}{n-1}, y)$.

For a toroidal bead model, we can also define a normalized multivalued height function h on $(\mathbb{R}/\mathbb{Z})^2$ analogously to Definition 6.3.1.

From now on, when we speak of the bead model with n threads defined on the unit square D, we mean a normalized bead model as above, with normalized height function extended to D.

Clearly the function h's horizontal partial derivative is equal to $\pm\frac{1}{2}$ almost everywhere and its vertical partial derivative equals to 0 almost everywhere. Restricted to the upper and lower boundaries of D, $h(x,1)$ and $h(x,0)$ are continuous in x, piecewise linear of slope $\pm\frac{1}{2}$, while restricted to the left and right boundaries of D, $h(0,y)$ and $h(1,y)$ are piecewise constant and increasing in y.

To describe the boundary condition by the normalized height function h, compare this to Section 5.1.4, we should introduce two imaginary threads $x = -\frac{1}{n-1}$ and $x = 1 + \frac{1}{n-1}$ where we define the boundary height function. So we sometimes consider a bead model on $[-\frac{1}{n-1}, 1+\frac{1}{n-1}] \times [0,1]$ if necessary. The domain of definition of the boundary height function depends on n, so we denote it by h_n^{∂}.

Definition 6.3.2. Consider a bead model with n threads defined on D. The normalized height function $h : D \to \mathbb{R}$ is said to have one of the boundary conditions below if there exists a normalized bead model height function $h' : [-\frac{1}{n-1}, 1+\frac{1}{n-1}] \times [0,1] \to \mathbb{R}$ such that $h'|_D = h$ and

(a) if $\mathcal{U}$ is a subspace of the functions $h_n^\partial : \partial\big([-\frac{1}{n-1}, 1+\frac{1}{n-1}] \times [0,1]\big) \to \mathbb{R}$, then we say h has a *boundary condition lying in* $\mathcal{U}$ if

$$h'|_{\partial\left([-\frac{1}{n-1},1+\frac{1}{n-1}]\times[0,1]\right)} \in \mathcal{U}.$$

(b) we say h has a *fixed boundary condition* $h_n^\partial : \partial\big([-\frac{1}{n-1}, 1+\frac{1}{n-1}] \times [0,1]\big) \to \mathbb{R}$ if $h'|_{\partial\left([-\frac{1}{n-1},1+\frac{1}{n-1}]\times[0,1]\right)} = h_n^\partial$, *i.e.*, $\mathcal{U}$ has only one element.

When $n \to \infty$, the domain $[-\frac{1}{n-1}, 1+\frac{1}{n-1}] \times [0,1]$ tends to the unit square D, so if we talk about an *asymptotic boundary condition*, it means a function h^∂ defined on ∂D, non-decreasing in y and $\frac{1}{2}$-Lipschitz in x.

Given an asymptotic height function h^∂, for any $n \in \mathbb{N}^*$, we want to consider a boundary height function h_n^∂ close to h^∂. However, as we will see later in Section 6.4, the dependence of the entropy of the bead model on the boundary condition is delicate, so the meaning of "close to h^∂" should be clarified with attention. We postpone this problem to Section 6.4, and in this section we focus on analytic results.

For every given asymptotic boundary condition h^∂, we define the space of *admissible functions* as the closure of the normalized height function, *i.e.*,

Definition 6.3.3. Given the unit square D and a boundary condition h^∂ defined on ∂D, a function h is called *admissible* if it is horizontally $\frac{1}{2}$-Lipschitz, vertically non decreasing, and when restricted on ∂D it is equal to h^∂. Denote by $\mathcal{H}$ the space of admissible functions.

We have the following generalization of Dini's theorem, which will be used later:

Lemma 6.3.4. *For any sequence of admissible functions $(h^i)_{i=1,2,\dots}$, if they converge pointwise to some continuous function, then the convergence is uniform.*

Proof. Denote the limiting function by h^∞. For any x, as $h^i(x,.)$ is non-decreasing and $h^\infty(x,.)$ is continuous, the convergence of $h^i(x,.)$ to $h^\infty(x,.)$ is uniform on $y \in [0,1]$ by Dini's theorem.

For all $\varepsilon > 0$ and for all x, there exists I_x such that for all $i > I_x$,

$$\sup_{y\in[0,1]} |h^i(x,y) - h^\infty(x,y)| < \frac{\varepsilon}{2}.$$

By the Lipschitz condition on x, for fixed x_0, for every x in the interval $[x_0 - \frac{\varepsilon}{2}, x_0 + \frac{\varepsilon}{2}]$ we have that

$$\sup_{y\in[0,1]} |h^i(x,y) - h^\infty(x,y)| < \varepsilon$$

for all $i > I_{x_0}$ and for all y. By compactness of $[0,1]$, we can choose I such that for $i > I$ we have

$$\sup_{y\in[0,1]} |h^i(x,y) - h^\infty(x,y)| < \varepsilon$$

for all $(x,y) \in D$. □

6.3.2 Statement of the entropy-maximizing problem

From now on we consider a specific case: the bead models on the unit square D with fixed asymptotic boundary condition

$$h|_{\partial D} = h^{\partial},$$

where the left and right boundary conditions are given by a constant function. More precisely, we have $h(0, y) = C_0$, $h(1, y) = C_1$ for $C_0, C_1 \in \mathbb{R}$, $h(x, 0)$ and $h(x, 1)$ are $\frac{1}{2}$-Lipschitz and $h(x, 1) \geq h(x, 0)$ for $x \in [0, 1]$. Recall that any such boundary condition corresponds to an asymptotic shape of (skew) Young diagram, and the bead model with this kind of boundary condition corresponds to the standard Young tableaux (Section 5.2.2). The shape of the diagram is given by the projection of $h(x, 0)$ and $h(x, 1)$ in the direction of y to the same plane:

$$\lambda = \{(x, z) : 2h(x, 0) \leq z \leq 2h(x, 1)\}. \tag{6.24}$$

In the case where $h(x, 0) = h(x, 1)$ for some $x \in]0, 1[$, the diagram can be decomposed into two independent regions, so without loss of generality we can always suppose that $h(x, 1) > h(x, 0)$ for all $x \in]0, 1[$.

We want to define a global entropy function $Ent(.)$ on the space of admissible functions. According to the definition, an admissible function is differentiable almost everywhere so $ent \circ \nabla h$ is well defined almost everywhere too. Naturally we can define the entropy of a function $h \in \mathcal{H}$ as the integral of $ent \circ \nabla h$ in D. However, for several reasons we are not satisfied with this choice.

The first problem is that under the common uniform norm, the space $\mathcal{H}$ is not equicontinuous, so an Arzelà-Ascoli-type theorem says that the space is not compact, and in a variational principle problem compactness is needed when we hope to prove the existence of an entropy-maximizer.

The second one is that if we take a discontinuous function as

$$h(x, y) = \begin{cases} h(x, 0) \text{ if } y \leq \frac{1}{2}, \\ h(x, 1) \text{ if } y > \frac{1}{2}, \end{cases}$$

then the integral of $ent \circ \nabla h$ is equal to 0. However, in the bead model this corresponds to a phenomenon where almost all the beads are located on one horizontal segment, which should be very rare. Even if we only consider the continuous functions, we can imagine a case where the vertical differential $\frac{\partial h}{\partial y}$ is 0 almost everywhere but the height changes (such a function can be constructed via Cantor set). In neither case the definition of a normal integral seems reasonable. To fix this problem, we could define an integral in the sense of distributions by finding a way to well define the integral of ent at the exploding points.

Instead, the solution we use is to think of a new space where we fix the $x-$axis and turn the space in the $y - z$ plane by $\frac{\pi}{4}$ so that the vertically monotonicity

converts to a 1−Lipshitz condition. This turning map is denoted by $\sim$, and the new coordinate system is denoted by $\tilde{x}$, $\tilde{y}$ and $\tilde{z}$.

After taking the map $\sim$, by properly choosing the 0 of the coordinates of the system or by thinking of a linear transformation within a constant, we have the following relation

$$\begin{cases} \tilde{x} = x, \\ \tilde{y} = \frac{\sqrt{2}}{2}(y+z), \\ \tilde{z} = \frac{\sqrt{2}}{2}(y-z), \end{cases} \qquad \begin{cases} x = \tilde{x}, \\ y = \frac{\sqrt{2}}{2}(\tilde{y}-\tilde{z}), \\ z = \frac{\sqrt{2}}{2}(\tilde{y}+\tilde{z}). \end{cases}$$

Consider the surface of any admissible function h as the set $S \subset \mathbb{R}^3$ containing the points (x, y, z) where for any x, y it contains such z that

$$\lim_{\delta \to 0^-} h(x, y+\delta) \leq z \leq \lim_{\delta \to 0^+} h(x, y+\delta).$$

We call the surface S under new coordinates as $\tilde{S}$ and let $\tilde{h} : \tilde{D} \to \mathbb{R}$ be the function that give the new surface $\tilde{S}$ under the turned coordinates, where $\tilde{D}$ is its domain of definition which is uniquely determined the boundary condition of $\mathcal{H}$. Denote by $\tilde{\mathcal{H}}$ the space $\{\tilde{h} : h \in \mathcal{H}\}$. We will still call the functions in $\tilde{\mathcal{H}}$ as admissible function, but under the coordinates $(\tilde{x}, \tilde{y})$.

The first advantage of this change is that the new space $\tilde{\mathcal{H}}$ is compact under the uniform metric, as we see that for fixed $x = \tilde{x}$, the monotonicity in y of $h(x, y)$ turns to 1-Lipschitz in $\tilde{y}$ of $\tilde{h}(\tilde{x}, \tilde{y})$. More precisely we have the following relations between (s, t) and $(\tilde{s}, \tilde{t})$ corresponding to the same point (x, y), $(\tilde{x}, \tilde{y})$:

$$\begin{cases} \tilde{s} = \frac{s}{t+1}, \\ \tilde{t} = \frac{t-1}{t+1}, \end{cases} \qquad \begin{cases} t = \frac{1+\tilde{t}}{1-\tilde{t}}, \\ s = \frac{2\tilde{s}}{1-\tilde{t}}. \end{cases}$$

Now consider in the double integral of $ent \circ \nabla h$ in D the change of variable (x, y) to $(\tilde{x}, \tilde{y})$. As the Jacobian is equal to

$$J = \frac{\partial x}{\partial \tilde{x}}\frac{\partial y}{\partial \tilde{y}} - \frac{\partial x}{\partial \tilde{y}}\frac{\partial y}{\partial \tilde{x}} = \frac{\sqrt{2}}{2}(1-\tilde{t}), \tag{6.25}$$

so the new entropy under the variable change is

$$\widetilde{ent}(\tilde{s}, \tilde{t}) = \frac{\sqrt{2}}{2} \ln \left(1 + \frac{(1-\tilde{t})\cos(\frac{2\pi\tilde{s}}{1-\tilde{t}})}{\pi(1+\tilde{t})} \right) (1+\tilde{t}).$$

Readers can verify that the new entropy $\widetilde{ent}$ is also strictly concave in the interior of its domain of definition.

We see that the entropy function $\widetilde{ent}$ is equal to $-\infty$ when the slope $\tilde{t} = \frac{\partial \tilde{h}}{\partial \tilde{y}}$ is equal to 1, the case corresponding to the discontinuity or quasi-discontinuity in $\mathcal{H}$. If we check the examples we considered as the typical cases that the integral of ent doesn't reflect the entropy, in the new integral they both give an integral equal to $-\infty$. So we take the following definition.

Definition 6.3.5. For any admissible function $\tilde{h} \in \tilde{\mathcal{H}}$, its *entropy* is defined as

$$\widetilde{Ent}(\tilde{h}) = \iint_{\tilde{D}} \widetilde{ent}\left(\frac{\partial \tilde{h}}{\partial \tilde{x}}, \frac{\partial \tilde{h}}{\partial \tilde{y}}\right) d\tilde{x}d\tilde{y},$$

and for any admissible function $h \in \mathcal{H}$, its *entropy* is defined as

$$Ent(h) = \widetilde{Ent}(\tilde{h}).$$

We can announce the main theorem of Section 6.3 now:

Theorem 6.3.6. *There exists a unique $h_0 \in \mathcal{H}$ (resp. $\tilde{h}_0 \in \tilde{\mathcal{H}}$) which maximizes $Ent(.)$ (resp. $\widetilde{Ent}(.)$) among all admissible functions of $\mathcal{H}$ (resp. $\tilde{\mathcal{H}}$).*

Later, Definition and Lemma 6.3.9 will show that there exists at least one admissible function whose entropy is not $-\infty$, so this set $\mathcal{H}$ (resp. $\tilde{\mathcal{H}}$)is not empty.

6.3.3 Proof of the existence and uniqueness of entropy-maximizer

We prove Theorem 6.3.6 in this section. For some technical reason that we will see soon, we still hope to calculate directly $Ent(h)$ by integrating $ent \circ \nabla h$ on D in the normal sense of Lebesgue.

Definition 6.3.7. Define the following subspace of the admissible functions:

$$\mathcal{H}_0 = \{h \in \mathcal{H} : \ Ent(h) = \iint_D ent \circ \nabla h dxdy\},$$

where $Ent(h) = \widetilde{Ent}(\tilde{h})$ (Definition 6.3.5). We define $\tilde{\mathcal{H}}_0$ as the image of $\mathcal{H}_0$ in $\tilde{\mathcal{H}}$.

Check the Jacobian in Equation (6.25), we directly get that

Lemma 6.3.8. *The space $\tilde{\mathcal{H}}_0$ is the subspace of $\tilde{\mathcal{H}}$ where for every function $\tilde{h} \in \tilde{\mathcal{H}}$, the Lebesgue measure of the set*

$$\{(\tilde{x}, \tilde{y}) : \frac{\partial \tilde{h}}{\partial \tilde{y}} = 1\}$$

is equal to 0.

In particular, any function in $\mathcal{H}_0$ is continuous, so a pointwise convergence of any sequence of admissible functions to a function in $\mathcal{H}_0$ is uniform (Lemma 6.3.4).

Obviously for any function $h \in \tilde{\mathcal{H}} \backslash \tilde{\mathcal{H}}_0$, $Ent(h) = \widetilde{Ent}(\tilde{h}) = -\infty$ (while its converse is false). As in Theorem 6.3.6 we are only interested in finding the maximizer of the entropy, we can restrict ourselves to any subspace which excludes only some functions whose entropy is $-\infty$, so it suffices to consider Theorem 6.3.6 in $\mathcal{H}_0$ and $\tilde{\mathcal{H}}_0$.

Although with the new coordinates we have compactness, the proof of the semi-continuity of [CKP01] does not apply here because the local entropy $\widetilde{ent}$ here is no longer bounded. Under the coordinates (x, y), it explodes (tends to $-\infty$) when the vertical slope tends to ∞, or when the horizontal slope tends to $\frac{1}{2}$ but the horizontal one is not 0. These are cases that we should take into consideration because later we will see that typically the slope explodes at some boundary points, which causes a singularity.

The method we use is to give a way to construct for every admissible function a good approximation. However, as the construction highly relies on the boundary condition, and it is hard to describe the boundary condition in $\tilde{\mathcal{H}}$ in a simple and clear way, we choose to do the construction still in $\mathcal{H}$. So in the remaining part of this section, we will often switch between $\tilde{\mathcal{H}}$ and $\mathcal{H}$. We hope that this inconvenience will not cause too many difficulties to the reader.

We introduce successive technical constructions which will be used in the proof of Theorem 6.3.6.

Definition and Lemma 6.3.9. Given a rectangular domain $[0,1] \times [a,b]$ with a boundary condition where $h(0,y)$ and $h(1,y)$ are constant, $h(x,a)$ and $h(x,b)$ are $\frac{1}{2}$-Lipschitz and $h(x,b) > h(x,a)$ for $x \in]0,1[$, then we can construct an admissible function

$$h^t : [0,1] \times [a,b] \to \mathbb{R},$$

whose vertical partial derivative $\frac{\partial h^t}{\partial y}$ only take two possible values, and $ent \circ \nabla h^t$ is bounded on D.

Proof. Since $h(x,b) > h(x,a)$ for all $x \in]0,1[$, there exists a $(\frac{1}{2} - \varepsilon)$-Lipschitz function $\bar{h}(x)$ for some $\varepsilon > 0$ such that $h(x,b) \geq \bar{h}(x) \geq h(x,a)$ for all $x \in [0,1]$. Let $A = \max_{x\in[0,1]}(\bar{h}(x) - h(x,a))$ and $B = \max_{x\in[0,1]}(h(x,b) - \bar{h}(x))$, consider D' as a subdomain of $[0,1] \times [a,b]$ given by

$$D' = \left\{(x,y) \in [0,1] \times [a,b] : \frac{b-a}{A+B}(A + h(x,a) - \bar{h}(x)) \leq y - a \leq \frac{b-a}{A+B}(A + h(x,b) - \bar{h}(x))\right\}.$$

We take

$$h^t(x,y) = \begin{cases} h(x,b) \text{ if } y \geq a + \frac{b-a}{A+B}(A + h(x,b) - \bar{h}(x)), \\ h(x,a) \text{ if } y \leq a + \frac{b-a}{A+B}(A + h(x,a) - \bar{h}(x)), \\ \lambda_a h(x,a) + \lambda_b h(x,b) \text{ otherwise,} \end{cases}$$

where $\lambda_a = \frac{a+\frac{b-a}{A+B}(A+h(x,b)-\bar{h}(x))-y}{\frac{b-a}{A+B}(h(x,b)-h(x,a))}$ and $\lambda_b = 1-\lambda_a$. In short, what we do is inscribing into the domain $[0,1] \times [a,b]$ a domain D' of shape corresponding to the boundary condition of D. Outside D' we have $\frac{\partial h^t}{\partial y} = 0$ so the height function on the boundary of D extends vertically to the boundary of D', and inside D' we construct the

surface of h^t by linking every pair of points with the same horizontal coordinate by line segment.

Outside D' we have $\frac{\partial h^t}{\partial y} = 0$ so $ent \circ \nabla h^t$ is equal to 0. Inside D' we always have

$$\begin{aligned} \frac{\partial h^t}{\partial y}(x,y) &= \frac{A+B}{b-a} \\ \frac{\partial h^t}{\partial x}(x,y) &= \frac{\partial \bar{h}}{\partial x}(x), \end{aligned}$$

so h^t satisfies the conditions in the statement. □

The construction of h^t is not unique: it depends on the choice of $\bar{h}$. Figure 6.6 is an illustration of an example h^t where the domain of definition is taken to be the unit square D and $h|_{\partial D}$ corresponds to the square Young diagrams and $\bar{h}$ is taken to be constant. In this example, h^t is piecewise linear.

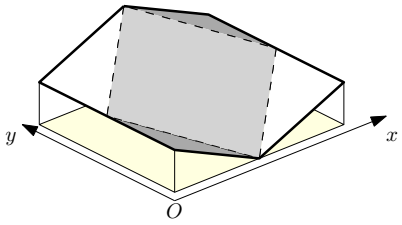

Figure 6.6: An example of h^t.

The following corollary is direct.

Corollary 6.3.10. *For all h^∂ as given asymptotic boundary function on ∂D satisfying that $h(0,y)$ and $h(1,y)$ are constant, $h(x,0)$ and $h(x,1)$ are $\frac{1}{2}$-Lipschitz, and $h(x,1) \geq h(x,0)$ for $x \in]0,1[$, there exists at least an admissible function whose entropy is not $-\infty$.*

We give a series of definitions for technical reasons. Although they are long and redundant, some of them may be used more than one time, so we decide to list them here rather than putting them separately into the proofs. Reader may skip this part and go back once some notion defined here appears later in an announcement or a proof.

Definition 6.3.11.

- For any $\delta \in]-\infty, \frac{1}{2}[$, D_δ is defined as the domain $[\delta, 1-\delta] \times [\delta, 1-\delta]$. Attention, when $\delta < 0$, the new domain is bigger than the unit square, see Figure 6.7 where the dashed square is the unit square D.

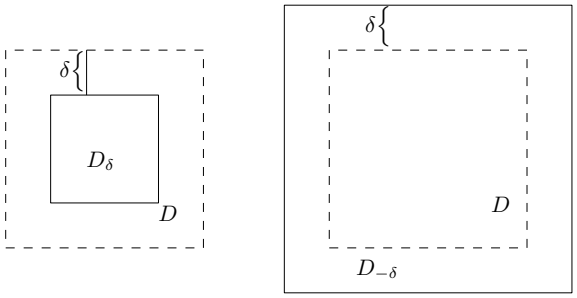

Figure 6.7: Examples of D_δ and $D_{-\delta}$ for $\delta > 0$.

- For any $\delta_1, \delta_2 \in]-\infty, \frac{1}{2}[$ and $z_0 \in \mathbb{R}$, define the operator of contraction

$$P_{\delta_1,\delta_2,z_0} : \{h : D_{\delta_1} \to \mathbb{R}\} \to \{h : D_{\delta_2} \to \mathbb{R}\},$$

  where for any bounded function $h : D_{\delta_1} \to \mathbb{R}$, we apply on the surface given by h the following map:

$$(x, y, z) \to \left(\frac{\delta_2 - \delta_1}{1 - 2\delta_1} + \frac{1 - 2\delta_2}{1 - 2\delta_1} x, \frac{\delta_2 - \delta_1}{1 - 2\delta_1} + \frac{1 - 2\delta_2}{1 - 2\delta_1} y, z_0 + \frac{1 - 2\delta_2}{1 - 2\delta_1} z \right).$$

  In other words, the surface of $P_{\delta_1,\delta_2,z_0}(h)$ is taken to be geometrically similar to that of h and to fit the domain D_{δ_2}.

- For any boundary function h^∂ which is respectively constant on the left and right boundaries of D, and for $\delta > 0$ and any function $h : D_\delta \to \mathbb{R}$ which is respectively constant on the left and right boundaries of D_δ, define $T_\delta(h) : D \to \mathbb{R}$ as the following extension of h on D whenever possible:

  - Respectively on $[0, \delta] \times [\delta, 1 - \delta]$ and on $[1 - \delta, 1] \times [\delta, 1 - \delta]$, $T_\delta(h)$ is taken to be flat and fitting the boundary conditions on ∂D and ∂D_δ.
  - If for the function constructed in the last step respectively we have

$$\begin{aligned} h(x, 1) &> T_\delta(h)(x, 1 - \delta) \quad \text{for } x \in]0, 1[, \\ h(x, 0) &< T_\delta(h)(x, \delta) \quad \text{for } x \in]0, 1[, \end{aligned}$$

    then extend $T_\delta(h)$ respectively on these two domains by using the function h^t in Definition and Lemma 6.3.9.

- For any admissible function $h \in \mathcal{H}$ and any $\delta > 0$, its flat extension on $D_{-\delta} = [-\delta, 1 + \delta] \times [-\delta, 1 + \delta]$ is the function

$$F_\delta(h) : D_{-\delta} \to \mathbb{R}$$

  which is the unique extension of h on $D_{-\delta}$ whose vertical partial derivative is equal to 0 everywhere outside D and the horizontal derivative is equal to 0 if $x \notin [0, 1]$.

Definition and Lemma 6.3.12. Fix a family of non-negative functions $U_\delta \in C^\infty(\mathbb{R}^2)$ parameterized by $\delta > 0$, whose integral is equal to 1 and whose support is contained in a disc centered at the origin and of radius δ. Define the operator

$$C_\delta : \mathcal{H} \to \{h : D_{-\delta} \to \mathbb{R}\}$$

such that for any admissible $h \in \mathcal{H}$, we extend h to

$$D_{-2\delta} = [-2\delta, 1 + 2\delta] \times [-2\delta, 1 + 2\delta]$$

by using the flat extension defined above, and $C_\delta(h)$ is taken to be the convolution of U_δ and the extended h on $D_{-\delta}$.

This new function $C_\delta(h)$ is horizontally $\frac{1}{2}$-Lipschitz and vertically non-decreasing. Moreover,
(a) the integral of $ent \circ \nabla C_\delta(h)$ on $D_{-\delta}$ is bigger than that of $ent \circ \nabla h$ on D.
(b) if $h \in \mathcal{H}_0$, then the integral of $ent \circ \nabla\big(C_\delta(h)\big)$ on $D_{-\delta}$ tends to $Ent(h)$ when $\delta \to 0$.

Remark: the letter C stands for convolution.

Proof. The function $C_\delta(h)$ is obviously horizontally $\frac{1}{2}$-Lipschitz and vertically non-decreasing.

To prove (a), it suffices to note that ent is concave and outside D the local entropy of the extended h is always 0, so for any admissible function h the value of $ent \circ \nabla(U_\delta * h)$ at any point is bigger than $U_\delta * ent \circ \nabla h$ (define by default $ent \circ \nabla h = 0$ on $D_{-2\delta} \backslash D$).

If $h \in \mathcal{H}_0$, then $Ent(h)$ is equal to the integral of $ent \circ \nabla h$ on D. As we have already proved (a), to prove the convergence it suffices to prove that

$$\limsup_{\delta \to 0} \int_{D_{-\delta}} ent \circ \nabla\big(C_\delta(h)\big) dxdy \leq \int_D ent \circ \nabla h dxdy.$$

Let δ_i be any sequence tending to 0, as $\nabla h \in L^1$, by property of the convolution we have the convergence in L^1 of $U_\delta * (\nabla h)$ to ∇h. We can take a subsequence δ_{i_j} of δ_i such that the convergence is almost everywhere, so $ent \circ \nabla C_\delta(h)$ tends to $ent \circ \nabla h$ almost everywhere for this subsequence of δ.

Since ent is a non-positive function, apply Fatou's lemma for this subsequence we have

$$\limsup_{j \to \infty} \int_{D_{-\delta_{i_1}}} \mathbb{1}_{D_{-\delta_{i_j}}} ent \circ \nabla\big(C_{\delta_{i_j}}(h)\big) dxdy \leq \int_{D_{-\delta_{i_1}}} ent \circ \nabla h dxdy,$$

while by construction the right hand side is equal to $Ent(h)$. As the sequence of δ_i can be chosen arbitrarily, so the inequality above is true for any $\delta \to 0$. □

We remark that the convolution provides us a function of better regularity but breaks the boundary condition. Using the convolution technique here above, in Lemma 6.3.13 we construct an admissible function of good enough regularity.

We also remark that, restricted on the left (resp. right) boundary of $D_{-\delta}$, it is constant and equal to the value of h on the left (resp. right) boundary of D, while its restriction on the upper and lower boundaries are functions that only depend on the boundary condition of h on the upper and lower boundaries of D.

Lemma 6.3.13. *For any given boundary condition, any $\delta < \frac{1}{2}$, and for any δ' small enough (depending on δ and the boundary condition), then there exists a family of operators*

$$A_{\delta,\delta'} : \mathcal{H} \to \mathcal{H},$$

parameterized by δ and δ', verifying that
(a) *for all functions $h \in \mathcal{H}$,*

$$Ent\big(A_{\delta,\delta'}(h)\big) \geq (1-2\delta)^2 Ent(h) + O(\delta \ln \delta),$$

where the function $O(.)$ only depends on δ and the boundary condition.
(b) *for any $h \in \mathcal{H}_0$, then for δ' sufficiently small depending on h, we have*

$$Ent\big(A_{\delta,\delta'}(h)\big) = (1-2\delta)^2 Ent(h) + O(\delta \ln \delta).$$

.
(c) *if $Ent(h) > -\infty$, then ent $\circ \nabla A_{\delta,\delta'}(h)$ is bounded from below on D by some constant depending on δ, δ' and $Ent(h)$ (and not on the precise h).*

The letter A stands for approximation.

Proof. Technically we will limit ourselves to the case that the domain

$$\lambda = \{(x,z) : x \in [0,1], z \in [2h(x,0), 2h(x,1)]\}$$

is *star convex*, *i.e.* there exist points (x_0, z_0) such that for any $\alpha \in]0,1[$ and $x \in [0,1]$, we have

$$\begin{aligned} \alpha(h(x,1) - z_0) &< h(x_0 + \alpha(x - x_0), 1) - z_0, \\ \alpha(h(x,0) - z_0) &> h(x_0 + \alpha(x - x_0), 0) - z_0. \end{aligned}$$

Moreover, we ask that every straight line passing (x_0, z_0) is not tangent to the boundary of this domain at any point. This assures a distance of order $1 - \alpha$ between the domain and the one multiplied by α, α close to 1.

For example, the function $h(x,1) = \frac{1}{2}|x - \frac{1}{2}|$ and $h(x,0) = -\frac{1}{2}|x - \frac{1}{2}|$ verify the condition above for $(x_0, y_0) = \frac{1}{2}$. In the case that the domain does not verify such condition, by the Lipschitz condition and compactness we can cut the domain vertically into disjoint parts such that every part verifies this condition. The following procedure still works with small modifications if we treat each part simultaneously.

Without loss of generality throughout the remainder of this chapter we will always suppose the star convexity with respect to $(x_0, z_0) = (\frac{1}{2}, 0)$. In this case, for every $\delta < \frac{1}{2}$, we take δ' small enough (to be specified below) so that we can define

$$T_\delta P_{-\delta',\delta,0} C_{\delta'}(h),$$

where T and P are operators defined in Definition 6.3.11. In this case, we just let

$$A_{\delta,\delta'} = T_\delta P_{-\delta',\delta,0} C_{\delta'}.$$

We will prove that such defined $A_{\delta,\delta'}$ verifies the conclusion in the Lemma. For h such that $Ent(h) = -\infty$, the results (a) and (b) are automatical. So without loss of generality we consider the h such that $Ent(h) > -\infty$, so these h are in $\mathcal{H}_0$, and

$$Ent(h) = \int_D ent \circ \nabla h \; dxdy.$$

As proved in Definition and Lemma 6.3.12, for any $h \in \mathcal{H}$,

$$\int_{D_{-\delta'}} ent \circ \nabla\big(C_{\delta'}(h)\big) dxdy \geq Ent(h), \tag{6.26}$$

and for any $h \in \mathcal{H}_0$, when $\delta' \to 0$,

$$\lim_{\delta' \to 0} \int_{D_{-\delta'}} ent \circ \nabla\big(C_{\delta'}(h)\big) dxdy = Ent(h). \tag{6.27}$$

The map $P_{-\delta',\delta,0}$ keeps gradient, so

$$\int_{D_\delta} ent \circ \nabla\big(P_{-\delta',\delta,0} C_{\delta'}(h)\big) dxdy = \frac{(1-\delta)^2}{(1+\delta')^2} \int_{D_{-\delta'}} ent \circ \nabla\big(C_{\delta'}(h)\big) dxdy. \tag{6.28}$$

Consider the function $P_{0,\delta,0}(h) : D_\delta \to \mathbb{R}$, and we claim that $T_\delta P_{0,\delta,0}(h)$ is well defined for δ small enough, *i.e.*, it is possible to fill in $D \backslash D_\delta$ piecewisely by h^t constructed in Definition and Lemma 6.3.9. Moreover, we will prove that the filling function will give a contribution of order $O(\delta \ln \delta)$ when $\delta \to 0$ in the integral of *ent*.

On $[0, \delta] \times [\delta, 1-\delta]$ and $[1-\delta, 1] \times [\delta, 1-\delta]$, it is always possible to define the extended function $T_\delta P_{0,\delta,0}(h)$, which is of 0 vertical slope so gives 0 contribution in *Ent*. In the following, without loss of generality we only treat the region near the upper boundary of D, that is $[0, 1] \times [1-\delta, 1]$.

By the star convex hypothesis, there exists a $(\frac{1}{2} - K\delta)$-Lipschitz function $\bar{h}$ for some constant $K > 0$ not depending on δ such that

$$h(x, 1) \geq \bar{h}(x) \geq P_{0,\delta,0}(h)(x, 1-\delta),$$

since $P_{0,\delta,0}(h)(x, 1-\delta)$ is already defined on $[0, 1] \times [\delta, 1-\delta]$. By construction (see Definition and Lemma 6.3.9), the local entropy *ent* is at most of order $O(\ln \delta)$, thus

the contribution of this region in Ent is at most of order $O(\delta \ln \delta)$. The function $O(.)$ only depends on the constant K we just mention.

Now consider $P_{-\delta',\delta,0}C_{\delta'}(h)$ instead of $P_{0,\delta,0}(h)$. Clearly for δ' small enough depending only on δ and the boundary condition, all the results above are still true.

Combining this with (6.26), (6.27) and (6.28), we prove (a) and (b).

To prove (c), it suffices to note that on D_δ, $A_{\delta,\delta'}(h)$ is constructed via convolution. By concavity of ent,

$$ent \circ \nabla\big(A_{\delta,\delta'}(h)\big)(x,y) \geq \frac{(1-\delta)^2}{(1+\delta')^2} U_{\delta'} * (ent \circ \nabla h(x,y))\,,$$

and the right hand side has a trivial lower bound depending on $Ent(h)$ and $U_{\delta'}$. Outside D_δ, $A_{\delta,\delta'}(h)$ is constructed via h^t in Definition and Lemma 6.3.9, whose local entropy function ent has also a lower bound only depending on the boundary condition and δ. Thus we prove (c). □

For any $\lambda \in \mathbb{R}^+$, let $\mathcal{H}^\lambda$ be the subspace of the admissible functions such that $ent \circ \nabla h(x,y) \geq -\lambda$ for $(x,y) \in \mathring{D}$ almost everywhere. Clearly $\mathcal{H}^\lambda$ is an increasing sequence of space of functions in λ. Definition and Lemma 6.3.9 constructs a function h^t whose entropy $ent \circ \nabla h^t$ is bounded, so $\mathcal{H}^\lambda$ is not empty for all λ bigger than some $\Lambda \in \mathbb{R}^+$.

We furthermore have the following two lemmas.

Lemma 6.3.14. *For δ and δ' such that $A_{\delta,\delta'}(h)$ verifies Lemma 6.3.13, for any $\varepsilon > 0$, there exists $l > 0$ such that we can construct a function h' as below:*
(a) *h' agrees with $A_{\delta,\delta'}(h)$ on $D\backslash D_\delta$.*
(b) *on D_δ it is piecewise linear on a triangle mesh of size $O(l)$.*
(c) *the sup norm between h' and $A_{\delta,\delta'}(h)$ is less than ε, and*

$$|Ent(A_{\delta,\delta'}(h)) - Ent(h')| < \varepsilon.$$

We need the triangulation to avoid the possible explosion of ent near the singularity $(s,t) = (\pm\frac{1}{2}, 0)$. Readers will see later that the lemma above plays the same role as Lemma 2.2 of [CKP01] where the authors give an approximation by triangulation, and it is interesting to compare them. In [CKP01], the main problem the authors deal with is the lack of smoothness, and thanks to Lemma 6.3.13 this is not the main focus in our case.

Proof. Define respectively for $+$ and $-$ the set of frozen points as

$$K^\pm := \left\{(x,y) \in D_\delta : \frac{\partial h}{\partial x}(x,y) = \pm\frac{1}{2}\right\},$$

and for all η, define respectively for $+$ and $-$ the set

$$K^\pm_\eta := \left\{(x,y) \in D_\delta : \mathrm{dist}((x,y), D\backslash K^\pm) \geq \eta\right\}.$$

For any δ' small enough we have the following equality:

$$K^{\pm}_{\delta'} = \left\{ (x,y) \in D_\delta : \frac{\partial A_{\delta,\delta'}(h)}{\partial x}(x,y) = \pm\frac{1}{2} \right\}.$$

The Lebesgue measure of $K^+_\eta \cup K^-_\eta$ is a decreasing function in η so it is continuous almost everywhere. From now on we take δ'' close enough to δ' such that δ'' is a continuous point of the measure of $K^+_\eta \cup K^-_\eta$, the sup norm between $A_{\delta,\delta''}(h)$ and $A_{\delta,\delta'}(h)$ is less than $\frac{\varepsilon}{2}$, and $|Ent(A_{\delta,\delta'}(h)) - Ent(A_{\delta,\delta''}(h))| < \frac{\varepsilon}{2}$ (by the arguments we used in the proof of Lemma 6.3.13 it is possible to do so).

The function $A_{\delta,\delta''}(h)$ belongs to some $\mathcal{H}^\lambda$.

For any l small enough and dividing $1-2\delta$, consider a l-grid on D_δ, and consider the mesh of isosceles right triangles constructed by linking the northeast and southwest vertices of every l-square of the grid. Consider the only function h' which is a linear function on every triangle of the mesh and agrees with $A_{\delta,\delta''}(h)$ on vertices of triangles and outside D_δ we just take $h' = A_{\delta,\delta''}(h)$.

As $A_{\delta,\delta''}(h)$ is C^∞ on D_δ, for l sufficiently small, h' agrees with h within $\frac{\varepsilon}{2}$, so the first approximation in (c) is direct.

We also conclude that there exists $\lambda' \in \mathbb{R}^+$ such that $h' \in \mathcal{H}^{\lambda'}$ (*i.e.* $ent \circ \nabla h'$ is bounded from below by $-\lambda'$ almost everywhere) and λ' is independent of l. The boundness on $D \backslash D_\delta$ is trivial. Inside D_δ, consider any triangle of the l-mesh. Its slope is equal to the integrals of the partial differentials of $A_{\delta,\delta''}(h)$ along the edge which is the diagonal of the l-square then normalized by the length $\sqrt{2}l$. Since on any point the partial differentials $(\partial A_{\delta,\delta''}(h)/\partial x, \partial A_{\delta,\delta''}(h)/\partial y)$ is within the set

$$\{(s,t) : ent(s,t) \geq -\lambda\},$$

the normalized integral of the partial differentials is within the convex hull of this set, which is easy to be shown to be included in $\{(s,t) : ent(s,t) \geq -\lambda'\}$ for some finite λ', so we get the wanted property.

We will respectively treat the case where $s = \pm\frac{1}{2}$ (note that whenever this is true we have also $\{t = 0\}$) and where $s \neq \pm\frac{1}{2}$. We show that for l small enough, $ent \circ \nabla h'$ approximates well $ent \circ \nabla h$ on most points in the interior of these sets, and the rest points have a contribution arbitrarily small.

As the Lebesgue measure of $K^\pm_\eta$ is continuous at δ'', for the ε given, find d small enough such that the Lebesgue measure of $(K^+_{\delta''} \cup K^-_{\delta''}) \backslash (K^+_{\delta''+d} \cup K^-_{\delta''+d})$ is less than $\frac{\varepsilon}{8\lambda'}$.

For any $l < \frac{d}{\sqrt{2}}$, the l-squares respectively intersecting $K^\pm_{\delta''+d}$ gives a cover of $K^\pm_{\delta''+d}$, and they are contained in $K^\pm_{\delta''}$. In other words, we give an inner approximation of $K^\pm_{\delta''}$ by disjoint squares of length l. The measure of the difference set is less than that of $(K^+_{\delta''} \cup K^-_{\delta''}) \backslash (K^+_{\delta''+d} \cup K^-_{\delta''+d})$, which is less than $\frac{\varepsilon}{8\lambda'}$.

Note that $ent \circ \nabla h'(x,y) = 0$ on $K^\pm_{\delta''+d}$, so the local entropy of the function h' is equal to that of $A_{\delta,\delta''}(h)$ there.

On the other hand, for any point $(x_0, y_0) \in D_\delta$ such that $\frac{\partial h}{\partial x}(x_0, y_0) \neq \pm\frac{1}{2}$, there exists r (which depends on (x_0, y_0)) such that within the r-neighborhood of (x_0, y_0), ∇h is within a small convex neighborhood of $\nabla h(x_0, y_0)$ where

$$|ent \circ \nabla h(x, y) - ent \circ \nabla h(x_0, y_0)| < \frac{\varepsilon}{4}.$$

This gives an open cover of the points that $\frac{\partial h}{\partial x} \neq \pm\frac{1}{2}$. We may choose ρ small enough such that the area of the union of the balls of diameters bigger than ρ is bigger than the measure of

$$\{(x, y) \in D_\delta : \frac{\partial h}{\partial x}(x, y) \neq \pm\frac{1}{2}\}$$

minus $\frac{\varepsilon}{8\lambda'}$.

Now take $l < \min\{\frac{d}{\sqrt{2}}, \rho\}$, for the piecewise linear function h', we have

$$|ent \circ \nabla h(x, y) - ent \circ \nabla h(x_0, y_0)| < \frac{\varepsilon}{4}$$

on all points except a set of measure $\frac{\varepsilon}{2\lambda'}$, thus

$$|Ent\big(A_{\delta,\delta''}(h)\big) - Ent(h')| < \frac{\varepsilon}{2},$$

thus we have finished the proof. □

Figure 6.8 gives an illustration of several notions used in the proof above: the l-mesh, the frozen point set $K^\pm$ and the set $K^\pm_{\delta''}$.

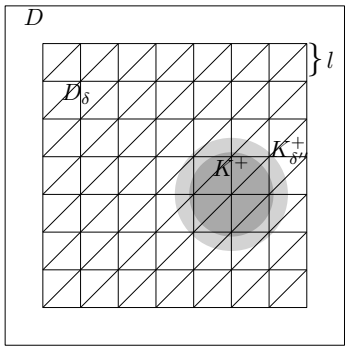

Figure 6.8: The l-mesh, the frozen point set $K^\pm$ and the set $K^\pm_{\delta''}$.

Lemma 6.3.15. *The space $\mathcal{H}^\lambda$ is compact and semicontinuous with respect to the sup norm of H, and there exists a unique function h_λ that maximizes $Ent(.)$ among all functions of $\mathcal{H}^\lambda$.*

Proof. When $\frac{\partial h}{\partial y}$ tends to plus infinity, the entropy $ent(\frac{\partial h}{\partial x}, \frac{\partial h}{\partial y})$ tends to minus infinity. So for any λ, the boundness condition implies that $\frac{\partial h}{\partial y}$ is bounded from

above by a constant depending on λ. Thus we have a Lipshitz condition on y for $\mathcal{H}^\lambda$, so $\mathcal{H}^\lambda$ is relative compact in $\mathcal{H}$ under the uniform norm.

To prove the compactness we should also prove that $\mathcal{H}^\lambda$ is closed in $\mathcal{H}$. This is because the constraint $ent \circ \nabla h(x,y) \geq -\lambda$ can be interpreted as a constraint on the horizontal and vertical slope. By the argument of the local convexity near the points $(\pm\frac{1}{2}, 0)$, a space verifying such geometric constraint is closed.

As for the semicontinuity of Ent, thanks to Lemma 6.3.14 and the boundness of ent on $\mathcal{H}^\lambda$, the proof is nothing different from Lemma 2.3 in [CKP01].

All these imply the existence of a maximizer: taking a sequence of height functions whose entropies tend to $\sup\{Ent(h) : h \in \mathcal{H}^\lambda\}$, then there exists a converging subsequence. By semicontinuity, the entropy of the limit height function is $\sup\{Ent(h) : h \in \mathcal{H}^\lambda\}$. □

Corollary 6.3.16. *We have*

$$\sup_{h\in\mathcal{H}} Ent(h) = \lim_{\lambda\to\infty} \sup_{h\in\mathcal{H}^\lambda} Ent(h).$$

Proof. This is a direct corollary of Lemma 6.3.13 and Lemma 6.3.15.

Proof of Theorem 6.3.6. Choose $I \in \mathbb{N}$ such that $\mathcal{H}^I$ is not empty. For any $i \geq I$, consider the function h_i as the maximizer of Ent among all functions of $\mathcal{H}^i$. We first take the turned coordinates $(\tilde{x}, \tilde{y})$. By compactness of $\tilde{\mathcal{H}}$, the sequence $\tilde{h}_i$ given by Corollary 6.3.16 has a converging subsequence $\tilde{h}_{i_j}$ under the uniform norm. Denote the limit by $\tilde{h}_0$, and denote its preimage by $h_0 \in \mathcal{H}$. The function h_0 is well defined except for the discontinuous points, and on these points we will take $h_0(x,y) = \limsup_{(a,b)\to(x,y)} h(a,b)$. It is easy to verify that the convergence of h_{i_j} to h_0 is pointwise except on the discontinuous points.

To simplify the notation, here rather than a subsequence of $\tilde{h}_i$, we suppose that the sequence $\tilde{h}_i$ converges. This simplification does not lose generality: we prove below that the limit of the subsequence is the unique function that maximizes $Ent(.)$, so by the uniqueness of the limit of the subsequence, the sequence itself converges to the same limit.

We now prove that $\tilde{h}_0 \in \tilde{\mathcal{H}}_0$. Otherwise, the set Δ defined by

$$\Delta = \{(\tilde{x}, \tilde{y}) \in \tilde{D} : \frac{\partial \tilde{h}_0}{\partial \tilde{y}} = 1\}$$

has a positive measure $\mu > 0$.

For all ε, there exists an open set $U \subset \mathbb{R}^2$ such that $\Delta \subset U$ and the $\mathbb{R}^2$-Lebesgue measure of U is less than $\mu(1+\varepsilon)$. Denote the $\mathbb{R}^2$-Lebesgue measure by $|\ .\ |$. The set U is the union of at most countable open discs, and we choose finite discs such that the $2-$Lebesgue measure of their union is bigger than μ, and we can cut their union into finite disjoint convex parts.

Let Δ_1, Δ_2,...,Δ_M respectively be their closures. The sum of $|\Delta_k|$ for $k = 1, 2, ..., M$ is less than $\mu(1+\varepsilon)$ and bigger than μ, and the sum of $|\Delta_k \cap \Delta|$ is bigger than $\mu(1-\varepsilon)$. Thus, there exists a subset K of $\{1, 2, ..M\}$ such that for every $k \in K$, $\frac{|\Delta_k \cap \Delta|}{|\Delta_k|} \geq 1-3\varepsilon$ and $\sum_{k\in K} |\Delta_k| \geq \frac{1}{3}\mu$.

For any $\tilde{h} \in \tilde{\mathcal{H}}$ and $k \in K$, define the average vertical slope on Δ_k as

$$av_y^{\Delta_k}(\tilde{h}) := \frac{1}{|\Delta_k|} \iint_{\Delta_k} \frac{\partial \tilde{h}}{\partial \tilde{y}} d\tilde{x} d\tilde{y}.$$

As $\frac{\partial \tilde{h}}{\partial \tilde{y}} \geq -1$, for all $k \in K$, we have

$$av_y^{\Delta_k}(\tilde{h}_0) \geq \frac{|\Delta_k \cap \Delta|}{|\Delta_k|} - \left(1 - \frac{|\Delta_k \cap \Delta|}{|\Delta_k|}\right) = 1 - 6\varepsilon.$$

As the convergence of $\tilde{h}_i$ to $\tilde{h}_0$ is uniform, there exists J such that for all $i \geq J$, $\tilde{h}_i$ is within a $\varepsilon \min_{k\in K}\{\text{diam}\Delta_k\}$-neighborhood of $\tilde{h}_0$, then $av_y^{\Delta_k}(\tilde{h}_i) \geq 1 - 8\varepsilon$ for all $k \in K$ and $i \geq J$.

By concavity of $\widetilde{Ent}$, negativity of $\widetilde{ent}$, we get

$$\widetilde{Ent}(\tilde{h}_i) \leq \sum_{k\in K} \iint_{\Delta_k} \widetilde{ent}\left(\frac{\partial \tilde{h}_i}{\partial \tilde{x}}, \frac{\partial \tilde{h}_i}{\partial \tilde{y}}\right) d\tilde{x} d\tilde{y} \leq \sum_{k\in K} \iint_{\Delta_k} \widetilde{ent}(av_x^{\Delta_k}, av_y^{\Delta_k}) d\tilde{x} d\tilde{y}, \quad (6.29)$$

where the average horizontal height change $av_x^{\Delta_k}$ is defined as analogue of $av_y^{\Delta_k}$. When $\varepsilon \to 0$, the average vertical slopes on all Δ_k uniformly tend to 1 so $\widetilde{ent}(av_x^{\Delta_k}, av_y^{\Delta_k})$ uniformly tend to $-\infty$. As the sum of the 2−Lebesgue measure of Δ_k is bigger than $\frac{1}{3}\mu$, we prove that $\widetilde{Ent}(\tilde{h}_i)$ tend to $-\infty$. However, by definition it should be finite and increasing, thus we get a contradiction and prove that $\tilde{h}_0 \in \tilde{\mathcal{H}}_0$, so $h_0 \in \mathcal{H}_0$.

By Lemma 6.3.13 for all h_i and h_0, for all $\varepsilon > 0$, there exist δ and δ' such that the function $O(\delta \ln \delta)$ depending only on the boundary condition is less than ε, and

$$\begin{aligned} &Ent\big(A_{\delta,\delta'}(h_i)\big) \geq (1-2\delta)^2 Ent(h_i) - \varepsilon, \ i = I, I+1, ... \\ &Ent\big(A_{\delta,\delta'}(h_0)\big) \in [(1-2\delta)^2 Ent(h_0) - \varepsilon, (1-2\delta)^2 Ent(h_0) + \varepsilon]. \end{aligned} \quad (6.30)$$

By construction, for all i,

$$Ent\big(A_{\delta,\delta'}(h_i)\big) \geq (1-2\delta)^2 Ent(h_I) - \varepsilon,$$

and by Lemma 6.3.13 (c) there exists $\Lambda(\delta, \delta') \in \mathbb{R}$ such that for all $i = I, I+1, ...$, $A_{\delta,\delta'}(h_i) \in \mathcal{H}^{\Lambda(\delta,\delta')}$.

The convergence of h_i to h_0 when $i \to \infty$ implies the convergence of $A_{\delta,\delta'}(h_i)$ to $A_{\delta,\delta'}(h_0)$. By semicontinuity of Ent for functions of $\mathcal{H}^{\Lambda(\delta,\delta')}$, we have

$$Ent\big(A_{\delta,\delta'}(h_0)\big) \geq \limsup_{i\to\infty} Ent\big(A_{\delta,\delta'}(h_i)\big).$$

Compare this inequality to (6.30), we prove that $Ent(h_0) \geq \limsup_{i\to\infty} Ent(h_i)$, and by Lemma 6.3.16, h_0 maximizes $Ent(.)$ among functions of $\mathcal{H}$. It is the unique maximizer because of the strict concavity of ent in the interior of its domain of definition. □

6.4 The variational principle

Our next step is to establish a variational principle to prove a large deviation result for the bead model that reveals a limit shape of the model when the size tends to infinity. In [CKP01], the authors prove that the number of dimer configurations of height functions around an admissible function is proportional to exponential of its entropy times n^2, by which they prove that in the limit the height functions converge to the entropy maximizing one in probability. As the bead model is a limit of the dimer model, we expect a similar behavior here.

Since a lot of notations will appear in this section and probably the readers may be confused, we decide to give here, in the very beginning of this section, a general convention on the use of notation.

- The number of beads or the number of horizontal lozenges is denoted by $N(n)$, where n emphasizes its dependence on the number of threads n.
- For any upper index u and lower index l,
  - $\mathcal{H}_l^u$ will denote the space of configurations.
  - X_l^u is a uniformly chosen random configuration of $\mathcal{H}_l^u$.
- If the lower index l is n, we mean the bead model with n threads, and if l is mn, n, that means we are considering a discrete approximation of the bead model by lozenge tilings.
- The letter h is used for the normalized bead height function. H with a lower index n means the un-normalized bead height function, and with a lower index mn, n means a height function of lozenge tiling.
- We use h_n^∂ to denote a fixed boundary condition of the normalized bead height function, while that of the lozenge tiling is given by the domain $R_{mn,n}$.

The main result of this section is the following theorem. Consider a fixed normalized boundary condition as in Section 6.3.2, *i.e.*, a normalized boundary function h^∂ defined on ∂D where D is the unit square, and we furthermore ask that $h^\partial(0, y)$, $h^\partial(1, y)$ viewed as functions of y are constant functions, while $h^\partial(x, 0) < h^\partial(x, 1)$ as functions of x are $\frac{1}{2}$-Lipschitz.

Fix the asymptotic boundary function h^∂. For any $n \in \mathbb{N}^*$, consider the following boundary height function h_n^∂ of a bead model with n threads and normalized into D:

$$h_n^\partial : \left([-\frac{1}{n-1}, 1 + \frac{1}{n-1}] \times [0, 1] \right) \to \mathbb{R}.$$

We furthermore ask that the function h_n^∂ is constant if restricted to $x = -\frac{1}{n-1}$ or $x = 1 + \frac{1}{n-1}$ and that for any $x \in [0, 1]$,

$$\max \left\{ |h_n^\partial(x, 0) - |h^\partial(x, 0)|, |h_n^\partial(x, 1) - |h^\partial(x, 1)| \right\} < \frac{1}{n-1}.$$

Theorem 6.4.1. *For any admissible function $h : D \to \mathbb{R}$ that agrees with h^∂ on ∂D and $Ent(h) > -\infty$, define $\mathcal{V}_\delta(h)$ as the δ-neighborhood of h under the supremum norm. For any $n \in \mathbb{N}^*$, consider the normalized bead model on D with n threads and fixed boundary condition h_n^∂. Let $\mathcal{H}_n^{\mathcal{V}_\delta(h)}$ be the space of configurations whose normalized height function is in $\mathcal{V}_\delta(h)$ and let $X_n^{\mathcal{V}_\delta(h)}$ be a random configuration uniformly chosen in this space, then we have*

$$\lim_{\delta\to 0}\lim_{n\to\infty}\frac{S(X_n^{\mathcal{V}_\delta(h)})}{n^2} = Ent(h), \tag{6.31}$$

where we recall that $S(X)$ is the adjusted combinatorial entropy of the random variable X.

Note that, in order to differ with $\mathcal{U}$ (the letter we use to a set of boundary condition), here we use $\mathcal{V}$ to denote the neighborhood of an admissible function h which is a subspace of the height functions of the bead configurations.

Here we give an outline of the proof of this theorem, which will later be formalized and proved via a series of lemmas and propositions. Recall that with the help of Lemma 6.1.5, we are able to approach the entropy S of a bead model via that of dimer model, which is well studied in [CKP01].

The main idea of the proof is to use triangulations. Although most results in this thesis are given for the bead model on the unit square, it is not hard to generalize the definition to triangles, discs or other simply connected regions. As we are going to prove the variational principle by using triangulation, it is particularly interesting to consider the isosceles right triangles. Proposition 6.4.13 proves that the entropy on the isosceles right triangles shares all the needed property of that on the squares.

We first study a bead model on the unit square D with almost planar boundary condition. Unlike in [CKP01], in the bead model, close boundary condition (under the uniform norm on ∂D) does not imply close entropy: if a boundary condition of the vertical sides has an arbitrarily small jump, then the entropy is equal to $-\infty$. Thus, in any neighborhood of a nearly planar boundary condition we can always find two boundary conditions that give entropies arbitrarily far apart.

To solve this problem, we give a more precise definition that clarify what is an "almost planar" boundary condition (Definitions 6.4.3 and 6.4.4). We prove that the normalized (and adjusted) entropy of a bead model with almost planar boundary condition converges (Lemma 6.4.5).

Then we prove a series of technical lemmas (Lemma 6.4.6, 6.4.7, 6.4.8) which the readers can find their origins in [CKP01] and [CEP96]. They serve to prove Lemma 6.4.9, which concludes that among all nearby boundary conditions, the almost planar ones have the biggest entropy. Theorem 6.4.10 proves that it is equal to $ent(.,.)$, and the entropy of the bead model whose boundary condition is the union of nearby functions in a neighborhood of an almost planar function has the same limit when the radius of the neighborhood tends to 0.

Lemma 6.3.14 and Lemma 6.4.14 give two triangulations of a surface of bead

configurations respectively for a lower bound and an upper bound of entropy. This proves Theorem 6.4.1, a variational principle of the bead model.

As a corollary of the variational principle, in the end of this section, we prove a limiting behavior for the bead model with fixed boundary condition: when $n \to \infty$, the random surface of the bead configuration converges in probability to the function h_0 that maximizes $Ent(h)$.

In the beginning we give a lemma which is somehow independent of the others. It proves that the combinatorial entropy S is bounded from above by a constant. This is reminiscent of the fact that the local entropy function *ent* is also bounded from above. This lemma will be used when we prove the upper bound of the entropy in Theorem 6.4.1.

Lemma 6.4.2. *We have a global constant C such that uniformly for any asymptotic fixed or periodic boundary condition of bead model, when $n \to \infty$, we have*

$$\limsup_{n\to\infty} \frac{S(X)}{n^2} \leq C.$$

Proof. We use the discretization based on Proposition 6.1.5 to prove this lemma. For any fixed or toroidal boundary condition of $N(n)$ beads, consider its discrete version of lozenge tiling of a rectangle-like region $R_{mn,n}$, so we should study

$$\limsup_{n\to\infty} \lim_{m\to\infty} \frac{1}{n^2}\Big(\ln Z_{mn,n} - \ln mN(n)\Big).$$

We consider the tiling of $R_{mn,n}$ column by column from left to right. Suppose that the number of horizontal lozenges on the i^{th} column is N_i. Given the positions of the i^{th} column, for the $i+1^{th}$ column, the number of possible positions of the columns are the product of the length of the intervals between the neighboring horizontal lozenges on the i^{th} thread, thus at most $\left(\frac{mn}{N_i}\right)^{N_{i+1}}$. Thus we have

$$Z_{mn,n} \leq \prod_{i=1}^{n} \left(\frac{mn}{N_i}\right)^{N_{i+1}}.$$

We derive that

$$\frac{1}{n^2}\Big(\ln Z_{mn,n} - \ln mN(n)\Big) \leq \frac{1}{n^2}\Big(\sum_{i=1}^{n} N_i(\ln n - \ln N_{i+1})\Big) \tag{6.32}$$

If $\min_{i=1,\ldots,n} N_i = 0$, then the model can be decomposed into independent models (one can be trivial, *i.e.* no bead at all). Without loss of generality we suppose that $\min_{i=1,\ldots,n} N_i \geq 1$.

For any $\varepsilon > 0$, we consider the following partition of $\{1, 2, ..., n\}$:

- set $I_{\leq \varepsilon n} := \{i : N_i \leq \varepsilon n\}$,
- set $I_{>\varepsilon n} := \{i : N_i > \varepsilon n\}$.

By construction, the numbers of beads on neighboring threads differ at most by 1, so for $i \in I_{\leq \varepsilon n}$, we have

$$\ln\left(\frac{N_i}{N_{i+1}}\right) \leq \ln 2,$$

so

$$N_i(\ln n - \ln N_{i+1}) \leq N_i(\ln n - \ln N_i) + \ln 2.$$

By the same reason, for $i \in I_{>\varepsilon n}$, we have

$$N_i(\ln n - \ln N_{i+1}) \leq N_i\left(\ln n - \ln N_i + \ln\left(\frac{1+\varepsilon n}{\varepsilon n}\right)\right) \leq N_i\left(\ln n - \ln N_i + \left(\frac{1}{\varepsilon n}\right)\right).$$

Thus, the right hand side of Inequality (6.32) is less than

$$\begin{aligned} & \frac{1}{n^2}\left(\sum_{i=1}^{n} N_i\big(\ln n - \ln N_i\big) + \sum_{i\in I_{\leq \varepsilon n}} \ln 2 N_i + \sum_{i\in I_{>\varepsilon n}} \left(\frac{1}{\varepsilon n}\right) N_i\right) \\ \leq \; & \frac{1}{n^2}\left(\sum_{i=1}^{n} N_i\big(\ln n - \ln N_i\big)\right) + \varepsilon \ln 2 + \frac{1}{\varepsilon} O\left(\frac{1}{n}\right), \end{aligned}$$

where we use the fact that $N(n) = O(n^2)$. Let $n \to \infty$, and by the fact that ε is arbitrarily small, the right hand side of Inequality (6.32) is less than

$$\frac{1}{n^2}\Big(\sum_i N_i(\ln n - \ln N_i)\Big) + o(1),$$

which takes maximum if N_i are almost all equal, thus less than

$$\frac{1}{n^2}\left(n\frac{N(n)}{n}\left(\ln n - \ln\frac{N(n)}{n}\right)\right) + o(1) = -\frac{N(n)}{n^2}\ln\frac{N(n)}{n^2} + o(1). \tag{6.33}$$

Let C be any constant bigger than $\max_{x>0}(-x\ln x) = \frac{1}{e}$ and we have finished the proof. □

Readers may compare this lemma to the expression of ent, and the term $-\frac{N(n)}{n^2}\ln\frac{N(n)}{n^2}$ of Equation (6.33) corresponds to the term $-t\ln t$ in $ent(s,t)$.

As we have already seen, the dependence of the entropy of a random bead configuration on the boundary condition is more delicate than that of the dimer model. So rather than roughly speaking that one boundary condition is close to a plane, we need to have a more precise definition.

Definition 6.4.3. Given a tilt $(s,t) \in]-\frac{1}{2},\frac{1}{2}[\times]0,+\infty[$, for any $n \in \mathbb{N}^*$, a fixed boundary condition $h_n^{\partial,0}$ of a bead model with n threads is called *almost planar* if there exists a plane of tilt (s,t) and $h_n^{\partial,0}$ is chosen to give the best approximation of that plane.

We remark that being chosen to give the best approximation of a plane implies that on the left and right boundaries of $[-\frac{1}{n-1}, 1+\frac{1}{n-1}]\times[0,1]$, the distances between neighboring jumps of $h_n^{\partial,0}$ are all equal.

We will equally need its discrete version:

Definition 6.4.4. Given a tilt $(s,t) \in]-\frac{1}{2},\frac{1}{2}[\times]0,+\infty[$, for any $n \in \mathbb{N}^*$ and $m \in \mathbb{N}^*$ large, *an almost planar region* $R^0_{mn,n}$ is a tall region tileable by lozenges corresponding to $h_n^{\partial,0}$ constructed as in Section 5.1.6.

According to the construction of $R^0_{mn,n}$, the distance between the neighboring cracks on the left and right boundaries of $R^0_{mn,n}$ are all equal except for an error smaller than 1. We also remark that an equivalent way to describe this region is that there exists a parallelogram in $\mathbb{R}^3$ corresponding to the tilt, and the boundary height function of $R^0_{mn,n}$ is chosen to fit best to that parallelogram.

By construction, the almost planar bead boundary condition (Definition 6.4.3) is the continuous limit of its discrete version (Definition 6.4.4). It is also clear that for any tilt (s,t), it is always possible to find at least one boundary function h_n^{∂} verifying Definition 6.4.3 and to find at least one region $R^0_{mn,n}$ verifying Definition 6.4.4.

Lemma 6.4.5. *For any tilt* $(s,t) \in]-\frac{1}{2},\frac{1}{2}[\times]0,\infty[$,
(a) *let* $\mathcal{H}_n^t(s,t)$ *be the space of bead configurations on the torus with* n *threads and the height change of* H *is equal to* $(\lfloor ns\rfloor, \lfloor nt\rfloor)$, *and let* $X_n^t(s,t)$ *be a randomly chosen element of* $\mathcal{H}_n^t(s,t)$, *then*

$$\liminf_{n\to\infty} \frac{S\big(X_n^t(s,t)\big)}{n^2} > -\infty.$$

(b) *let* $\mathcal{H}_n^0(s,t)$ *be the space of almost planar bead configurations on* D *with* n *threads best fitting a plane of tilt* (s,t), *and let* $X_n^0(s,t)$ *be a randomly chosen element of* $\mathcal{H}_n^0(s,t)$, *then*

$$\liminf_{n\to\infty} \frac{S\big(X_n^0(s,t)\big)}{n^2} > -\infty.$$

Proof. The existence of the $\liminf_{n\to\infty}$ is a result of subadditivity. □

We give a series of technical lemmas following [CEP96, CKP01].

Lemma 6.4.6. *For any two bead models having the same number of threads but with different boundary conditions, consider the un-normalized height function* H. *If the two boundary conditions differ by at most* Δ, *then on every common vertex, the expected value of these two unnormalized height functions differ by at most* $\Delta+2$ *under the supremum norm.*

Proof. This is a corollary of Proposition 20 of [CEP96]'s analog in the case of lozenge tilings.

Define the distance between two vertices as the length of the shortest path between them, and define the distance between two sets as the sup inf of the distances between vertices from two sets. Proposition 20 of [CEP96]'s analog in lozenge tiling says that, for any two lozenge-tileable domains, if their boundaries differ by Δ_1, and if for any pair of points on the first and the second domain with a distance smaller Δ_1 their heights differ at most by Δ_2, then the average height function of these two domains differ at most by $\Delta_1 + \Delta_2 + 1$.

For the bead model, suppose that the number of thread is n, and for any $m \in \mathbb{N}^*$ big enough, consider the discrete version where we consider two regions $R^i_{mn,n}$, $i = 1, 2$, both with n columns, tileable by lozenges and corresponding to the boundary conditions given in this lemma. The distance between their left-most (or right-most) boundaries is 1, and for the upper and lower boundaries, the difference of the boundary height functions at a point on the boundaries of the bead model is equal to the vertical distance of the boundaries of the corresponding lozenge tiling model. Thus we can apply Proposition 20 of [CEP96] and take the limit $m \to \infty$. □

Lemma 6.4.7. *For a bead model with n threads, if the average height function is vertically A-Liptshitz, then there exists a constant $C > 0$ and $C' > 0$ depending on A such that for any simply connected region contained in D with given boundary condition of the bead model and two points (x_1, y_1) and (x_2, y_2) in the this region, the probability that $h(x_1, y_1) - h(x_2, y_2)$ differs from its expected height change by more than $\alpha\sqrt{\frac{|x_1-x_2|+|y_1-y_2|}{n-1}}$ is less than $Ce^{-C'\alpha^2}$.*

Proof. This is the bead-model-version of Theorem 21 and Proposition 22 of [CEP96]. To prove this, consider the path

$$\big((n-1)x_1, (n-1)y_1\big) \to \big((n-1)x_2, (n-1)y_1\big) \to \big((n-1)x_2, (n-1)y_2\big)$$

in the domain $[0, n-1] \times [0, n-1]$, and consider the height function $(n-1)h(x, y)$ (attention, this is not the un-normalized height function H).

Let $N_1 = \lfloor (n-1)|x_1 - x_2| \rfloor$ be the number of threads between these two points. For the first step (the horizontal step), consider the same martingale as in Theorem 21 of [CEP96], and using Azuma's inequality [AS16], the probability that the difference between the exact height change and expected height change is bigger than $\frac{1}{2}\alpha\sqrt{N_1}$ is less than $C_1 e^{-C_2\alpha^2}$ for some constant $C_1, C_2 > 0$.

Now consider the vertical step. To do this, we turn the space by $\frac{\pi}{4}$ again so that the new space is vertically Lipshitz (see Section 6.3.2) under the turned coordinates $(\tilde{x}, \tilde{y}, \tilde{z})$ and the surface is $\tilde{z} = \tilde{H}(\tilde{x}, \tilde{y})$. Since the space is Lipschitz, we can apply Azuma's inequality again. Take a discretization in $\tilde{y}$ and for any two points on the same thread and with vertical coordinates $\tilde{y}_1$, $\tilde{y}_2$, the number of steps is equal to $\lfloor (n-1)|\tilde{y}_1 - \tilde{y}_2| \rfloor$, and we get a result for $\tilde{y}$ similar to that for x. For any surface

$(n-1)h$, turning $(\tilde{x}, \tilde{y}, \tilde{z})$ back into the original space (x, y, z) will lead to another difference, but it is bounded by a constant depending on A times the difference of the real and expected height change of $(n-1)h$. Thus, there exist constants $C_3, C_4 > 0$ such that $(n-1)h(x, y)$ changes by more than $\frac{1}{2}\alpha\sqrt{N_2}$ is less than $C_3 e^{-C_4\alpha^2}$, where $N_2 = \lfloor (n-1)|y_1 - y_2| \rfloor$.

In conclusion, the probability that h and its expected value differs by more than $\alpha\sqrt{\frac{|x_1-x_2|+|y_1-y_2|}{n-1}}$ is at most $Ce^{-C'a^2}$ for well chosen C and C'. □

For any tilt $(s, t) \in]-\frac{1}{2}, \frac{1}{2}[\times]0, +\infty[$, any $\delta > 0$ and $n \in \mathbb{N}^*$, define $\mathcal{U}_{\delta,n}(s, t)$ as the space of fixed boundary condition of the normalized bead model with n threads, where the boundary functions h_n^∂ are in the δ-neighborhood of a plane of tilt (s, t).

Lemma 6.4.8. *Under the setting above, for n sufficiently large, for any fixed boundary condition $h_n^\partial \in \mathcal{U}_{\delta,n}(s, t)$, the average normalized height function of the bead model is given within $\delta + o(1)$ by that plane, $o(1)$ tending to 0 when $n \to \infty$.*

Proof. This is a direct corollary of Proposition 3.4 of [CKP01]. □

Lemma 6.4.9. *Under the same setting of Lemma 6.4.8, for any $\varepsilon > 0$, if we let $X_n^{h_n^\partial}$ be any random bead model whose fixed boundary condition is given by $h_n^\partial \in \mathcal{U}_{\delta,n}(s, t)$, then for δ sufficiently small and n sufficiently large, we have*

$$\frac{S(X_n^{h_n^\partial})}{n^2} \leq \frac{S\big(X_n^0(s, t)\big)}{n^2} + \varepsilon,$$

where recall that $X_n^0(s, t)$ is the random bead configuration with an almost planar fixed boundary condition.

This lemma corresponds to Proposition 3.6 of [CKP01], where the authors prove that the entropies of the dimer models of nearby boundary conditions are close. As we have already explained, this is no longer true for the bead model, and the lemma above tells that among all the boundary conditions near a planar, the one that is almost planar has the biggest entropy, with an error tending to 0 when $n \to \infty$. In short, we have an approximating inequality rather than an approximating equality.

We remark that in the proof below there is a technical assumption. We don't succeed to find a rigorous proof of this point but we have reason to believe that it is true.

Proof. To prove this lemma, we will look at the discrete version of the bead model. There we use the same idea of [CKP01], where the authors compare the entropy of two different boundary conditions by applying a coupling-like method between the surfaces. In our case this is more complicated since even a tiny region may have big negative contribution in the entropy, so some more detailed construction is needed.

Given a tilt $(s, t) \in]-\frac{1}{2}, \frac{1}{2}[\times]0, +\infty[$, we define $h^{\partial,0} : \partial D \to \mathbb{R}$ as the linear function fitting a plane of tilt (s, t). For any $n \in \mathbb{N}^*$, we denote by $h_n^{\partial,0}$ an almost

planar boundary condition fitting best $h^{\partial,0}$, and for any $m \in \mathbb{N}^*$ large, consider an almost planar region $R^0_{mn,n}$ as in Section 5.1.6.

Now given any other boundary condition $h^\partial_n \in \mathcal{U}_{\delta,n}(s,t)$, consider another region $R_{mn,n}$ that corresponds to h^∂_n as in Section 5.1.6.

As rising the whole boundary by the same amount doesn't change the entropy, without loss of generality we can suppose that $h^\partial_n \geq h^{\partial,0}_n$. We superpose $R^0_{mn,n}$ and $R_{mn,n}$ in such a way that their left and right sides are on the same lines (except for the positions of cracks corresponding to the jumps of $h^{\partial,0}_n$ and h^∂_n), and the upper and lower boundaries differ by at most $O(\delta n)$.

Define respectively $\mathcal{H}_{mn,n}$ and $\mathcal{H}^0_{mn,n}$ as the space of tilings of $R_{mn,n}$ and of $R^0_{mn,n}$, and a random tiling uniformly chosen respectively from $\mathcal{H}_{mn,n}$ and $\mathcal{H}^0_{mn,n}$ is denoted by $X_{mn,n}$ and $X^0_{mn,n}$. We want to compare the adjusted entropies of $X_{mn,n}$ and $X^0_{mn,n}$. To do this, we use a surface coupling method as in [CKP01] but more delicate (in some sense).

For a given tilt (s,t), we fix some $\rho > 0$ such that the ρ-neighborhood of (s,t) lies within $]-\frac{1}{2},\frac{1}{2}[\times]0,\infty[$. Define $h^{0,+} : D \to \mathbb{R}$ as the supremum of the admissible function fitting $h^{\partial,0}$ on ∂D and of tilt within the ρ-neighborhood of (s,t) almost everywhere. Such $h^{0,+}$ is a piecewise linear surface on D. For any n, we let $h^{0,+}_n$ be a bead height function that fits best to $h^{0,+}$ and let $H^{0,+}_{mn,n}$ be a height function of tiling of $R^0_{mn,n}$ which approximates $h^{0,+}$ best when normalized horizontally by n and vertically by mn.

For any $r \in]0,\frac{1}{2}[$, for every $H_{mn,n}$, whenever possible, define $\gamma_r(H_{mn,n})$ to be the maximal curve made up by the points of the intersection of $H_{mn,n}$ and $H^{0,+}_{mn,n}$ and enclosing $D_r = [r,1-r]\times[r,1-r]$. Here the "curve" means a path along the edges of lozenges, and "maximal" means having the biggest enclosed area.

We decompose the set of tilings of $R_{mn,n}$ by $\gamma_r(H_{mn,n})$. In case that $\gamma_r(H_{mn,n})$ doesn't exist, we just note $\gamma_r(H_{mn,n}) = \emptyset$. According to Lemma 6.1.3, we have the following decomposition for $\gamma \in \{\gamma_r(H_{mn,n}) : H_{mn,n} \in \mathcal{H}_{mn,n}\} \cup \{\emptyset\}$:

$$S(X_{mn,n}) - \ln mN(n) = \sum_\gamma p_\gamma \big(-\ln p_\gamma + S(X_{mn,n}|_{\gamma_r(H_{mn,n})=\gamma}) - \ln mN(n)\big), \quad (6.34)$$

where $N(n)$ is the number of horizontal tiles in a tiling of $R_{mn,n}$ and p_γ is the probability that $\gamma_r(H_{mn,n}) = \gamma$. We will compare this to $S(X^0_{mn,n}) - \ln mN^0(n)$, where $N^0(n)$ is the number of horizontal tiles in a tiling of $R^0_{mn,n}$.

We first treat the term $\gamma = \emptyset$ and fix $r = \frac{2\delta}{\rho}$ as a function of δ. The probability that $\gamma = \emptyset$ is less than the probability that there is some point on ∂D_r such that on the corresponding point in the discrete version we have $H_{mn,n} > H^{0,+}_{mn,n}$.

By Lemmas 6.4.6 and 6.4.7, on any such point this probability is exponentially small in n. Moreover, there are only $O(n)$ points that need to be checked: on the upper and lower sides there are only $O(n)$ point, and on the other two sides it suffices to check $O(n)$ with fixed distance between neighboring ones. The unit distance should be small enough depending on ρ so that if two neighboring points

verify the condition then on the whole interval the same condition is automatically verified. Thus, the total probability tends to 0 when $\delta \to 0$ and $n \to \infty$, and the term $-p_\gamma \ln p_\gamma$ tends to 0 too.

By Lemma 6.4.2 the remaining part is bounded from above by a global constant times the area, so in conclusion, we can choose δ small enough so that this term is less than $\frac{\varepsilon}{4}$ for any n large enough.

We now restrict ourselves to the case where $\gamma \neq \emptyset$. For any γ, denote respectively the number of horizontal lozenges on the curve by N^γ, the number of lozenges not enclosed by γ by N^γ_{out} and the number of lozenges enclosed by γ by N^γ_{in}. Conditioned to γ, the tiling of the regions inside and outside γ are independent, so we can write every term (corresponding to γ) in the sum on the right hand side of (6.34) as a sum of:
(a) p_γ times the adjusted entropy of a tiling of the region enclosed by γ,
(b) that of a tiling of the region not enclosed by γ,
(c) $p_\gamma(-\ln p_\gamma - \ln mN^\gamma)$.

We take the following technical assumption: we assume that for δ small enough, when $n \to \infty$ and $m \to \infty$ (depending on n), the term (c) summed over all γ and normalized by n^2 will be finally smaller than $\frac{\varepsilon}{4}$. In fact, the sum over all γ of (c) can be viewed as an expectation, and we consider a typical boundary. If on the left piece there are N_l horizontal lozenges, and we suppose that the winding contributes not too much so the left piece behaves as a lazy random walk with fixed number of moves, starting position and ending position. The way to take this piece is around $\binom{nm}{\frac{N_l}{2}}^2$, so typically the probability is of order $\binom{mn}{N^\gamma}^{-1}$, and

$$\frac{1}{n^2}\mathbb{E}\Big[\sum_\gamma p_\gamma(-\ln p_\gamma - \ln mN^\gamma)\Big]$$

should be of order $\frac{\ln n}{n}$. By this argument, our assumption seems to be reasonable, but we wish to find a way to make this argument rigorous.

For terms (a) and (b), we consider the following subspaces of the tiling of $R^0_{mn,n}$: for every given γ, define

$$\mathcal{H}^{0,+}_{mn,n}(\gamma) = \{H^0_{mn,n} \in \mathcal{H}^0_{mn,n} : H^0_{mn,n}|_\gamma = H^{0,+}_{mn,n}|_\gamma\}. \tag{6.35}$$

Denote by $X^{0,+}_{mn,n}(\gamma)$ a random tiling uniformly chosen in this space. We prove that the normalized and adjusted entropy

$$\frac{1}{n^2}\Big(S(X^{0,+}_{mn,n}(\gamma)) - \ln m(N^0(n) - N^\gamma)\Big)$$

is at least not much smaller than

$$\frac{1}{n^2}\Big(S(X_{mn,n}|_{\gamma_r(H_{mn,n})=\gamma} - \ln m(N(n) - N^\gamma)\Big).$$

In fact, both of them can be written as a sum of the adjusted and normalized entropy on the region enclosed by γ and that on the region not enclosed by γ.

Obviously their contributions of the region enclosed by γ in the entropy are equal. On the region not enclosed by γ, by Lemma 6.4.2 we have

$$\frac{1}{n^2}\Big(S(X^{out}_{mn,n}|_{\gamma_r(H_{mn,n})=\gamma}) - \ln mN^{\gamma}_{out}\Big)$$

is less than a global constant C times the area of region, which tends to 0 when $\delta \to 0$ (so $r \to 0$). Here $X^{out}_{mn,n}|_{\gamma_r(H_{mn,n})=\gamma}$ is the conditioned random tiling outside the region enclosed by γ and of boundary condition $\partial R_{mn,n}$.

Meanwhile, if let $X^{out,0,+}_{mn,n}|_{\gamma_r(H_{mn,n})=\gamma}$ be the conditioned random tiling outside the region enclosed by γ and of boundary condition $\partial R^0_{mn,n}$, then for

$$\frac{1}{n^2}\Big(S(X^{out,0,+}_{mn,n}|_{\gamma_r(H_{mn,n})=\gamma}) - \ln mN^{\gamma,0}_{out}\Big),$$

where $N^{\gamma,0}_{out} = N^0(N) - N^{\gamma} - N^{\gamma}_{in}$ is the number of horizontal lozenges outside γ, its boundary condition restricted on $\partial R^0_{mn,n}$ and γ fits best to a piecewise linear function $h^{0,+}$. We can decomposed the region into a union of disjoint squares, and by Lemma 6.4.5, the adjusted normalized ventropy normalized entropy is bounded from below by some constant (depending on (s,t) and ρ) times the area of this region when $n \to \infty$ and $m \to \infty$ depending on n. Since when $\delta \to 0$, the normalized area of the region between curve γ and ∂R^0_{mn} also tends to 0, as conclusion, for δ small enough, for n big enough and for m big enough, we have

$$\frac{1}{n^2}\Big(S(X^{out,0,+}_{mn,n}|_{\gamma_r(H_{mn,n})=\gamma}) - \ln mN^{\gamma,0}_{out}\Big) > -\frac{\varepsilon}{4}.$$

Finally, since the space $\mathcal{H}^{0+}_{mn,n}|_{\gamma_r(H_{mn,n})=\gamma}$ is a subspace of $\mathcal{H}^0_{mn,n}$, the normalized adjusted entropy of $X^{0+}_{mn,n}|_{\gamma_r(H_{mn,n})=\gamma}$ for every γ is less than that of $X^0_{mn,n}$. Together with the technical assumption on (c), in conclusion we have: for δ small enough, n large enough, we have

$$\sum_{\gamma} p_{\gamma}\big(-\ln p_{\gamma} + S(X_{mn,n}|_{\gamma_r(H_{mn,n})=\gamma}) - \ln mN(n)\big) < \frac{1}{n^2}\Big(S(X^0_{mn,n}) - \ln mN^0(n)\Big) + \varepsilon.$$

□

Lemma 6.4.9 proves that among the fixed boundary conditions that are close to a plane, the almost planar one has almost the biggest entropy. As a corollary, we have the following theorem. Recall that for bead models with n threads, $X^t_n(s,t)$ is the random bead configuration of toroidal boundary condition given by tilt (s,t), and $X^0_n(s,t)$ is that of almost planar fixed boundary condition.

Theorem 6.4.10. *For any tilt $(s,t) \in]-\frac{1}{2},\frac{1}{2}[\times]0,+\infty[$, we have*

$$\lim_{n\to\infty}\frac{S\big(X^t_n(s,t)\big)}{n^2} = \lim_{n\to\infty}\frac{S\big(X^0_n(s,t)\big)}{n^2} = ent(s,t).$$

Moreover, for any $\delta > 0$, $n \in \mathbb{N}^*$, if we consider the union of bead models with fixed boundary conditions taken in $\mathcal{U}_{\delta,n}(s,t)$, then the combinatorial entropy of a random bead configuration in this set normalized by n^2 is also equal to $ent(s,t) + o(1)$ when $n \to \infty$ and $\delta \to 0$.

If we take any two fixed boundary function of $\mathcal{U}_{\delta,n}(s,t)$, they do not necessarily have the same number of beads. So to define the adjusted combinatorial entropy for the union of boundary conditions in $\mathcal{U}_{\delta,n}(s,t)$, we need Definition 6.1.4, which a priori furthermore asks fixing the probability that a random bead configuration has some given number of beads. However, in the proof below, we show that the choice of the probability doesn't affect the limit of the normalized adjusted entropy.

Proof. By Lemmas 6.4.2 and 6.4.5, for any tilt (s,t), $\frac{S\left(X_n^t(s,t)\right)}{n^2}$ is bounded, so there exists a subsequence n_k of n, and along this subsequence, for every n_k we can choose an almost planar boundary conditions whose normalized entropies as sequence in n_k converge.

Lemma 6.4.9 proves that among all nearby boundary conditions the almost planar one has the almost biggest normalized entropy. In particular, this implies that for any given tilt (s,t) and any $n \in \mathbb{N}^*$ big enough, two almost planar boundary conditions have close entropy. Thus, the convergence along n_k in the last paragraph doesn't depend on the choice of the precise almost planar boundary condition.

Moreover, this convergence is not just for a subsequence of n_k but a convergence in n. In fact, in the following we prove that along n_k, the normalized adjusted entropies converge to $ent(s,t)$. As this is also true for any subsequence of n, we conclude that the normalized adjusted entropy converge as $n \to \infty$. Thus, without loss of generality, in the following we only consider a sequence in n.

Now for every $n \in \mathbb{N}^*$ fix the sequence $N(n) \propto n^2$ and consider the bead models with n threads, $N(n)$ beads and with boundary conditions be any function in $\mathcal{U}_{\delta,n}(s,t)$. We claim that the normalized entropy of this sequence of models converges to the same limit of $\frac{S(X_n^0(s,t))}{n^2}$ when $\delta \to 0$ and $n \to \infty$. This claim corresponds to the second part of this theorem.

We first suppose that upper, lower and right boundaries are fixed and the left boundary boundary is free within δ neighborhood of the almost planar one. The number of beads on the left boundary is fixed (by the given upper and lower boundaries) and we denote it by K. For all m, consider the discrete version where we tile $R_{mn,n}$ by lozenges. There are $\binom{mn}{K}$ different possibilities, and by Stirling's formula

$$\begin{aligned}
&\frac{\ln\binom{mn}{K} - K\ln m}{n^2} \\
=\ & \frac{1}{n^2}\Big[\ln\Big(\frac{\sqrt{2\pi mn}}{\sqrt{2\pi(mn-K)2\pi K}}\frac{(mn)^{mn}}{(mn-K)^{mn-K}K^K}\Big) + o(1) - K\ln m\Big] \\
=\ & \frac{1}{n^2}\Big[\ln\sqrt{\frac{mn}{2\pi(mn-K)K}} - K\ln\frac{K}{n} + (mn-K)\ln\frac{mn}{mn-K} + o(1)\Big] \\
=\ & \frac{1}{n^2}\Big[\ln\sqrt{\frac{mn}{2\pi(mn-K)K}} - K\ln\frac{K}{n} + \frac{mn-K}{mn}K + o(1)\Big] \\
=\ & O(\frac{1}{n}),
\end{aligned}$$

where $o(1)$ is for m big enough. Thus, the entropy of the bead model of free left

boundary will be at most $O(\frac{1}{n})$ bigger than that of the fixed almost planar one. It is not hard to show that for any of other three boundaries there is a similar result. Thus, if the number of $N(n)$ is fixed, then our claim is true.

Now we allow $N(n)$ to vary but under the constraint that the boundary functions are within $\mathcal{U}_{\delta,n}(s,t)$. For any n and δ, denote by $\mathcal{N} = \mathcal{N}(s,t,\delta,n)$ be the set of possible $N(n)$, then $|\mathcal{N}|$ is of order $O(2\delta n^2)$. According to Definition 6.1.4, if for any $N_i \in \mathcal{N}$, the probability that $N(n) = N_i$ is given and equal to p_{N_i}, then the entropy of the bead configurations with boundary conditions taken in $\mathcal{U}_{\delta,n}(s,t)$ is equal to

$$-\sum_{N_i\in\mathcal{N}} p_{N_i}\ln p_{N_i} + \sum_{N_i\in\mathcal{N}} p_{N_i} S_{N_i}, \tag{6.36}$$

where S_{N_i} is the entropy of the model whose number of beads is equal to N_i. Since we have proved that $\frac{S_{N_i}}{n^2}$ is at most $\frac{S(X_n^0(s,t))}{n^2} + o(1)$, and $\frac{-\sum_{N_i\in\mathcal{N}} p_{N_i}\ln p_{N_i}}{n^2}$ is at most of order $\frac{\ln n}{n^2}$, we have proved our claim that the normalized entropies of the bead configurations with $\mathcal{U}_{\delta,n}(s,t)$-boundary condition converge to the same limit of $\frac{S(X_n^0(s,t))}{n^2}$ when $n\to\infty$ and $\delta\to 0$.

It remains to prove the first part of this theorem.

First, by construction, we can find an almost planar boundary condition whose opposite sides matches. So we have

$$\lim_{n\to\infty}\frac{S\big(X_n^t(s,t)\big)}{n^2} \geq \lim_{n\to\infty}\frac{S\big(X_n^0(s,t)\big)}{n^2}.$$

On the other hand, given a toroidal boundary condition (so the number of beads is fixed), consider the fixed boundary conditions of $\mathcal{U}_{\delta,n}(s,t)$ that yield the same number of beads. Since the bead configuration with periodic boundary condition not included in $\mathcal{U}_{\delta,n}(s,t)$ has a negligible contribution, by our claim proved above, we have

$$\lim_{n\to\infty}\frac{S\big(X_n^t(s,t)\big)}{n^2} \leq \lim_{n\to\infty}\frac{S\big(X_n^0(s,t)\big)}{n^2}.$$

Finally, as for any $\delta > 0$, $\mathcal{U}_{\delta,n}(s,t)$ also includes the almost planar boundary conditions of tilts near (s,t), by applying a similar argument as above we conclude that for (s',t') close to (s,t), $\frac{S\left(X_n^t(s',t')\right)}{n^2}$ is also close to $\frac{S\left(X_n^0(s,t)\right)}{n^2}$. Thus, $\frac{S\left(X_n^t(s,t)\right)}{n^2}$ is continuous in the tilt. This allows us to use the Legendre transform in Section 6.2.2, so we have proved this theorem. □

Definition 6.4.11. For any $\varepsilon > 0$ and for any $(s,t) \in]-\frac{1}{2},\frac{1}{2}[\times]0,1[$, define

$$\rho^{\varepsilon}(s,t) = \sup_{\rho>0}\left\{\rho : (||(s',t')-(s,t)|| < \rho) \Rightarrow (|ent(s,t) - ent(s',t')| < \varepsilon)\right\}.$$

The following lemma is a direct corollary of Lemma 6.4.9 and Theorem 6.4.10.

Lemma 6.4.12. *Consider the unit square D. For any $\varepsilon > 0$, and for any tilt*

$$(s,t) \in]-\frac{1}{2},\frac{1}{2}[\times]0,+\infty[,$$

consider the bead model on D with n treads and with the fixed boundary condition fitting to a plane of tilt (s,t) within $\rho^{\varepsilon}(s,t)$. Then for n sufficiently large, the entropy S of the bead configurations normalized by n^2 is at most the entropy of a bead model with an almost planar periodic boundary condition $h_n^{\partial,0}$ plus $\varepsilon + o(1)$ where $o(1)$ tends to 0 when $n \to \infty$.

Proposition 6.4.13. *Lemma 6.4.9 and Theorem 6.4.10 hold if the region is an isosceles right triangle instead of a square.*

Proof. The proof is exactly the same as that of Corollary 4.2 of [CKP01]. An isosceles right triangle can be approached from interior by a union of squares, and combining two triangles gives a square. These operations naturally yield a lower bound and an upper bound of the entropy of a bead model on a isosceles right triangle, which is both equal to $ent(s,t) + o(1)$ when $n \to 0$.

The following Lemma is another version of Lemma 6.3.14 which we will see is related to an upper bound of the entropy S.

Lemma 6.4.14. *For any admissible function h such that $Ent(h) > -\infty$ and for any $\varepsilon_1, \varepsilon_2 > 0$, for $l > 0$ sufficiently small, then the piecewise linear function h' on the l-right-triangle mesh verifies the following two properties.*
(a) *For all but a fraction of ε_1 of the triangles in the mesh, for every triangle, denote the tilt of h' on that triangle by (s,t), then the function h is within $\rho^{\varepsilon_2}(s,t)l$ of h'.*
(b) *$Ent(h') < Ent(h) + \varepsilon_2$.*

Proof. The proof of part (a) is the same as in Lemma 2.2 of [CKP01]. We now prove (b). Define the space of possible tilts as

$$V_0 = [-\frac{1}{2},\frac{1}{2}] \times [0,+\infty[,$$

and for any $A > 0$, $d > 0$, define the following subset of V_0:

$$V_0^{A,d} = \{(s,t) : |s - \frac{1}{2}| < d, \text{ or } |s + \frac{1}{2}| < d, \text{ or } t > A\}.$$

Since $Ent(h) > -\infty$ and $ent(.,0) = 0$, we can take A sufficiently large and d sufficiently small so that the points

$$\left\{(x,y) : \left(\frac{\partial h}{\partial x}, \frac{\partial h}{\partial hy}\right)(x,y) \notin V_0^{A,d}\right\}$$

gives a contribution of absolute value less than $\frac{\varepsilon_2}{4}$ in $Ent(h)$.

Let $V_1, V_2, ..., V_n$ be a open cover of $V_0 \backslash V_0^{A,d}$ such that within each set V_i the function $ent(s,t)$ changes at most by $\frac{\varepsilon_2}{4}$. For any $i \in \{1,2,...,n\}$ and for any

$\eta_i \in]0,1[$, consider the set $\bar{S}(V_i, \eta_i)$ which is composed of possible tilts $(\bar{s}, \bar{t})$ that there exists a probability density function (in the sense of distribution) on V_0 such that the average slope is equal to $(\bar{s}, \bar{t})$, and a proportion bigger than η_i is in V_i. This gives a family of convex subsets of V_0 indexed by η_i. When $\eta_i \to 1$, the set $\bar{S}(V_i, \eta_i)$ tends to $V_i + \{0\} \times \mathbb{R}^+$, where the sum of two sets is defined as the set of the sums of any pair of elements.

By the property of *ent*, for η_i close enough to 1 we have that for any average tilt $(\bar{s}, \bar{t}) \in \bar{S}(V_i, \eta_i)$,

$$ent(\bar{s}, \bar{t}) \leq \sup_{(s,t) \in V_i} ent(s,t) + \frac{\varepsilon_2}{8},$$

and

$$(1 - \eta_i) \inf_{(s,t) \notin V_0^{A,d}} ent(s,t) \geq -\frac{\varepsilon_2}{4}.$$

Now we can apply an argument of metric density from [Rud87] similar to the way [CKP01] uses it. For any $\varepsilon' > 0$, $\eta_i > 0$, if l_i is sufficiently small, then for any $\delta \leq l_i$, on all but an $1 - \varepsilon'$ fraction of the points (x, y) such that $\left(\frac{\partial h}{\partial x}, \frac{\partial h}{\partial y}\right) \in V_i$, at least a η_i fraction of the ball centered at (x, y) and of radius δ lies in V_i.

If there is some triangle where h verifies (a) for some ε', the tilt of the piecewise linear function h' differs from the average tilt on that triangle by at most $2\varepsilon'$. Take ε' less than $\frac{\varepsilon_1}{2}$ such that for all i and for all (s,t) in the $2\varepsilon'$ neighborhood of $\bar{S}(V_i, \eta_i)$ we have

$$ent(s,t) \leq \sup_{(s,t) \in V_i} ent(s,t) + \frac{\varepsilon_2}{4}. \tag{6.37}$$

Also, for ε' small enough, the integral of $ent \circ \nabla h$ is bigger than $-\frac{\varepsilon_2}{4}$ on any subset of D whose measure is less than $2\varepsilon'$.

For all $l \leq \min_i\{l_i\}$ and less than the l in (a) where we replace ε_1 by some ε' less than ε_1 and verifying the conditions above, on at least a $1 - \varepsilon'$ fraction of the triangles, (a) is verified.

Now compare $Ent(h)$ to $Ent(h')$ where h' is the piecewise linear function on the l-mesh. There is at least a $1 - 2\varepsilon'$ fraction of triangles such that for each triangle, there exists i such that in this triangle a proportion of at least η_i of points (x, y) verifies that $ent \circ \nabla h(x, y)$ is contained in V_i, thus the average slope of h is in $\bar{S}(V_i, \eta_i)$. Meanwhile, as the tilt of h' lies within $2\varepsilon'$-neighborhood of the average slope of h, according to (6.37) we have that on this triangle

$$ent \circ \nabla h' \leq \sup_{(s,t) \in V_i} ent(s,t) + \frac{\varepsilon_2}{4} \leq \inf_{(s,t) \in V_i} ent(s,t) + \frac{\varepsilon_2}{2}.$$

In conclusion, we compare $Ent(h)$ and $Ent(h')$ respectively for the following two cases:

- On the $2\varepsilon'$ fraction of triangles and on the points in the $1 - 2\varepsilon'$ fraction of triangles where $ent \circ \nabla h(x, y) \in V_0^{A,d}$:

  - the integral of $ent \circ \nabla h$ is bigger than $-\frac{\varepsilon_2}{2}$ by construction.
  - the integral of $ent \circ \nabla h$ is less than 0 by negativity.

- On the $1 - 2\varepsilon'$ fraction of triangles and where $ent \circ \nabla h(x, y) \notin V_0^{A,d}$, for each triangle, there exists i such that a proportion bigger than η_i of points is in V_i. The contribution of the other $(1 - \eta_i)$ proportion of points in $Ent(h)$ is most $-\frac{\varepsilon_2}{4}$ times the area. On other points,

$$ent \circ \nabla h' < ent \circ \nabla h + \frac{\varepsilon}{4},$$

  so the contribution of these points in $Ent(h') - Ent(h)$ is at most $\frac{\varepsilon}{2}$.

Thus we have proved the lemma. □

Now we can prove our main theorems of this section.

Proof of Theorem 6.4.1. We will separately prove that $Ent(h)$ is asymptotically the upper bound and lower bound of the normalized entropy on the left hand side of (6.31).

We begin by the part of lower bound. For any $\varepsilon > 0$, by Lemma 6.3.13, we can find some $\tilde{h}$ such that $||\tilde{h} - h||_{L^\infty} < \frac{\delta}{4}$, $|Ent(\tilde{h}) - Ent(h)| < \frac{\varepsilon}{4}$, and there exists some K such that $ent \circ \nabla \tilde{h} > -K$ on D (in other words $\tilde{h} \in \mathcal{H}^K$). By Lemma 6.3.14, for any l small enough, we can construct a l-isosceles-right-triangle mesh and find a function h' such that on every triangle of the mesh h' is linear and $||h' - \tilde{h}||_{L^\infty} < \frac{\delta}{4}$ and $|Ent(h') - Ent(\tilde{h})| < \frac{\varepsilon}{4}$.

By Theorem 6.4.10 and Proposition 6.4.13, on any triangular of the mesh, when $n \to \infty$, the entropy normalized by n^2 of the bead model with fixed almost planar boundary condition fitting the boundary of triangle converges to the contribution of this triangle in $Ent(h')$, and the configurations whose maximal height difference from h' is bigger than $\frac{\delta}{4}$ is exponentially small in n. The fixed boundary conditions of the triangles together with the control on the maximal height difference gives a lower bound of $S(X_n^{\mathcal{V}_\delta(h)})$, so as conclusion we prove that for any δ and for n small enough,

$$\frac{S(X_n^{\mathcal{V}_\delta(h)})}{n^2} \geq Ent(h) - \varepsilon.$$

Now we prove the upper bound. For any $\varepsilon > 0$, since h has no atom and $Ent(h) > -\infty$, there exists ε_1 such that for any subset of D of Lebesgue measure less than ε_1, the integral of $ent \circ \nabla h$ on that set is bigger than $-\frac{\varepsilon}{4}$. By Lemma 6.4.14, for $l > 0$ small enough, the piecewise linear function h' on the l-right-triangle mesh satisfies that
(a) for at least a fraction of $1 - \varepsilon_1$ of triangles in the mesh, on every triangle, the function h is within $\rho^{\frac{\varepsilon}{2}}(s, t)l$ of h' where (s, t) is the tilt of that triangle.
(b) $Ent(h') < Ent(h) + \frac{\varepsilon}{4}$.

Lemma 6.4.2 says that the at most ε_1 fraction of triangles, the entropy S is at most C times the area of the triangles, and Theorem 6.4.10 says that on every triangle, if the tilt h' is (s,t) there, then the normalized entropy of all the configurations whose height on the boundary of the triangle is within $\rho^{\frac{\varepsilon}{2}}(s,t)l$ is less than $ent(s,t)+\frac{\varepsilon}{2}+o(1)$ times the area of the triangle, $o(1)$ converging to 0 when n tends to infinity. Summing this gives an upper bound of entropy, which is less than $Ent(h)+\varepsilon+o(1)$. This finishes the proof. □

The above large-deviation theorem naturally yields the following theorem about the convergence of a random bead configuration.

Theorem 6.4.15. *Given an asymptotic boundary condition function h^∂ defined on ∂D which is constant if restricted to $x=1$ or $x=0$, for any $n\in\mathbb{N}^*$, consider the bead model on D with n threads and with fixed boundary condition that approximates best h^∂. Then the normalized height function h converges (under the uniform norm) in probability when $n\to\infty$ to an admissible function h_0, which is the unique maximizer of $Ent(.)$.*

Proof. Theorem 6.4.1 proves that for any admissible function $h:D\to\mathbb{R}$ such that $Ent(h)>-\infty$, for any $\delta>0$, when $n\to\infty$, $\frac{S\left(X_n^{\mathcal{V}_\delta(h)}\right)}{n^2}$ converges to $Ent(h)$ when $n\to\infty$. We should also take the functions that $Ent(h)=-\infty$ into consideration.

If $h\in\mathcal{H}_0$, it is easy to see that Lemma 6.3.14 and the upper bound part of Theorem 6.4.10 still apply. Thus, for any $h\in\mathcal{H}_0$ such that $Ent(h)=-\infty$, we have

$$\lim_{\delta\to 0}\lim_{n\to\infty}\frac{S\left(X_n^{\mathcal{V}_\delta(h)}\right)}{n^2}=-\infty.$$

If $h\notin\mathcal{H}_0$, we consider the turned space $\tilde{\mathcal{H}}$ under the uniform norm. By definition, if $h\notin\mathcal{H}_0$, then there exists a subset of $(\tilde{x},\tilde{y})$ with Lebesgue measure $\mu>0$ where $\frac{\partial\tilde{h}}{\partial\tilde{y}}=1$. By the same argument of metric density used in Lemma 6.4.14, for all $\varepsilon>0$ small enough, there exists a subset of $\tilde{D}$ as a union of disjoint squares such that on every square the average vertical slope is bigger than $1-\varepsilon$ and the measure of this subset is bigger than $\mu-\varepsilon$. It is not hard to see that if we take $\varepsilon>0$ arbitrarily small, then for $\tilde{\delta}$ small enough, the entropy within the $\tilde{\delta}$-neighborhood in $\tilde{\mathcal{H}}$ of $\tilde{h}$ can be arbitrarily small.

An open set of admissible functions in the original height function space $\mathcal{H}$ is also an open set in the turned space $\tilde{\mathcal{H}}$, and the turned space $\tilde{\mathcal{H}}$ is compact under the uniform norm. Thus, from any open cover of the admissible functions we can choose a finite cover. By the definition of entropy, if we consider all the bead configurations with the same fixed boundary condition, then for any $\delta>0$, any admissible function h such that $Ent(h)>-\infty$ and for n large enough, the probability that a random bead configuration is in $\mathcal{V}_\delta(h)$, which by definition is equal to the proportion of the volume of this set with respect to the volume of the whole set of possible configurations, is proportional to $e^{Ent(h)n^2}$. When $n\to\infty$, the

probability that h is within the neighborhood of h_0 dominates the other possibilities, and we have proved the theorem. □

6.5 Solutions of the entropy maximizing problem

In this section, we will characterize h_0, the solution of the variational principle. The variational principle naturally yields a Euler-Lagrange equation of the limit shape h_0: since *ent* is smooth, to maximize the integral of *ent* over a region with given boundary condition, the height function should satisfies the equation:

$$\mathrm{div}\nabla ent \circ \nabla h = 0,$$

which implies

$$\pi^2(1+\tan^2(\pi h_x))h_y h_{xx} + \frac{h_{yy}}{h_y} + 2\pi h_{xy}\tan(\pi h_x) = 0. \tag{6.38}$$

However, in general it is hard to solve Equation (6.38) directly, and we hope to have a systematical way to find the solutions. A possible option is applying directly the results of [KO07] to the bead model, where the authors prove that finding the solution h of the Euler-Lagrange equation can be done via finding and solving a system of algebraic equations. To do so, we prove in Theorem 6.5.1 that the maximizer of the bead model is a properly normalized limit of those of the dimer models.

This theorem can be summarized by a commutative diagram (6.39) here below. For any given asymptotic fixed boundary condition h^∂ defined on ∂D and constant if restricted to $x = 0$ or $x = 1$, for any n, we consider the bead model with n threads and an almost planar boundary condition h_n^∂. Moreover, for any m big enough we consider $R_{mn,n}$ as the domain constructed in Section 5.1.6. We have:

$$\begin{array}{ccc} \text{Lozenge tiling of } R_{mn,n}, & \xrightarrow[m\to\infty]{} & \text{Bead configuration with } n \text{ threads}, \\ \Big\downarrow n\to\infty & \circlearrowleft & \Big\downarrow n\to\infty \\ \text{Limit shape of a uniformly chosen tiling of } R_{mn,n}, & \xrightarrow[m\to\infty]{} & \text{Limit shape of the bead model.} \end{array} \tag{6.39}$$

This result seems quite natural as the bead model is a continuous scaling limit of the dimer model. However, it is not trivial since there is no theory yet that ensures the commutativity of the limit in m (from dimer models to bead models) and that in n (from finite cases to asymptotic limit).

For every $R_{mn,n}$, rather than considering $m \to \infty$ while keeps n as when we defined the bead model, here we consider the limit $n \to \infty$ while keeping the asymptotic shape of the region. Let R_m be the region $R_{mn,n}$ normalized by n. Define

$$\sigma := \sup\{|y_1 - y_2| : (x_1, y_1), (x_2, y_2) \in R_m\} - m.$$

In other words, the height of the region R_m is equal to $m+\sigma$. Thus, if we vertically normalize R_m by $m+\sigma$, then the new region, denoted by D^m, fits inside the unit square D.

The boundary condition of D^m also naturally yields a boundary condition of D by vertically extending the boundary height function of D^m, *i.e.* for $x \in [0,1]$,

$$h(x,1) = h(x, \sup\{y : (x,y) \in D^m\}),$$
$$h(x,0) = h(x, \inf\{y : (x,y) \in D^m\}),$$

while $h(0,y)$ and $h(1,y)$ are constant.

The (dimer) admissible function on R_m, defined as the closure of the height function H of lozenge tilings normalized to D^m as above (see Figure 5.3), forms the space of functions on R_m which are horizontally $\frac{1}{2}$-Lipschitz, vertically non-decreasing and 1-Lipschitz. If naturally extended from D^m to the whole of D, they forms such following subspace of functions $\mathcal{H}_0$: define

$$\bar{\mathcal{H}}_m = \left\{ h \in \mathcal{H}_0 : \frac{\partial h}{\partial y}\Big|_{D\setminus D^m} = 0,\ h \text{ is } (m+\sigma)\text{-Lipschitz} \right\}.$$

It is easy to see that $(\bar{\mathcal{H}}_m)_m$ form an increasing subsequence exhausting $\mathcal{H}_0$ when $m \to \infty$.

Recall that $ent^\diamond$ as the local entropy function of the dimer model on the hexagon lattice. Considering Proposition 6.2.5, we define ent_m as the normalized and adjusted local entropy function of the dimer model, *i.e.*,

$$ent_m(s,t) = (m+\sigma)\ ent^\diamond(s, t/(m+\sigma)) - \ln(m+\sigma)t, \tag{6.40}$$

and for any $h \in \bar{\mathcal{H}}_m$ define

$$Ent_m(h) = \int_D ent_m \circ \nabla h\ dxdy.$$

Recall that Proposition 6.2.5 says that the right side of Equation (6.40) converges to $ent(s,t)$ for any (s,t) and the convergence is uniform on any compact of slopes that doesn't contain exploding points. We also remark that the concavity of ent simply implies the concavity of ent_m.

By [CKP01], for any $m \in \mathbb{N}^*$, there exists a unique height function $\bar{h}_m \in \bar{\mathcal{H}}_m$ that maximizes Ent_m. The following theorem is the main result of this section.

Theorem 6.5.1. *The normalized height functions $\bar{h}_m$ converge to h_0 on D when $m \to \infty$.*

Proof. Similar to Theorem 6.3.6, if we consider the turned space $\tilde{\mathcal{H}}$, by compactness there is a converging subsequence of $(\tilde{\bar{h}}_m)_m$, saying $(\tilde{\bar{h}}_{m_l})_l$. Denote the limit function's preimage in $\mathcal{H}$ by $\bar{h}_0$ (it may depends on the choice of the subsequence but we will prove that this is not the case).

We prove that it is the same function as h_0, and we do this by showing that $Ent(\bar{h}_0)$ is equal to $Ent(h_0)$. The proof is divided into the following three parts. We first prove that

$$Ent(h_0) \leq \liminf_{l\to\infty} Ent_{m_l}(\bar{h}_{m_l}), \tag{6.41}$$

then we show that $\bar{h}_0 \in \mathcal{H}_0$, so we can apply Lemma 6.3.13, and finally we prove that

$$Ent(\bar{h}_0) \geq \limsup_{m\to\infty} Ent_{m_l}(\bar{h}_{m_l}), \tag{6.42}$$

thus $Ent(\bar{h}_0) \geq Ent(h_0)$. By uniqueness of Theorem 6.3.6 we prove that $\bar{h}_0 = h_0$.

Finally, as we can apply this argument to any subsequence of $(\bar{\bar{h}}_m)_m$ and prove that any subsequence has a converging subsubsequence whose limit is h_0, so the convergence of subsequence is in fact a convergence of the sequence $(\bar{\bar{h}}_m)_m$ itself. Thus, without loss of generality, here below we suppose $(\bar{\bar{h}}_m)_m$ converges so as to simplify the notation.

Begin by proving Inequality (6.41), and without loss of generality we still take the setting of star-convexity used in Lemma 6.3.13. For any $\varepsilon > 0$, by Lemma 6.3.13 and Lemma 6.3.14 there exist $\delta, \delta' > 0$, functions $A_{\delta,\delta'}(h)$ and h', such that the function h' agrees with $A_{\delta,\delta'}(h)$ on $D\backslash D_\delta$, is piecewise linear on a l-triangle mesh of D_δ, and

$$Ent(h') \geq Ent(h_0) - \frac{\varepsilon}{2}.$$

The local entropy $ent \circ \nabla h'$ is bounded, so by the same reason mentioned in the proof of Lemma 6.3.15, there exists some $M \in \mathbb{Z}^+$ such that the vertical partial derivative is less than M. Still by construction, on the band $[0,1] \times [1-\delta, 1]$ and that $[0,1] \times [0,\delta]$, we have some frozen-like regions of shapes corresponding to the height function near the boundaries, so there exists $M' \in \mathbb{Z}^+$ such that outside $D^{M'}$ the vertical slope of h' is 0.

Thus, for all $m \geq \max\{M, M'\}$ we have $h' \in \bar{\mathcal{H}}_m$. Especially,

$$Ent_m(\bar{h}_m) \geq Ent_m(h').$$

As h' is piecewise linear on D_δ and the number of pieces is finite, and on $D\backslash D_\delta$ it is taken to be the naive function in Definition and Lemma 6.3.9, $\nabla h'$ only takes the values of $t = 0$ together with a finite number of possible values. By Lemma 6.2.5,

$$\lim_{m\to\infty} Ent_m(h') = Ent(h')$$

so for m sufficiently large we have

$$Ent_m(h') \geq Ent(h') - \frac{\varepsilon}{2}.$$

In conclusion, we have that for m sufficiently large,

$$Ent_m(\bar{h}_m) \geq Ent(h_0) - \varepsilon,$$

which proves Inequality (6.41).

Now we prove that $\tilde{\bar{h}}_0 \in \widetilde{\mathcal{H}}_0$. As in Theorem 6.3.6, if the set that $\frac{\partial \tilde{\bar{h}}_0}{\partial \tilde{y}} = 1$ is positive, then for any $\varepsilon > 0$, there exist a finite number of disjoint convex compacts $K_j, j = 1, 2, ..., J$ of a positive measure independent of ε and $M \in \mathbb{Z}^*$ such that on each compact the average vertical height change $av_y^{\Delta_k}(\tilde{\bar{h}}_m)$ is greater than $1 - 8\varepsilon$ if $m \geq M$. By an argument similar to that used in Theorem 6.3.6, it can be proved that

$$\limsup_{m\to\infty} \widetilde{Ent}_m(\tilde{\bar{h}}_m) = -\infty.$$

However, this contradicts to Inequality (6.41) which says that

$$\widetilde{Ent}_m(\tilde{\bar{h}}_m) = Ent_m(\bar{h}_m)$$

has a lower bound, so we have proved that $\bar{h} \in \mathcal{H}_0$.

Now we are allowed to use Lemma 6.3.13 to approximate $\bar{h}_0$ by a function of better regularity. For all $\varepsilon > 0$, we can choose δ, δ' small enough so that

$$Ent\big(A_{\delta,\delta'}(\bar{h}_0)\big) = (1 - 2\delta)^2 Ent(\bar{h}_0) + O(\delta \ln \delta),$$

so for any $\varepsilon > 0$ we may choose δ and δ' so that the absolute value of the term $O(\delta \ln \delta)$ is less than ε.

Furthermore, by construction of the operator $A_{\delta,\delta'}$, for the same δ and δ' as above, we have that for any admissible function h:
(a) if $h \in \bar{\mathcal{H}}_m$, then the integral of local entropy function ent_m of $A_{\delta,\delta'}(h)|_{D_\delta}$ is bigger than that of $h|_{D_\delta}$ (by concavity of ent_m).
(b) $A_{\delta,\delta'}(h)|_{D\backslash D_\delta}$ is the same function for any h, with two possible vertical derivative, and when the vertical derivative is non-zero, the horizontal one is bounded away from $\pm\frac{1}{2}$ by some constant of order δ. Thus, the integral of $ent_m \circ (\nabla A_{\delta,\delta'}(h))$ on $D\backslash D_\delta$ converges in m uniformly for all h to a term of absolute value less than ε.

In conclusion, for any $\varepsilon > 0$, there exists $\delta, \delta' > 0$ and $M \in \mathbb{N}^*$ such that for any $m \geq M$ we have

$$Ent_m\big(A_{\delta,\delta'}(\bar{h}_m)\big) \geq (1 - 2\delta)^2 Ent_m(\bar{h}_m) - \varepsilon.$$

The boundness of $Ent_m(\bar{h}_m)$ and concavity of ent_m implies the uniform boundness of $ent_m \circ \nabla A_{\delta,\delta'}(\bar{h}_m)$ on D.

We also claim that $\nabla A_{\delta,\delta'}(\bar{h}_m)$ converges uniformly to $\nabla A_{\delta,\delta'}(\bar{h}_0)$ on D. In fact, by construction, they are all identical on $D\backslash D_\delta$ so have the same gradient there, and on D_δ we have that for any m,

$$\nabla A_{\delta,\delta'}(\bar{h}_m) = -\nabla U_{\delta'} * P_{0,\delta,0}\bar{h}_m.$$

According to Lemma 6.3.4, $P_{0,\delta,0}\bar{h}_m$ converge uniformly to $P_{0,\delta,0}\bar{h}_0$, so the convergence of $\nabla A_{\delta,\delta'}(\bar{h}_m)$ to $\nabla A_{\delta,\delta'}(\bar{h}_0)$ is uniform.

Define $\left(K_l(A_{\delta,\delta'}(\bar{h}_0))\right)_{l=1,2,\ldots}$ as the following increasing sequence of subsets of D:

$$K_l(A_{\delta,\delta'}(\bar{h}_0)) = \left\{(x,y) \in D : \frac{\partial A_{\delta,\delta'}(\bar{h}_0)}{\partial x}(x,y) \in [-\frac{1}{2}+\frac{1}{l}, \frac{1}{2}-\frac{1}{l}] \times [0,A]\right\},$$

and the limit of this sequence is

$$K_\infty(A_{\delta,\delta'}(\bar{h}_0)) = \left\{(x,y) \in D : \frac{\partial A_{\delta,\delta'}(\bar{h}_0)}{\partial x}(x,y) \in]-\frac{1}{2}, \frac{1}{2}[\times[0,A]\right\}.$$

By the uniform convergence of $\nabla A_{\delta,\delta'}(\bar{h}_m)$ to $\nabla A_{\delta,\delta'}(\bar{h}_0)$, for all l, there exists M such that for all $m > M$, on $K_l(A_{\delta,\delta'}(\bar{h}_0))$ we have

$$\frac{\partial A_{\delta,\delta'}(\bar{h}_m)}{\partial x} \in [-\frac{1}{2}+\frac{1}{2l}, \frac{1}{2}-\frac{1}{2l}],$$

By Lemma 6.2.5 argument (a), the convergence of $ent_m(s,t)$ to $ent(s,t)$ is uniform for any $(s,t) \in [-\frac{1}{2}+\frac{1}{2l}, \frac{1}{2}-\frac{1}{2l}] \times [0,A]$, *i.e.*, for any $\varepsilon > 0$, there exists M' such that for all $m' > M'$ and all $(s,t) \in [-\frac{1}{2}+\frac{1}{2l}, \frac{1}{2}-\frac{1}{2l}] \times [0,A]$, we have

$$|ent_m(s,t) - ent(s,t)| < \frac{\varepsilon}{2}. \tag{6.43}$$

The uniform convergence also implies that the space

$$\{ent_m(.,.), m \geq M\} \cup \{ent(.,.)\}$$

viewed as a subspace of continuous functions on the compact set

$$(s,t) \in [-\frac{1}{2}+\frac{1}{2l}, \frac{1}{2}-\frac{1}{2l}] \times [0,A]$$

is compact. Especially, by Arzela-Ascoli, they are equicontinuous: for the same ε, there exists $\varepsilon' > 0$ such that for any (s,t) and (s',t') in $[-\frac{1}{2}+\frac{1}{2l}, \frac{1}{2}-\frac{1}{2l}] \times [0,A]$ and for any $m > M$,

$$||(s,t)-(s',t')|| < \varepsilon' \Rightarrow |ent_m(s,t) + ent_m(s',t')| < \frac{\varepsilon}{2}.$$

Again by the uniform convergence of $\nabla A_{\delta,\delta'}(\bar{h}_m)$ to $\nabla A_{\delta,\delta'}(\bar{h}_0)$, there exists $M'' > M$ such that for all $m'' \geq M''$,

$$\sup_{(x,y)\in K_l} ||\nabla A_{\delta,\delta'}(\bar{h}_{m''}) - \nabla A_{\delta,\delta'}(\bar{h}_0)|| < \varepsilon'.$$

Thus for all $m' > M'$, $m'' > M''$, $(x, y) \in K_l$, we have

$$\begin{aligned} & |ent_{m'} \circ \nabla A_{\delta,\delta'}(\bar{h}_{m''})(x,y) - ent \circ \nabla A_{\delta,\delta'}(\bar{h}_0)(x,y)| \\ \leq\ & |ent_{m'} \circ \nabla A_{\delta,\delta'}(\bar{h}_{m''})(x,y) - ent_{m'} \circ \nabla A_{\delta,\delta'}(\bar{h}_0)(x,y)| \\ & + |ent_{m'} \circ \nabla A_{\delta,\delta'}(\bar{h}_0)(x,y) - ent \circ \nabla A_{\delta,\delta'}(\bar{h}_0)(x,y)| \\ \leq\ & \varepsilon. \end{aligned}$$

Thus, on K_l, we have the following uniform convergence on m' and m'':

$$\lim_{m' \to \infty, m'' \to \infty} ent_{m'} \circ \nabla A_{\delta,\delta'}(\bar{h}_{m''})(x,y) = ent \circ \nabla A_{\delta,\delta'}(\bar{h}_0)(x,y),$$

so

$$\lim_{m \to \infty} Ent_m^{K_l}(A_{\delta,\delta'}(\bar{h}_m)) = Ent^{K_l}(A_{\delta,\delta'}(\bar{h}_0)). \tag{6.44}$$

When l tends to infinity, by bounded convergence, the right hand side of (6.44) tends to $Ent^{K_\infty}(A_{\delta,\delta'}(\bar{h}_0))$ which is equal to $Ent(A_{\delta,\delta'}(\bar{h}_0))$. For the left hand side, the difference between $Ent_m^{K_l}(A_{\delta,\delta'}(\bar{h}_m))$ and $Ent_m^{K_\infty}(A_{\delta,\delta'}(\bar{h}_m))$ also converges to 0 by bounded convergence, and the difference between $Ent_m^{K_\infty}(A_{\delta,\delta'}(\bar{h}_m))$ and $Ent_m(A_{\delta,\delta'}(\bar{h}_m))$ is equal to

$$\iint_{D \setminus K_\infty} ent_m(A_{\delta,\delta'}(\bar{h}_m))dxdy,$$

and by Lemma 6.2.5 (b), for l sufficiently large, then for m large enough, the term above will be uniformly bounded from above by ε.

In conclusion, for m large enough, we have

$$Ent\big(A_{\delta,\delta'}(\bar{h}_0)\big) \geq Ent_m\big(A_{\delta,\delta'}(\bar{h}_m)\big) - 2\varepsilon,$$

and let $\varepsilon \to 0$ we get

$$Ent(\bar{h}_0) \geq \limsup_{m \to \infty} Ent_m(\bar{h}_m),$$

which is Inequality (6.42). □

Inspired by the results of [KO07], in the following part of this section, we are furthermore interested in the case where the asymptotic upper and lower boundary functions of the bead model are piecewise linear where every piece is of slope $\pm\frac{1}{2}$ and that the length of every piece is rational.

Consider the discrete version of this bead model, *i.e.* tiling a regions $R_{mn,n}$ by lozenges for $m, n \in \mathbb{N}^*$ large enough. Consider a subsequence of n such that $\frac{1}{n}$ divides the length of every piece of the boundary. The advantage of taking this subsequence is that it verifies the the assumptions of [KO07]. Meanwhile, by Theorem 6.4.15, the limit shape along such subsequence of n is the same for the sequence in n itself.

Thus, without loss of generality, we can apply the results of [KO07] to our case about the limit shape when $n \to \infty$ for fixed m.

By [KO07], for every $R_{mn,n}$, we can complete the boundary by adding some imaginary vertical edge so that the region can be viewed as a polygon whose boundary is made up of the edges clockwise (or anticlockwise) repeated in the directions of the edges of the honeycomb lattice. If the number of edges is $3d$, [KO07] proves that when $n \to \infty$, the limiting height function ($\bar{h}_m$ if normalize this to D) exists and is determined by

$$\nabla h = \frac{1}{\pi}(\mathrm{Arg}w, -\mathrm{Arg}z),$$

in the liquid region, where w and z are found by solving a system of algebraic equations

$$\begin{aligned} P(z,w) &= 0, \\ Q_0(z,w) &= xzP_z + ywP_w, \end{aligned}$$

$P(z,w)$ as the characteristic polynomial and Q being a polynomial of degree at most d. We remark that coefficients of Q_0 effectively depend on m. Also, there is an algebraic arctic curve (the frozen boundary) of degree at most $2d-2$ that separates the liquid and frozen region, see Section 2.4.1 for a summary.

Theorem 6.5.1 says that the normalized limit height functions $\bar{h}_m$ converge to h_0 (the limit height function of the bead model) when $m \to \infty$, so the frozen boundary converges too. Denote the frozen boundaries of $\bar{h}_m$ by γ_m and that of h_0 by γ_0. The algebraic curves of degree less than some integer d is a finite dimensional object, so the convergence of these algebraic curves is equivalent to the convergence of their coefficients, which means that γ_0 is still an algebraic curve whose degree is at most $2d-2$. Moreover, γ_m is tangent to every side of the polygon (perhaps on the extended line). As $m \to \infty$, these tangent relations is interpreted to be the tangent relations between γ_0 and ∂D. It is easy to see that the only possibility is given by the following proposition.

Proposition 6.5.2. *Suppose that the upper boundary of D can be divided into the following $2k_u$ intervals*

$$[0,1] = \bigcup_{i=1,\ldots,k_u} \left([a_u^i, b_u^i] \cup [b_u^i, a_u^{i+1}]\right),$$

(by convention we take $a_u^1 = 0$, $a_u^{k_u+1} = 1$), and on every interval of $[a_u^i, b_u^i]$ (resp. $[b_u^i, a_u^{i+1}]$) the upper boundary height function $h(.,1)$ is of slope $\frac{1}{2}$ (resp. $-\frac{1}{2}$). Similarly, suppose that the lower bound of D can be divided into the intervals

$$[0,1] = \bigcup_{j=1,\ldots,k_l} \left([a_l^j, b_l^j] \cup [b_l^j, a_l^{j+1}]\right),$$

and on every interval of $[a_l^j, b_l^j]$ (resp. $[b_l^j, a_l^{j+1}]$) the upper boundary height function $h(.,0)$ is of slope $-\frac{1}{2}$ (resp. $\frac{1}{2}$). Then the frozen boundary h_0 is an algebraic curve

of degree $2(k_u + k_l) - 2$ *and genus* 0 *such that it is tangent to* ∂D *at the points*

$$\Big(\bigcup_{i=1,\dots,k_u} \{(b_u^i, 1)\} \Big) \cup \Big(\bigcup_{j=1,\dots,k_l} \{(b_l^j, 0)\} \Big),$$

tangent to the lines $x = a_u^i$, $i = 2, \dots, k_u$ *and the lines* $x = a_l^j$, $i = 2, \dots, k_l$ *in the interior of* D *with cusp singularities, and tangent to the left and right boundaries of* D.

We give an explicit example here below. Consider a boundary condition we considered in Chapter 1:

$$f(x,y) = \begin{cases} \frac{1}{4} - \frac{1}{2}|x - \frac{1}{2}| & \text{if } y \leq 0, \\ -\frac{1}{4} + \frac{1}{2}|x - \frac{1}{2}| & \text{if } y > 0. \end{cases}$$

Here $d = 2$, so the frozen boundary is of degree at most $2d - 2 = 2$. By symmetry and we have at once that the frozen boundary is a circle, the only degree 2 algebraic curve that verifies Proposition 6.5.2. Moreover, this boundary condition corresponds to an hexagonal domain in the dimer model, a particular case studied in [CLP98] where the author gives explicit solutions. If we let the length of two vertical edges tend to infinity, readers can easily verify that the following function $h(x,y) = \frac{1}{2\pi} H(2x-1, 2y-1)$, where

$$H(x,y) = \begin{cases} \arctan \frac{y}{\sqrt{1-x^2-y^2}} - x \arctan \frac{xy}{\sqrt{1-x^2-y^2}} \text{ if } x^2 + y^2 \leq 1 \\ \frac{\pi}{2}(1 - |x|) \text{ if } x^2 + y^2 > 1, y > \frac{1}{2} \\ \frac{\pi}{2}(|x| - 1) \text{ if } x^2 + y^2 > 1, y < \frac{1}{2} \end{cases}$$

is a particular solution of the Euler-Lagrange equation (6.38).

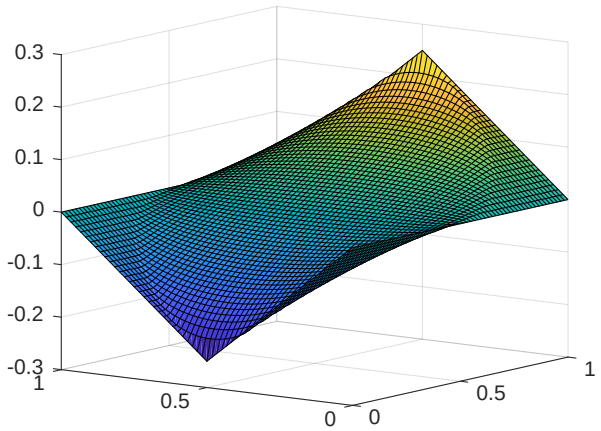

Figure 6.9: The function h_0 for this boundary condition.

We remark that this shape corresponds to a square Young diagram. We will use this result to recover the limit shape of a random square Young tableau calculated in [PR07].

6.6 Limit shape of standard Young tableaux

6.6.1 Limit shape of standard (skew) Young tableaux

In this section we study the limiting behavior of a random standard Young tableau with a given asymptotic shape (which can be skew). We use the map from uniform bead configurations and the convergence result of a random bead configuration.

More precisely, we fix an arbitrarily chosen (skew) shape of Young diagram λ, given by two $\frac{1}{2}$-Lipschitz function

$$h(.,0), h(.,1) : [0,1] \to \mathbb{R}$$

such that $h(x,1) - h(x,0) > 0$ on $]0,1[$, and λ is given by

$$\lambda = \{(x,z) : 2h(x,0) \leq z \leq 2h(x,1)\}.$$

Without loss of generality we can suppose that $h(0,0) = h(0,1) = 0$. Readers can compare this to (6.24), page 86.

For any $n \in \mathbb{N}^*$, define λ_n as the normalized (skew) diagram that approximates λ to an order of $O(\frac{1}{n})$, and the diagram is made of boxes of edge length $\frac{\sqrt{2}}{n}$ and written under the Russian convention. We use the $x - z$ coordinates.

Recall that $\mathcal{T}_{\lambda_n}$ is the set of standard tableaux of diagram λ_n. We can view a random tableau $T \in \mathcal{T}_{\lambda_n}$ as a random piecewise constant function on λ_n.

Consider Ω as a probability space, and consider $\mathbf{B}_n = \mathbf{B}_n(\omega)$ be a random bead configuration for the bead model corresponding to λ_n. By the map $\mathcal{Y}$ constructed in Section 5.2.2 from bead configurations to the standard Young tableaux, we define the following random surface

$$\begin{array}{rccl} \tau_n : & \mathbb{R}^2 \times \Omega & \to & [0,1], \\ & (x,z;\omega) & \mapsto & \mathbb{1}_{(x,z)\in\lambda_n} \dfrac{\mathcal{Y}(\mathbf{B}_n(\omega))(x,z)}{|\lambda_n|}, \end{array}$$

where we extend the function to the whole $\mathbb{R}^2$ plane and outside λ_n we take 0 by default. We have the following theorem.

Theorem 6.6.1. *For a sequence of (skew) Young diagram λ_n with an asymptotic shape λ, when $n \to \infty$, the random surfaces τ_n converge on any compact subset of the interior of λ in probability and under uniform metric to a surface $\mathcal{S}$ supported on λ. The surface $\mathcal{S}$ is explicitly determined by the unique function $h_0 \in \mathcal{H}$ that maximizes $Ent(.)$ with a boundary condition corresponding to λ. If we define for any $x \in [0,1]$*

$$z_-(x) = \inf\{z : (x,z) \in \lambda\},$$
$$z_+(x) = \sup\{z : (x,z) \in \lambda\},$$

and for any value $e \in [h(x,0), h(x,1)]$, define

$$h_{0,x}^{-1}(e) = \inf\{y \in [0,1] : h_0(x,y) \geq e\},$$

then the surface is given by

$$\mathcal{S}(x,z) = \begin{cases} h_{0,x}^{-1}\left(\frac{h_0(x,0)(z_+(x)-z)+h_0(x,1)(z-z_-(x))}{z_+(x)-z_-(x)}\right) & \text{if } (x,z)\in\lambda, \\ 0 & \text{otherwise.} \end{cases}$$

Proof. Consider the corresponding sequence of bead models, which by construction has an asymptotic boundary condition h^∂ determined by λ. By Theorem 6.4.15, the normalized height function h converges in probability to h_0 under the uniform metric.

For any such compact K in the interior of λ, there exists $N(K)\in\mathbb{N}^*$ such that for any $n > N(K)$ we have $K \subset \lambda_n$. To prove that τ_n converges to $\mathcal{S}$ on K, we define another random function η_n. Recall that $y_{i,j} = y_{i,j}(\omega)$ is the random vertical coordinate of the j^{th} bead on the i^{th} thread (page 63). For any bead configuration $\mathbf{B}_n$ with n threads, $n > N(K)$, consider

$$\begin{aligned} \eta_n : \quad K \quad &\to [0,1], \\ (x,z;\omega) \quad &\mapsto y_{\lfloor xn\rfloor,\lfloor (z-z_-(x))n\rfloor}(\omega), \end{aligned}$$

i.e., for all n we associate the box containing the point (x,z) to a value equal to the y-coordinate of the bead corresponding to that box.

When $n\to\infty$, the random function η_n converges in probability to $\mathcal{S}(x,z)$ on K. In fact, restricted to every x, $\eta_n(x,.,\omega)$ viewed as a stepwise constant function of z is roughly the inverse (which can be well defined by using inf and sup) of the normalized height function h as a stepwise constant function of y. Meanwhile, still restricted to x, the surface $\mathcal{S}$ viewed as a function of z is merely the inverse function of h_0 as a function of y, while the degenerating case (where the inversion fails) only happens in the frozen region of h_0, and by construction this doesn't matter. Thus the fact that a random surface h converges to h_0 implies that η_n converges to $\mathcal{S}$.

Now consider the difference between τ_n and η_n. For any bead configuration, conditioning to any ordering of $y_{i,j}$, the difference of τ_n and η_n on a box i,j is just equal to the difference of $y_{i,j}$ and its rank normalized by $|\lambda_n|$. So

$$\sup_{(x,z)\in K}|\tau_n-\eta_n|(x,z) \le \sup_{k=1,2,\dots,|\lambda_n|}\left|y_{i_k,j_k}-\frac{k}{|\lambda_n|}\right|,$$

where the right hand side converges to 0 in probability since the array $(y_{i_k,j_k})_{k=1,2,\dots,|\lambda_n|}$ is of the same law than a random ordered $|\lambda_n|$-dimensional array under the uniform measure on $[0,1]$. □

We remark that the random surface η_n in the proof can be viewed as the limit of a normalized plane partition, which also gives the bead model. So the convergence of η_n when $n\to\infty$ is nothing different from the convergence of bead configurations in Theorem 6.4.15.

We call Theorem 6.6.1 the "surface version" convergence of a random (skew) Young tableau. It will be interesting to recover for a general skew case the results of [PR07] and [Ś06], which we call as the "contour curve version" convergence.

For any (skew) Young diagram λ_n, any standard tableau $T \in \mathcal{T}_{\lambda_n}$, and for any $\alpha \in]0,1[$, define $Y_{\alpha,n}(T)$ as the set composed of the boxes whose entries are less than $\alpha|\lambda_n|$, *i.e.* a sub (skew) diagram of λ_n given by

$$Y_{\alpha,n}(T) := \left\{ \left(\frac{i}{n}, \frac{j}{n} \right) : T(i,j) \leq \alpha|\lambda_n| \right\}. \tag{6.45}$$

If we consider T as a random standard tableau, then $Y_{\alpha,n}$ such defined is a random subdiagram of λ_n. We have

Theorem 6.6.2. *When $n \to \infty$, the Dirac measures of the upper boundary of $Y_{\alpha,n}$ converges to a Dirac measure on a curve determined explicitly by h_0. The curve is the contour line of height α of the surface $\mathcal{S}$ in Theorem 6.6.1.*

Proof. Consider a boundary condition on D of the bead model corresponding to λ and a line segment $y = \alpha$ in D. Then for any $n \in \mathbb{N}^*$, define the following random subdiagram of λ_n formed by the boxes corresponding to the beads under the line $y = \alpha$, *i.e.*,

$$Y'_{\alpha,n} = \left\{ \left(\frac{i}{n}, \frac{j}{n} \right) : y_{i,j} \leq \alpha|\lambda_n| \right\}.$$

The upper boundary of $Y'_{\alpha,n}$ normalized by n is a 1-Lipschitz function on $[0,1]$. By the same reason than in Theorem 6.6.1, this curve converges to a limiting curve determined by h_0.

Consider the difference of the diagrams $Y'_{\alpha,n}$ and $Y_{\alpha,n}$. If $\alpha|\lambda_n| \leq y_{i_{\lfloor \alpha|\lambda_n| \rfloor}, j_{\lfloor \alpha|\lambda_n| \rfloor}}$, then $Y'_{\alpha,n} \leq Y_{\alpha,n}$ and if $\alpha|\lambda_n| \geq y_{i_{\lfloor \alpha|\lambda_n| \rfloor}, j_{\lfloor \alpha|\lambda_n| \rfloor}}$ then $Y'_{\alpha,n} \geq Y_{\alpha,n}$. In either case, their difference is a random skew diagram, and the number of boxes in this diagram is

$$\big|\alpha|\lambda_n| - y_{i_{\lfloor \alpha n \rfloor}, j_{\lfloor \alpha n \rfloor}}|\lambda_n| + O(1)\big|.$$

Thus, the area of this diagram normalized into λ is equal to the difference of α and the $\lfloor \alpha|\lambda_n| \rfloor^{th}$ biggest element in a random array uniformly taking $|\lambda_n|$ points in $[0,1]$, which converges to 0 in probability when $n \to \infty$. By the Lipshictz condition of the upper boundary of a Young diagram under the Russian convention, the norm sup of these upper boundaries converges to 0 in probability. Thus the Dirac measure of the upper boundary of $Y_{\alpha,n}$ converges to the same limit than that of $Y'_{\alpha,n}$. □

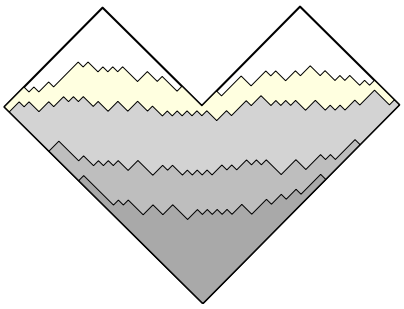

Figure 6.10: Contour curves of a Young tableaux for $\frac{1}{6}$, $\frac{1}{3}$, $\frac{2}{3}$ and $\frac{5}{6}$.

As an example, we consider the boundary function

$$f(x,y) = \begin{cases} \frac{1}{4} - \frac{1}{2}|x - \frac{1}{2}| & \text{if } y \le 0, \\ -\frac{1}{4} + \frac{1}{2}|x - \frac{1}{2}| & \text{if } y > 0, \end{cases}$$

which corresponds to the shape of a random square standard Young tableau. For a sequence of odd positive integers n, let λ_n be a sequence of squares $\frac{n+1}{2} \times \frac{n+1}{2}$, so the corresponding bead model has n threads. This is the case studied in Section 6.5, where h_0 is given explicitly via an existing result of [CLP98]. For any $\alpha \in]0,1[$, if we write the square diagram under the Russian convention and let the scale be $[0,1] \times [0,1]$, define $z_\alpha(x)$ as the limiting upper boundary of the first α proportion of boxes. This corresponds to a level line $y = \alpha$, and the difference of $z_\alpha(x)$ and the lower boundary of the diagram (*i.e.* $z = |x - \frac{1}{2}|$) corresponds to the number of beads on the thread x and between $y = \alpha$ and $y = 0$. Since the total area is $\frac{1}{2}$, we have that

$$\begin{aligned} z_\alpha(x) &= 2\big(h_0(x,\alpha) - h_0(x,0)\big) + |x - \frac{1}{2}| \\ &= \begin{cases} \frac{1}{\pi}\left(\arctan \frac{1-2\alpha}{\sqrt{1-(1-2x)^2-(1-2\alpha)^2}} - (1-2x)\arctan \frac{(1-2\alpha)(1-2x)}{\sqrt{1-(1-2x)^2-(1-2\alpha)^2}}\right) + \frac{1}{2} \\ \qquad\qquad \text{if } 1-(1-2x)^2-(1-2\alpha)^2 \ge 0, \\ |x - \frac{1}{2}| \qquad \text{if } 1-(1-2x)^2-(1-2\alpha)^2 < 0,\ \alpha < \frac{1}{2}, \\ 1 - |x - \frac{1}{2}| \qquad \text{if } 1-(1-2x)^2-(1-2\alpha)^2 < 0,\ \alpha > \frac{1}{2}. \end{cases} \end{aligned}$$

Thus we recover the result in [PR07].

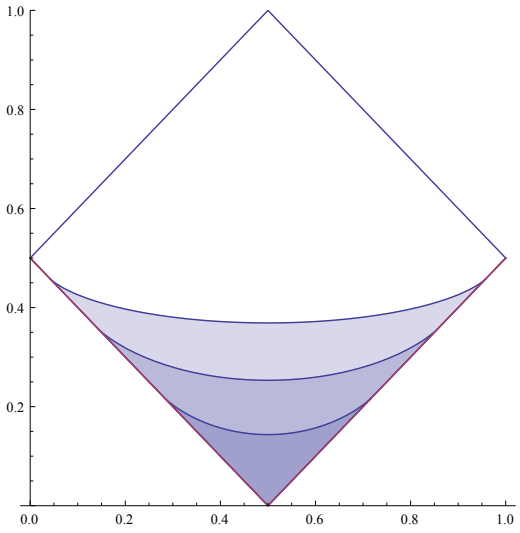

Figure 6.11: Level line of a standard square tableau, for $\alpha = 0.05$, 0.15 and 0.3.

6.6.2 Arctic curve of a uniform particle jumping process

We end this chapter by considering a particle jumping process encoding the standard Young tableaux, proposed in [Rom12], where the author finds an arctic curve

separating frozen regions and mixing regions. This behavior has an obvious similarity to those of the bead model and dimer model, and we show that they are in fact equivalent.

The jumping process we consider is as follows. Suppose on $\mathbb{Z}$ there are p particles. Every particle occupies a site of $\mathbb{Z}$ at time 0, which we call as the initial state, which can be viewed as a set $E_0 \subset \mathbb{Z}$ where $|E_0| = p$. At every time $t \in \mathbb{N}^*$, there is exactly one particle which jumps, at it is allowed to jump one unit to its right if that site is not occupied. We also fix a time $\mathbf{T}$ as well as the ending state $E_1 \subset \mathbb{Z}$, $|E_1| = p$. It is obvious that there exists such a jump process if and only if for any $k \in \mathbb{Z}$, the number of the elements of E_0 that is less than k is smaller than that of the elements of E_1. Moreover, we have

$$\mathbf{T} = \sum_{k \in E_1} k - \sum_{k' \in E_0} k'.$$

We will consider the uniform probability measure on this process, *i.e.* every possible configuration has the same probability.

For every (skew) Young diagram, there exists a corresponding particle jumping process such that every configuration of the jumping process corresponds to exactly one standard tableau. The process is constructed as below. For any (skew) Young diagram λ, write the diagram under the Russian convention. As in Figure 6.12, we draw one line above the diagram and on below the diagram. For every northwest-southeast going edge on the lower (resp. upper) boundary of the diagram, we associate to it a particle right below (resp. above) it on the line.

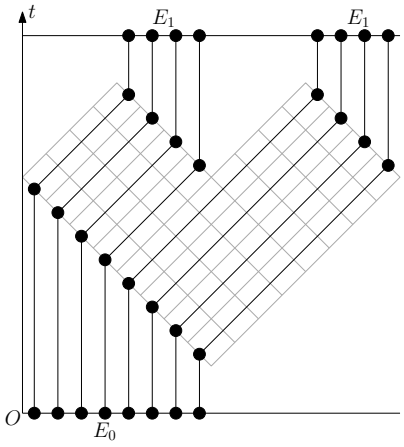

Figure 6.12: An example of associating a Young diagram to 8 particles.

Obviously the number of particles on the line below the diagram is equal to that on the line above the diagram, and this is equal to the number of rows of the diagram (under the French convention). We associate the i^{th} row (under the French convention) to the i^{th} particles counted from right on the line above and below the diagram. Given any standard tableau $T \in \mathcal{T}_\lambda$, let particles begin at their positions on the line below the diagram, and at every time t, $t \in \{1, 2, ..., |\lambda|\}$, if $T_{i,j} = t$, then the i^{th} particle jump one step to its right, and finally it will go to the position

of the i^{th} particle on the line above the diagram, see Figure 6.13 for an illustration. It is clear that this correspondence between standard tableaux and configurations of particle jump process is 1 to 1 and measure preserving if both are under uniform measure.

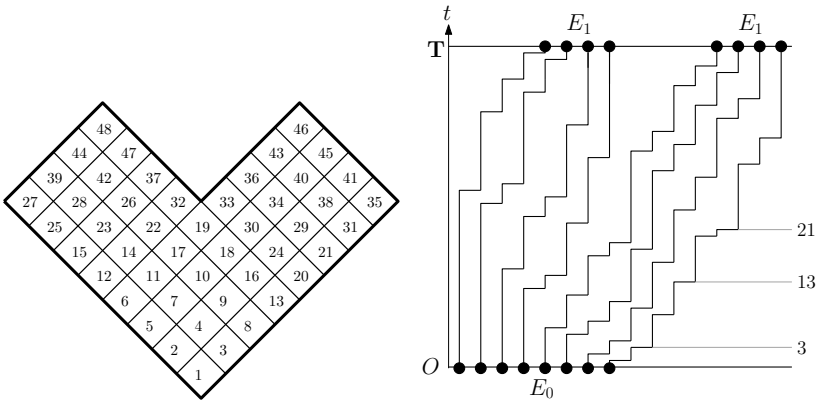

(a) Young tableau. (b) Corresponding process.

Figure 6.13: The process corresponding to a random tableau, 8 particles.

When the size of the diagram goes to infinity, we observe the appearance of an arctic curve. Figure 6.14 gives a simulation of 40 particles.

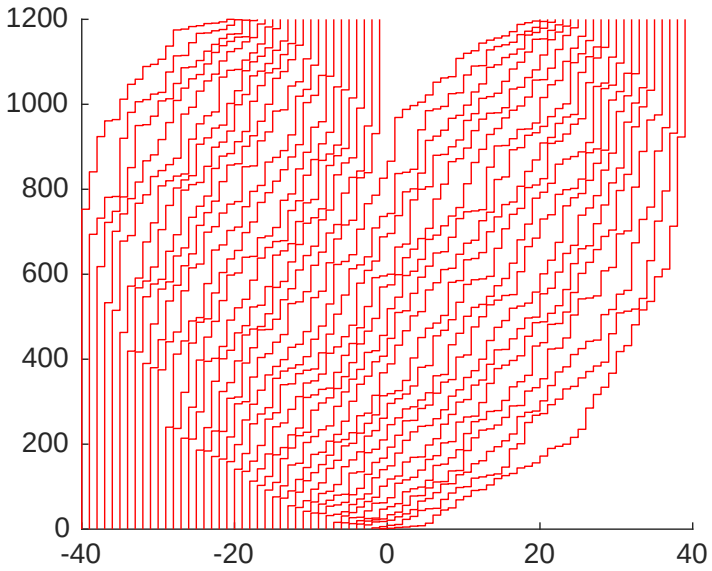

Figure 6.14: The process corresponding to a random tableau of shape Figure 6.12, 40 particles.

We have the following result as a generalization of Theorem 2 of [Rom12] for

more general diagrams.

Suppose that there is a shape of Young diagram λ written under the Russian convention whose boundary is piecewise linear and the projection of every piece on the x axis is rational. Suppose that n_0 is the smallest positive integer such that the length of every piece of boundary of λ is integer if multiplied by n_0. Then we consider a sequence of diagram $\lambda_{kn_0} = kn_0\lambda$.

Consider the jump processes corresponding to λ_{kn_0}. Clearly, the number of particles is proportional to k and the number of jumps (equal to $|\lambda_{kn_0}|$) is proportional to k^2. To simplify the notation we let $n = kn_0$.

Scale this process into a unit square $[0,1] \times [0,1]$, so the horizontal step size is $\frac{1}{n-1}$ and the vertical step size is $\frac{1}{|\lambda_n|}$. For any $i \in \mathbb{N}*$, define $t_n^-(i)$ (resp. $t_n^+(i)$) be the first (resp. last) moment that there is a particle jump from or jump into the line $x = \frac{i}{n-1}$. Then we have the following arctic-curve theorem for random (skew) Young tableaux.

Proposition 6.6.3. *The exist two functions*

$$\varphi_\pm : [0,1] \to [0,1],$$

such that for any $\varepsilon > 0$, when $n \to \infty$, the probability of the event

$$\left\{ \max_{1\le i\le n-1} \left| \frac{t_n^-(i)}{|\lambda_n|} - \varphi_-(\frac{i}{n-1}) \right| < \varepsilon \right\} \cap \left\{ \max_{1\le i\le n-1} \left| \frac{t_n^+(i)}{|\lambda_n|} - \varphi_+(\frac{i}{n-1}) \right| < \varepsilon \right\}$$

converges to 1.

Proof. It suffices to note that the constructed point process is nothing else but a discretization of a bead model: for any bead configuration with vertical coordinates ordered as

$$y_{i_1,j_1} < y_{i_2,j_2} < ... < y_{i_{|\lambda_n|},j_{|\lambda_n|}},$$

then the corresponding process replaces y_{i_k,j_k} by k for any $k \in \{1,2,...,|\lambda_n|\}$. Since

$$\max_{k\le|\lambda_n|} \left| y_{i_k,j_k} - \frac{k}{|\lambda_n|} \right|$$

converges to 0 in probability, the proposition is just a corollary of the corresponding result on the bead model where there is an arctic curve in the limit that separating frozen regions and non-frozen one(s) if the boundary condition is given by piecewise linear functions. □

Appendix A

We give a summary of two papers that study the limit shape of standard Young tableaux when the sizes go to infinity.

Section A.1 is based on the work of [PR07], where the authors use the hook formula for non-skew diagrams to prove and explicitly compute the limit shapes for rectangular shapes. We give a short summary of the hook formula(s), including a general hook formula [Nar14] that enumerates the standard tableaux of skew shapes. But note that this tool does not directly allow us to generalize the results of [PR07].

Section A.2 is based on the work of [Śni06] and also [VK77, Bia98, Bia01, IO02a]. The limit shape of a random diagram has been studied in [Bia01, Bia98, IO02b, LS77], where the authors consider the representations of symmetric groups. The limit shape of a random tableau is in correspondence with a subrepresentation. Section A.2.1 provides background on representation theory and Section A.2.2 concludes with the existence of a limit shape of a random tableau. It is not obvious how to explicitly calculate the limit shape of standard tableaux using this approach, and not obvious that this result can be generalized to skew shapes.

A.1 Limit shape of standard Young tableaux via hook formula

A.1.1 Hook formula(s)

In this section we give a short summary of an important combinatorial result about the standard Young tableaux, the hook formula(s).

The classical hook formula is first proved in [FRT54] and later by several different approaches ([Ban08, CFKP11, GNW79, Kra95, NPS97, Pak02, Rem82, Ver89] and others). It is generalized to skew shapes first by Naruse [Nar14] and a series of papers [MPP16, MPP17] continue this work.

Consider the standard Young tableaux of shape λ, $|\lambda| = n$. The number of such tableaux is given by the *hook formula*: for each cell at the position (i, j) in the

Young diagram λ, let $h_\lambda(i,j)$ be the number of the cells of position (i',j') such that either $i'=i$, $j'\geq j$ or $i'\geq i$, $j'=j$. Then the number of standard Young tableaux of diagram λ, denoted by $|\mathcal{T}_\lambda|$, is equal to

$$|\mathcal{T}_\lambda| = \frac{n!}{\prod_{(i,j)\in\lambda} h_\lambda(i,j)}. \tag{A.1}$$

This formula gives an easy way to count the number of standard Young tableaux of a given shape. The fact that the right hand side of (A.1) is written as a product yields the possibility of approximating the normalized logarithm of $|\mathcal{T}_\lambda|$ by an integral. This is one of the crucial facts that leads to [PR07], see Section A.1.2 below.

For the skew shapes, in [Nar14] the following result is proved.

An *excited move* is a family of mappings between skew Young diagrams of the same number of boxes. A hole (a location without box) (i,j) can be moved to $(i+1,j+1)$ if both $(i,j+1)$ and $(i+1,j)$ are occupied by a box.

Let $\mu\leq\lambda$ be two Young diagrams. For the skew Young diagram $\lambda\backslash\mu$, a (skew) Young diagram ξ is called its excited diagram if ξ can be obtained from $\lambda\backslash\mu$ via successive excited moves. Denote the set of the excited diagrams of $\lambda\backslash\mu$ by $\Xi(\lambda\backslash\mu)$, then the number of standard skew Young tableaux of the shape $\lambda\backslash\mu$ is equal to

$$|\mathcal{T}_{\lambda\backslash\mu}| = \sum_{\xi\in\Xi(\lambda\backslash\mu)} \frac{n!}{\prod_{(i,j)\in\xi} h_\xi(i,j)}. \tag{A.2}$$

where $n=|\lambda\backslash\mu|$.

Note that the skew hook formula (A.2) gives a sum of products rather than a single product, so the generalization of the sum-to-integral method to study asymptotic behavior is not direct.

A.1.2 A variational principle for rectangular Young tableaux via the hook formula

In [PR07], the authors prove the existence of a limit shape of the rectangular Young tableaux and explicitly compute its shape. The tool they use is the classical hook formula. Similar arguments also appeared in [LS77, VK77] and others.

Consider without losing generality a square Young diagram λ_n of size $n\times n$ written under the Russian convention (the same approach will apply to any rectangle shape without difficulty), and we normalize the diagram λ_n by n. Denote by $\mathcal{T}_{\lambda_n}$ the set of standard Young tableaux. For any $T\in\mathcal{T}_{\lambda_{\lambda_n}}$ and any $k\in\mathbb{N}^*$, $1\leq k\leq n^2$, let λ_T^k be the union of the boxes of T whose entrance is not bigger than k. Clearly, such λ_T^k is a sub Young diagram of λ of dimension k, and its upper boundary is a 1-Lipschitz function having k boxes below it.

If we fix this Lipschitz upper boundary function, denoted by f, the boxes below the boundary and those above it form two Young diagrams. Denote them respectively by λ_f^- and λ_f^+. If we consider the uniform measure on the standard Young

tableaux, then the probability that the upper boundary of the set of the smallest k boxes is f is

$$\mathbb{P}(T \in \mathcal{T}_{\lambda_n} : \lambda_T^k = \lambda_f^-) = \frac{k!}{\prod_{(i,j)\in\lambda_f^-} h_{i,j}} \frac{(n^2-k)!}{\prod_{(i,j)\in\lambda_f^+} h_{i,j}} \frac{1}{|\mathcal{T}_{\lambda_n}|}.$$

When $n \to \infty$, this product formula, as mentioned in the last section, naturally yields the use of an integral to approximate the logarithm of the probability of finding a specific f in a random tableau. Authors of [PR07] prove that, when $n \to \infty$,

$$\frac{\ln \mathbb{P}(T \in \mathcal{T}_{\lambda_n} : \lambda_T^k = \lambda_f^-)}{n^2} = -I\left(f, \frac{k}{n^2}\right) + o(1).$$

This formula gives a variational principle. Together with some other arguments, it yields that for any $\alpha \in]0,1[$, when $n \to \infty$, the normalized upper boundary of the set of first $\lfloor \alpha n^2 \rfloor$ boxes of a random tableau of size $n \times n$ converges uniformly to a function f that minimizes the functional $I(f, \alpha)$.

The authors also get the explicit minimizer f_α via such approach. They provide a technique for systematically deriving it using an inversion formula for Hilbert transforms on a finite interval.

The above method has raised a beautiful and fruitful result. However, it applies (as far as we know) only to rectangular Young diagrams, as this is the only case where the number of tableaux of the diagram above and below a given path can be written in the forms of products. If we apply this to a general shape, we would have at least one skew diagram, and unluckily the hook-type formula for a skew shape is no longer a single product but rather a sum of products.

A.2 Limit shape of standard Young tableaux via representation theory

A.2.1 Young diagrams, Young tableaux and representation theory

The Young tableaux and diagrams are useful in representation theory. As the Young diagrams of size n are in bijection with the partitions of n, they are in one-to-one correspondence with the conjugacy classes of irreducible representations of the symmetric group S_n. If ρ is an interesting finite dimensional representation of S_n (for example we can take the defining representation or regular representation, which respectively is the representation of S_n on $\mathbb{C}[\mathbf{1}, \mathbf{2}, ..., \mathbf{n}]$ or $\mathbb{C}[S_n]$), then we have the following decomposition of ρ:

$$\rho = \oplus_{\lambda \vdash n} m^\lambda \rho^\lambda, \tag{A.3}$$

where ρ^λ is an irreducible representation of S_n corresponding to the diagram λ and m^λ is its multiplicity in ρ. For any ρ we can define a canonical probability measure on all Young diagrams $\{\lambda : \lambda \vdash n\}$ to be proportional to the total dimension of the irreducible components of diagram λ in ρ, *i.e.*,

$$\mathbb{P}(\lambda) = \frac{m^\lambda \dim\rho^\lambda}{\dim\rho}, \tag{A.4}$$

where $\dim\rho = \sum_{\lambda\vdash n} \dim\rho^\lambda$.

Consider the Specht module on the space of polytabloids (for the details we refer the readers to the references on the representation theory of the symmetric group, for example [Sag01]). There, a basis of $(\rho^\lambda)_{\lambda\vdash n}$ in the decomposition (A.3) is given by the standard tableaux of λ. The dimension of ρ^λ is equal to the number of the standard Young tableaux of λ, and as all the ρ^λ such that $\lambda \vdash n$ form a complete list of irreducible representations, the dimension is also equal to the multiplicity m^λ. Then we recover the relation

$$\sum_{\lambda\vdash n} (|\mathcal{T}_\lambda|)^2 = n!,$$

where $|\mathcal{T}_\lambda|$ is the number of the standard tableaux of λ.

This identity can also be found by using a purely combinatorial method called the Robinson-Schensted algorithm [Rob38, Sch61], which gives a bijection between S_n and the pairs of standard Young tableaux of size n such that the tableaux of each pair is of the same shape.

The measure defined by (A.4) is the Plancherel measure

$$\mathbb{P}(\lambda) = \frac{(|\mathcal{T}_\lambda|)^2}{n!}.$$

This measure is also known to describe the measure of the longest increasing subsequence of a random permutation under the uniform probability measure [Sch61].

Now consider a chosen diagram λ, $\lambda \vdash n$, and let ρ^λ be the irreducible representation corresponding to λ in (A.3). For $l \leq n$ consider $\rho^\lambda \downarrow_{S_l}^{S_n}$, which is the restriction of ρ^λ to S_l as a subgroup S_n. As a S_l representation, we have the following decomposition of $\rho^\lambda \downarrow_{S_l}^{S_n}$:

$$\rho^\lambda \downarrow_{S_l}^{S_n} = \oplus_i m_i \rho^{(i)}, \tag{A.5}$$

where $\rho^{(i)}$ are pairwise inequivalent irreducible representations of S_l of dimension d^i and m_i are the corresponding multiplicities.

For any Young sub-diagram μ, $\mu \leq \lambda$ and $|\mu| = l$, let ρ^μ be the space spanned by the elements of the basis of ρ^λ where the numbers no-bigger than l are all included in μ (the notation ρ^μ is not exact as it depends on λ, and we hope that this simplification in notation will not cause ambiguity). Clearly, ρ^μ is invariant under S_l, so ρ^μ gives a subrepresentation of S_l. This subrepresentation can be decomposed into a direct sum of the copies of the Specht module for $S_{|\mu|}$, whose dimension is $|\mathcal{T}_\mu|$,

and the multiplicity (co-dimension) is just the number of the skew Young tableaux of $\lambda\backslash\mu$. Finally, it is easy to see that the following decomposition is unique (so this gives a decomposition of ρ^λ into irreducible representations):

$$\rho^\lambda \downarrow_{S_l}^{S_n} = \oplus_{\mu,\ \mu\leq\lambda} |\mathcal{T}_{\lambda\backslash\mu}| \rho^\mu.$$

Consider the probability measure defined as an analogue of (A.4): for $\mu \leq \lambda$, $\mu \vdash l$,

$$\mathbb{P}_\lambda^l(\mu) = \frac{|\mathcal{T}_{\lambda\backslash\mu}| \dim\rho^\mu}{\dim\rho^\lambda}, \tag{A.6}$$

then $\mathbb{P}_\lambda^l$ is in fact the marginal measure of the support of the first l elements under the uniform λ-Young tableaux measure. With this observation, the limiting behavior of Young tableaux, which is our main interest, can be translated as the limiting behavior of the subrepresentation of the symmetric group, which is studied in [Śni06] and is to be summarized in Section A.2.2.

A.2.2 The existence of the limit shape of standard Young tableaux via representation theory

The main result in this appendix is a corollary of Theorem 8 of [Śni06] which proves the existence of a limit shape of the standard Young tableaux of given asymptotic shape. The tools are originally used to study the limit shape of the Young diagrams. From Appendix A.2.1 we see that both can be reduced to the problem of the limiting behavior of the symmetric group S_n.

The problem of the limit shape of Young diagrams of size n while n tends to infinity is a topic discussed in a number of papers, including but not limited to [VK77, Bia98, Bia01, IO02a, Śni06].

The results we summarize below in this appendix are mainly taken from [Bia01] and [Śni06]: if we consider the canonical measure (A.4) (as a particular example they are interested in the Plancherel measure so we may take the regular representation or equivalently the Specht module), then if the normalized representation approximately factorizes (the definition will be given later), the Young diagrams' contribution to some finite-dimensional reducible representation of the symmetric group S_n will concentrate around some limit shape. More precisely, the measure of the boundary will converge in probability to a Dirac measure of the limit shape.

In this appendix we only summarize the necessary notions and results used to prove the existence of the limit shape of Young tableaux. In fact the Gaussian fluctuation of this limit shape is also indicated by these results.

Consider the canonical measure (A.4) when the representation ρ verifies certain properties yet to be precised. The authors of [Bia01] and [Śni06] consider the space of continuous Young diagrams, which are the 1-Lipschitz functions ω such that $\omega(x) - |x|$ is non-negative and of compact support. Readers can easily see that this

is the space of the properly scaled Young diagrams under the Russian convention. We define a function $s : \mathbb{R} \to \mathbb{R}$, $s(x) = \frac{1}{2}(\omega(x) - |x|)$, and we consider s'' as a (signed) measure in the sense of distributions. This measure is of compact support, so the following map [Bia01, IO02a]

$$\tilde{p}_n(\lambda) = \int_{\mathbb{R}} x^n s''(x)dx \tag{A.7}$$

determines uniquely the Young diagram λ. Thus the existence of the limit shape can be reduced to the convergence of $\tilde{p}_n$ (both properly normalized), so we call $\tilde{p}_n$ the *shape functionals*.

Define the *transition measure* μ^ω on the continuous Young diagrams as

$$\log \int_{\mathbb{R}} \frac{1}{z-x} d\mu^\omega(x) = -\frac{1}{2}\int_{\mathbb{R}} \frac{1}{z-x} s'(x)dx = -\int_{\mathbb{R}} \log(z-x)s''(x)dx. \tag{A.8}$$

The Cauchy transform appearing here is reminiscent of Appendix A.1.2 where we have mentioned the Hilbert transform used in calculating the limit shape of a rectangle Young tableau. We mention it here but we have no intent to go deep into the comparison of these results.

Let M_n be the n^{th} moment of μ^ω, then the Cauchy transform of μ^ω is given by

$$G_\mu(z) = \frac{1}{z} + \sum_{n\geq 1} M_n z^{-n-1}.$$

Let K_μ be the inverse of G_μ, and the free cumulants R_n of μ are defined as the coefficient in the expansion

$$K_\mu(z) = \frac{1}{z} + \sum_{n\geq 1} R_n z^{n-1}.$$

The classical cumulants are the coefficients of the formal expansion of the logarithm of the multidimensional Fourier transform. For more introduction to the free cumulants, we refer the readers to [Spe03]. The shape functionals (A.7) can be expressed as polynomials in the free cumulants and vice versa. So Theorem A.2.1 [Ś06] in the following implies the existence of the limit shape of the Young tableaux (and the Gaussian fluctuation of the boundary measure).

Before we announce the theorem we need to introduce the notion of approximating factorization [Bia01, Bia98, Ś06]. For given n, and for any $\sigma \in S_n$, we define the length of σ (denoted by $|\sigma|$) as the minimal number of transpositions that σ can be decomposed into their product. A functional χ of the permutations is said to *approximately factorize* if for any permutations $\sigma_1, \sigma_2, ..., \sigma_k$, if their supports (the non-fixed points) are disjoint, then we have

$$\chi(\sigma_1\sigma_2...\sigma_k) \approx \chi(\sigma_1)...\chi(\sigma_k),$$

where the $\approx$ means with an error term of order

$$O(n^{-\frac{|\sigma_1|+|\sigma_2|+...+|\sigma_k|+2(k-1)}{2}}),$$

where note that the order of $\chi(\sigma)$ is $n^{-\frac{|\sigma|}{2}}$ [Bia01].

Here in practice we will take the functional χ as the normalized character of the representation ρ, *i.e.*, for any π, $\chi(\pi)$ is equal to the trace of $\rho(\pi)$ divided by $\mathrm{Tr}(\rho(\epsilon))$. The regular representation is one of the example that verifies the approximate factorization.

It is the following theorem that proves the existence of the limit shape of the Young tableaux and its Gaussian fluctuations.

Theorem A.2.1. [Śni06] *Suppose that the sequence of representation ρ_q has the character factorization property. Let m_q be a sequence of integers such that $m_q \geq q$ and the limit $\alpha = \lim_{q\to\infty} \frac{q}{m_q}$ exists. Then if we consider ρ'_q as the restriction of the representation ρ_{m_q} to the subgroup $S_q \subseteq S_{m_q}$, then*

- *The sequence $(\rho'_q)_q$ also have the factorization property.*
- *Consider the free cumulants related to ρ'. For every l, there exists the limit $\lim_{q\to\infty} \mathbb{E}(R_l)q^{-\frac{l}{2}}$, and the joint distribution of*

$$q^{-\frac{i-2}{2}}(R_i - \mathbb{E}R_i)$$

converges to a Gaussian distribution in the weak topology.

In Appendix A.2.1 we have shown that the canonical measure associated to the representation $\rho^\lambda \downarrow_{S_l}^{S_n}$ (we recall that it is the representation ρ^λ restricted to S_l) is in fact the uniform measure of the standard Young tableaux corresponding to diagram λ. So to apply Theorem A.2.1 to our case, it suffices to note that for any given shape λ_1, let $(\lambda_n)_n$ be a sequence of Young diagrams of the same shape but with a scale of n times that of λ_1 (so $|\lambda_n| = n^2|\lambda_1|$), then the representation ρ^{λ_n}, as a subrepresentation of the regular representation, also has the approximate factorization. So for any $\alpha \in]0,1[$, the representation

$$\rho^{\lambda_n} \downarrow_{S_{\lfloor \alpha|\lambda_n| \rfloor}}^{S_{|\lambda_n|}}$$

is the ρ'_q in Theorem A.2.1, thus by the theorem the limit shape exists.

Bibliography

[AS16] Noga Alon and Joel H. Spencer. *The probabilistic method*. Wiley Series in Discrete Mathematics and Optimization. John Wiley & Sons, Inc., Hoboken, NJ, fourth edition, 2016.

[Ban08] Jason Bandlow. An elementary proof of the hook formula. *Electron. J. Combin.*, 15(1):Research paper 45, 14, 2008.

[BdT10] Cédric Boutillier and Béatrice de Tilière. The critical Z-invariant Ising model via dimers: the periodic case. *Probab. Theory Related Fields*, 147:379–413, 2010.

[Bia98] Philippe Biane. Representations of symmetric groups and free probability. *Adv. Math.*, 138(1):126–181, 1998.

[Bia01] Philippe Biane. Approximate factorization and concentration for characters of symmetric groups. *Internat. Math. Res. Notices*, (4):179–192, 2001.

[BK17] Alexey Bufetov and Alisa Knizel. Asymptotics of random domino tilings of rectangular aztec diamonds. 2017.

[BLPS01] Itai Benjamini, Russell Lyons, Yuval Peres, and Oded Schramm. Uniform spanning forests. *Ann. Probab.*, 29(1):1–65, 2001.

[Bou09] Cédric Boutillier. The bead model and limit behaviors of dimer models. *Ann. Probab.*, 37(1):107–142, 2009.

[BP93] Robert Burton and Robin Pemantle. Local characteristics, entropy and limit theorems for spanning trees and domino tilings via transfer-impedances. *Ann. Probab.*, 21(3):1329–1371, 1993.

[BR10] Yuliy Baryshnikov and Dan Romik. Enumeration formulas for Young tableaux in a diagonal strip. *Israel J. Math.*, 178:157–186, 2010.

[CEP96] Henry Cohn, Noam Elkies, and James Propp. Local statistics for random domino tilings of the Aztec diamond. *Duke Math. J.*, 85(1):117–166, 1996.

[CFKP11] Ionuţ Ciocan-Fontanine, Matjaž Konvalinka, and Igor Pak. The weighted hook length formula. *J. Combin. Theory Ser. A*, 118(6):1703–1717, 2011.

[Chh12] Sunil Chhita. The height fluctuations of an off-critical dimer model on the square grid. *J. Stat. Phys.*, 148(1):67–88, 2012.

[CKP01] Henry Cohn, Richard Kenyon, and James Propp. A variational principle for domino tilings. *J. Amer. Math. Soc.*, 14(2):297–346 (electronic), 2001.

[CLP98] Henry Cohn, Michael Larsen, and James Propp. The shape of a typical boxed plane partition. *New York J. Math.*, 4:137–165, 1998.

[CR07] David Cimasoni and Nicolai Reshetikhin. Dimers on surface graphs and spin structures. I. *Comm. Math. Phys.*, 275(1):187–208, 2007.

[DG15] Julien Dubédat and Reza Gheissari. Asymptotics of height change on toroidal Temperleyan dimer models. *J. Stat. Phys.*, 159(1):75–100, 2015.

[DM15] Erik Duse and Anthony Metcalfe. Asymptotic geometry of discrete interlaced patterns: Part I. *Internat. J. Math.*, 26(11):1550093, 66, 2015.

[Elk03] Noam D. Elkies. On the sums $\sum_{k=-\infty}^{\infty}(4k+1)^{-n}$. *Amer. Math. Monthly*, 110(7):561–573, 2003.

[For93] Robin Forman. Determinants of Laplacians on graphs. *Topology*, 32(1):35–46, 1993.

[FR37] RH Fowler and GS Rushbrooke. An attempt to extend the statistical theory of perfect solutions. *Transactions of the Faraday Society*, 33:1272–1294, 1937.

[FRT54] J. S. Frame, G. de B. Robinson, and R. M. Thrall. The hook graphs of the symmetric groups. *Canadian J. Math.*, 6:316–324, 1954.

[GL99] Anna Galluccio and Martin Loebl. On the theory of Pfaffian orientations. I. Perfect matchings and permanents. *Electron. J. Combin.*, 6:Research Paper 6, 18, 1999.

[GNW79] Curtis Greene, Albert Nijenhuis, and Herbert S. Wilf. A probabilistic proof of a formula for the number of Young tableaux of a given shape. *Adv. in Math.*, 31(1):104–109, 1979.

[Häg95] Olle Häggström. Random-cluster measures and uniform spanning trees. *Stochastic Process. Appl.*, 59(2):267–275, 1995.

[IO02a] Vladimir Ivanov and Grigori Olshanski. Kerov's central limit theorem for the Plancherel measure on Young diagrams. In *Symmetric functions 2001: surveys of developments and perspectives*, volume 74 of *NATO Sci. Ser. II Math. Phys. Chem.*, pages 93–151. Kluwer Acad. Publ., Dordrecht, 2002.

[IO02b] Vladimir Ivanov and Grigori Olshanski. Kerov's central limit theorem for the Plancherel measure on Young diagrams. In *Symmetric functions 2001: surveys of developments and perspectives*, volume 74 of *NATO Sci. Ser. II Math. Phys. Chem.*, pages 93–151. Kluwer Acad. Publ., Dordrecht, 2002.

[Kas61] P. W. Kasteleyn. The statistics of dimers on a lattice : I. the number of dimer arrangements on a quadratic lattice. *Physica*, 27:1209–1225, December 1961.

[Kas63] P. W. Kasteleyn. Dimer statistics and phase transitions. *J. Mathematical Phys.*, 4:287–293, 1963.

[Kas67] P. W. Kasteleyn. Graph theory and crystal physics. In *Graph Theory and Theoretical Physics*, pages 43–110. Academic Press, London, 1967.

[Ken97] Richard Kenyon. Local statistics of lattice dimers. *Ann. Inst. H. Poincaré Probab. Statist.*, 33(5):591–618, 1997.

[Ken09] Richard Kenyon. Lectures on dimers. 2009.

[Ken11] Richard Kenyon. Spanning forests and the vector bundle Laplacian. *Ann. Probab.*, 39(5):1983–2017, 2011.

[KO06] Richard Kenyon and Andrei Okounkov. Planar dimers and harnack curves. *Duke Math. J.*, 131(3):499–524, 2006.

[KO07] R. Kenyon and A. Okounkov. Limit shapes and the complex burgers equation. *Acta mathematica*, 199(2):263–302, 2007.

[KOS06] Richard Kenyon, Andrei Okounkov, and Scott Sheffield. Dimers and amoebae. *Ann. of Math. (2)*, 163(3):1019–1056, 2006.

[KPW00] R.W. Kenyon, J.G. Propp, and D.B. Wilson. Trees and matchings. *Electron. J. Combin*, 7(1):R25, 2000.

[Kra95] C. Krattenthaler. Bijective proofs of the hook formulas for the number of standard Young tableaux, ordinary and shifted. *Electron. J. Combin.*, 2:Research Paper 13, approx. 9 pp. 1995.

[KU08] Takahiro Kazami and Kôhei Uchiyama. Random walks on periodic graphs. *Trans. Amer. Math. Soc.*, 360(11):6065–6087, 2008.

[LPS03] Russell Lyons, Yuval Peres, and Oded Schramm. Markov chain intersections and the loop-erased walk. *Ann. Inst. H. Poincaré Probab. Statist.*, 39(5):779–791, 2003.

[LS77] B. F. Logan and L. A. Shepp. A variational problem for random Young tableaux. *Advances in Math.*, 26(2):206–222, 1977.

[Mac12] Diane Maclagan. Introduction to tropical algebraic geometry. In *Tropical geometry and integrable systems*, volume 580 of *Contemp. Math.*, pages 1–19. Amer. Math. Soc., Providence, RI, 2012.

[MPP16] Alejandro H. Morales, Igor Pak, and Greta Panova. Hook Formulas for Skew Shapes I. q-analogues and bijections. 2016.

[MPP17] Alejandro H. Morales, Igor Pak, and Greta Panova. Hook Formulas for Skew Shapes II. Combinatorial Proofs and Enumerative Applications. *SIAM J. Discrete Math.*, 31(3):1953–1989, 2017.

[Nar14] Hiroshi Naru. Shubert calculus and hook formula. *Talk slides at 73rd Sem. Lothar. Combin, Strobl., Austria*, 2014.

[NPS97] Jean-Christophe Novelli, Igor Pak, and Alexander V. Stoyanovskii. A direct bijective proof of the hook-length formula. *Discrete Math. Theor. Comput. Sci.*, 1(1):53–67, 1997.

[Pak02] Igor Pak. Hook length formula and geometric combinatorics. *Sém. Lothar. Combin.*, 46:Art. B46f, 13, 2001/02.

[Pem91] Robin Pemantle. Choosing a spanning tree for the integer lattice uniformly. *Ann. Probab.*, 19(4):1559–1574, 1991.

[Pet14] Leonid Petrov. Asymptotics of random lozenge tilings via Gelfand-Tsetlin schemes. *Probab. Theory Related Fields*, 160(3-4):429–487, 2014.

[Pet15] Leonid Petrov. Asymptotics of uniformly random lozenge tilings of polygons. Gaussian free field. *Ann. Probab.*, 43(1):1–43, 2015.

[PR07] Boris Pittel and Dan Romik. Limit shapes for random square Young tableaux. *Adv. in Appl. Math.*, 38(2):164–209, 2007.

[Rem82] J. B. Remmel. Bijective proofs of formulae for the number of standard Young tableaux. *Linear and Multilinear Algebra*, 11(1):45–100, 1982.

[Rob38] G. de B. Robinson. On the Representations of the Symmetric Group. *Amer. J. Math.*, 60(3):745–760, 1938.

[Rom12] Dan Romik. Arctic circles, domino tilings and square Young tableaux. *Ann. Probab.*, 40(2):611–647, 2012.

[Rud87] Walter Rudin. *Real and complex analysis*. McGraw-Hill Book Co., New York, third edition, 1987.

[Ś06] Piotr Śniady. Gaussian fluctuations of characters of symmetric groups and of Young diagrams. *Probab. Theory Related Fields*, 136(2):263–297, 2006.

[Sag01] Bruce E. Sagan. *The symmetric group*, volume 203 of *Graduate Texts in Mathematics*. Springer-Verlag, New York, second edition, 2001. Representations, combinatorial algorithms, and symmetric functions.

[Sch61] C. Schensted. Longest increasing and decreasing subsequences. *Canad. J. Math.*, 13:179–191, 1961.

[She03] Scott Sheffield. *Phd. Thesis, Standford Univ.*, 2003.

[Spe03] R. Speicher. Free probability theory and random matrices. In *Asymptotic combinatorics with applications to mathematical physics (St. Petersburg, 2001)*, volume 1815 of *Lecture Notes in Math.*, pages 53–73. Springer, Berlin, 2003.

[Tem74] Combinatorics. pages 202–204, 1974. London Mathematical Society Lecture Note Series, No. 13.

[Tes00] Glenn Tesler. Matchings in graphs on non-orientable surfaces. *J. Combin. Theory Ser. B*, 78(2):198–231, 2000.

[TF61] H. N. V. Temperley and Michael E. Fisher. Dimer problem in statistical mechanics—an exact result. *Philos. Mag. (8)*, 6:1061–1063, 1961.

[Ver89] A. M. Vershik. The hook formula and related identities. *Zap. Nauchn. Sem. Leningrad. Otdel. Mat. Inst. Steklov. (LOMI)*, 172(Differentsialcprime naya Geom. Gruppy Li i Mekh. Vol. 10):3–20, 169, 1989.

[VK77] A. M. Vershik and S. V. Kerov. Asymptotic behavior of the Plancherel measure of the symmetric group and the limit form of Young tableaux. *Dokl. Akad. Nauk SSSR*, 233(6):1024–1027, 1977.

[Wil96] David Bruce Wilson. Generating random spanning trees more quickly than the cover time. pages 296–303, 1996.

[You28] Alfred Young. On Quantitative Substitutional Analysis. *Proc. London Math. Soc. (2)*, 28:255–292, 1928.

[You30] A. Young. Corrigenda. On Quantitative Substitutional Analysis. *Proc. London Math. Soc. (2)*, 31:556, 1930.